STRUCTURAL MRI AND CALIBRATED fMRI DURING A COGNITIVE STROOP TASK IN THE NORMAL AGED HUMAN BRAIN

Thesis submitted in accordance with the requirements of the University of Liverpool for the degree of Doctor in Philosophy

By

Rafat Saeed Mohtasib

December 2011

UNIVERSITY OF LIVERPOOL

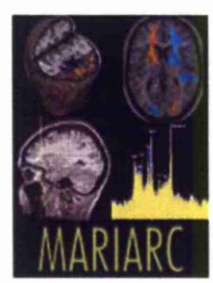

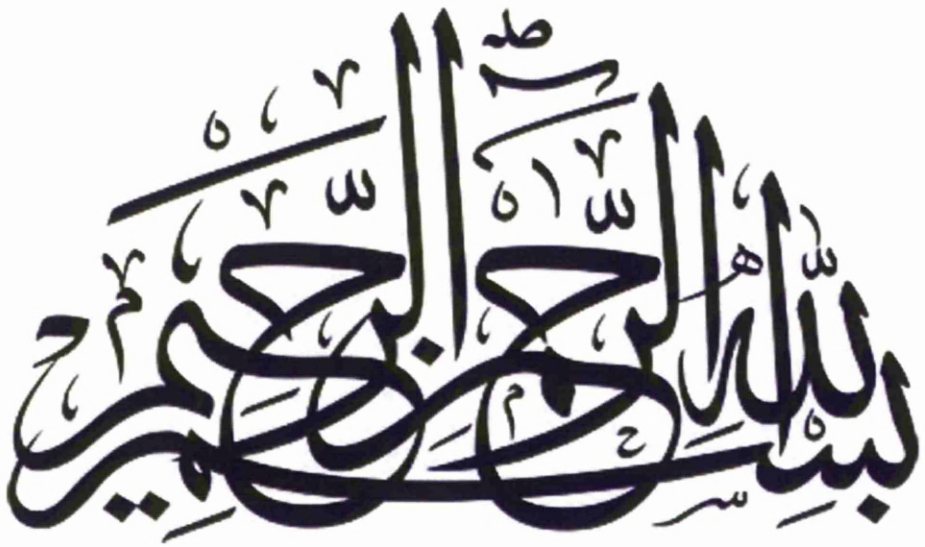

In the Name of Allah, the Most Gracious, the Most Merciful

Table of Contents

DECLARATION

The work presented in this thesis is the result of my own work. The material contained in this thesis has not been presented, nor is currently being presented, either wholly or in part, for any other degree or qualification.

_____

Rafat Mohtasib

_____

Dr. Vanessa Slumming

ACKNOWLEDGEMENTS

This work was the most worthwhile part of my life and whatever is the outcome, it has been such an enrich-able experience that will enlightens my future. I would like to thank my supervisors Dr. Vanessa Slumming, Dr. Tony Marson and Dr. Laura Parkes; the nicest and most talented people I have ever met, and with whom it has been my honour to learn from and work with over the last four years. I would also like to thank my colleagues from MARIARC, Dr. Jonathan Goodwin who developed many of the protocols described in this thesis, senior radiographer Valerie Adams, Andrew Irwin (research nurse), and Guy Lumley who helped me out during the scans and cognitive tests. Very big special thanks to my best friend Jaman Alghamdi who always stand by my side and supported me.

I would also like to acknowledge Medical Research Council and King Faisal Specialist Hospital and Research centre for their financial support of my PhD research, without which, none of it would have been possible.

My family and close friends enrich my life and I thank them all. I would, however, like to make special mention of my mother (Khyryiah), brothers (Majdi and Ramzi), sisters (Manal, Maram, Halah, Rawiyah and Suha), my sweet heart (Layla) and my kids (Majdi, Aseel, Ghida, Hadeel and Abdulrhman) for their encouragements and ongoing support. I take this opportunity to also thank you for all the love, care and comprehension you have had throughout every stage of my life. I will never be able to express how much you mean to me.

Rafat Mohtasib 2011

Abstract of Thesis

Background: In recent years, structural magnetic resonance imaging (MRI) studies have shown dramatic age-associated changes in grey matter volume, density and cortical thickness. Calibrated functional magnetic resonance (fMRI) has become a recognized technique for quantifying both the cerebral blood flow (CBF) and oxygen metabolism ($CMRO_2$) changes associated with neural activation. It has been used as an advanced approach for examining the physiological effects of age-related changes in the brain, which may be difficult to interpret if measured by the blood oxygen level dependent (BOLD) signal alone. fMRI studies of aging have revealed increased BOLD response to tasks of executive function with advancing age, which is generally interpreted as increased neural activity. However, changes in the cerebrovascular system with age can alter the BOLD signal, complicating this interpretation. Arterial spin labeling (ASL) allows simultaneous acquisition of BOLD and CBF information and can be used to quantify the component parts of the BOLD signal.

Aims: Hyperoxia calibration was applied during fMRI to study neurovascular alterations and correlations with age. We aimed: (1) address if age-related differences in the BOLD signal develop from age-related neural plasticity or age-related cerebrovascular changes during a cognitive Stroop task. (2) Understand the underlying physiology of the BOLD signal change that is seen with aging. (3) Determine regional variation in physiological changes with age. (4) Determine regional changes in grey matter density and cortical thickness with increasing age. (5) Assess the impact of this structural change on physiological change.

Methods: We used calibrated fMRI approach in 55 healthy participants over an age range of 18–71 years to determine the relative vascular and neuronal contributions to the age-related BOLD changes in response to a Stroop task. We analysed the structural data with the new VBM-DARTEL technique. The cortical thicknesses were analysed using the FreeSurfer tools.

Results: The BOLD response increased significantly with increasing age but the CBF response did not alter, such that the BOLD increase is attributed to a significant reduction in $CMRO_2$ response with increasing age. Hence, in this study, the BOLD increase with age should be interpreted as a reduction in neural activity, which would be consistent with neurodegeneration. The greatest BOLD increases with age were found in left and right medial frontal gyri and primary motor cortex and were again linked to a reduction in $CMRO_2$. Age-related decline in grey matter density and cortical thickness were widespread, but the frontal regions, in general, exhibit greater thickness changes than parietal, temporal and occipital. The strongest correlations between age and (BOLD activations, grey matter density, cortical thickness) were found mainly in the frontal cortices. The cortical structure–function relationships are different for each sex. Finally, better performance had been observed to be associated with larger frontal grey matter density and thicker cortex on some executive tasks, and increased frontal $CMRO_2$ response.

Conclusions: This study demonstrates the relationship between structure, function, and cognition, as well as the need to take into account alterations in vascular-metabolic coupling and resting blood volume when interpreting changes in the BOLD response with aging. It also highlights the added benefit that calibrated fMRI offers in terms of interpreting the underlying physiological changes that give rise to the measured BOLD response.

List of tables

List of figures

Publications

PAPERS

- **Mohtasib, R.S.,** Lumley, G., Goodwin, J.A., Emsley, H.C., Sluming, V. & Parkes, L.M. 2011. Calibrated fMRI during a cognitive Stroop task reveals reduced metabolic response with increasing age. *Neuroimage.*

ABSTRACTS

- **Mohtasib RS,** Sluming V, Parkes LM "Calibrated fMRI during a cognitive Stroop task in the aging brain" ISMRM Stockholm [2010].

- **Mohtasib RS**, Sluming V, Parkes LM "Calibrated fMRI: alteration in neurovascular coupling during a cognitive Stroop task in aging brain" HBM Barcelona [2010].

- Cox DJ, **Mohtasib RS,** Montaldi D, Parkes LM "Increased resting state connectivity between left and right hemispheres with increasing age" ISMRM Stockholm [2010].

- Parkes LM, Lumley G, **Mohtasib RS,** Emsley H, Goodwin JA "Calibrated fMRI reveals altered neurovascular coupling with age during a cognitive Stroop task' ISMRM Honolulu [2009].

Abbreviations

- ACC Anterior Cingulate cortex
- ATP: Adenosine Triphosphate
- ASL: Arterial Spin Labeling
- B_0: Static magnetic field applied in MRI
- BOLD: Blood Oxygen Level Dependent
- CASL: Continuous Arterial Spin Labeling
- CBF: Cerebral Blood Flow
- CBV: Cerebral Blood Volume
- $CMRO_2$: Cerebral Metabolic Rate of Oxygen
- CNS: Central Nervous System
- CSF: Cerebrospinal Fluid
- DARTEL: Diffeomorphic Anatomical Registration using Exponentiated Lie Algebra
- dHb: Deoxyhaemoglobin
- DLPFC: Dorsolateral pre-frontal cortex
- DMPFC Dorsomedial pre-frontal cortex
- EPI: Echo Planar Imaging
- EPISTAR: Echo Planar Imaging and Signal Targeting with Alternating Radiofrequency
- FA: Flip Angle
- FAIR: Flow-Sensitive Alternating Inversion Recovery
- FDR False Discovery Rate Correction
- FID: Free induction decay
- FL: Frontal Lobe
- fMRI: Functional MRI
- FOV: Field-of-View
- FWE: Family Wise Error
- FWHM: Full-Width-at-Half-Maximum
- GE: Gradient echo
- GM: Grey Matter
- Hb: Haemoglobin
- LFP's: Local Field Potentials
- M1: Primary Motor Area
- MARIARC: Magnetic Resonance & Image Analysis Research Centre
- MFG: Middle Frontal Gyrus
- MRI: Magnetic Resonance Imaging
- MPRAGE Magnetization-Prepared Rapid Gradient Echo
- *n:* Neurovascular Coupling
- NMR: Nuclear Magnetic Resonance
- NMV: Net Magnetization Vector
- OEF: Oxygen Extraction Fraction
- OL: Occipital Lobe
- PASL: Pulsed Arterial Spin Labeling
- PICORE: Proximal Inversion with a Control for off-Resonance Effects
- PL: Parietal Lobe

- Q2TIPS QUIPSS II with Thin-Slice TI1 Periodic Saturation
- QUIPSS Quantitative Imaging of Perfusion using a Single Subtraction
- PFC: Prefrontal Cortex
- r Correlation Coefficient
- R_2*: The relaxation parameter
- RF: Radio Frequency
- ROI: Region-Of-Interest
- SE: Spin Echo
- SMA: Supplementary Motor Area
- SNR: Signal to Noise Ratio
- T1 Longitudinal magnetization recovery constant
- T2 Transverse magnetization decay constant
- T2* Transverse magnetization decay constant including field inhomogeneity effects
- TE: Echo Time
- TI Inversion Time
- TIV: Total Intracranial Volume
- TL: Temporal Lobe
- TOF: Time of Flight
- TR: Repetition Time
- VBM: Voxel-Based Morphometric
- WM: White Matter
- γ Gyromagnetic Ratio

CHAPTER 1: Introduction

1.1 Introduction

The human brain has always been one of the organs that has most enthused the interest of researchers throughout the years. Recently, the science of neuroimaging has made great progress in helping researchers gain a clearer understanding of age-related brain changes. The aging population increases, it is of increasing importance to understand how the brain changes with age and how we might be able to preserve healthy brain function with age.

Neuroimaging has helped to advance understanding of the brain aging process, in particular the relationship between cognitive decline and physiological changes. The aging process involves remarkable changes in brain morphology and function. As a person ages, significant changes occur in cellular metabolism (Simic et al., 1997), cortical density (Good et al., 2001b, Sowell et al., 2003, Tisserand et al., 2004, Van Laere and Dierckx, 2001) and cerebrovascular function (Leenders et al., 1990, Parkes et al., 2004). It is well documented that aging is accompanied by a decline in cognitive function (Coffey et al., 1992, Golomb et al., 1994, Gong et al., 2005, Zimmerman et al., 2006), as well as reductions in grey matter volume (Coffey et al., 1992, Pfefferbaum et al., 1994, Raz et al., 1997) and thinning of the cortex (Fjell et al., 2009, Salat et al., 2004, Thambisetty et al., 2010, Ziegler et al., 2010). Age-related changes in brain anatomy, neuronal density, or cerebral metabolism could significantly influence the blood oxygenation level dependent (BOLD) signal (Huettel et al., 2001), as measured with fMRI.

Functional magnetic resonance imaging (fMRI) has become an increasingly important tool. Most fMRI experiments make use of the BOLD signal as an indirect measure of neural activity which reflects local changes in deoxyhemoglobin content, which is a complex function of dynamic changes in cerebral blood flow (CBF), cerebral blood volume (CBV), and the cerebral metabolic rate of oxygen ($CMRO_2$). Interestingly, structural studies of the aging brain indicate that prefrontal cortices (PFC) experience the highest degree of age-related atrophy (Cowell et al., 1994, Gur et al., 2000, Raz et al., 2004, Salat et al., 1999). However, even with the susceptibility of the PFC to aging, greater PFC BOLD activation has been revealed in many fMRI studies of aging (Cabeza et al., 2002, Langenecker et al., 2004, Milham et al., 2002, Reuter-Lorenz et al., 2000, Zysset et al., 2007), suggesting a compensatory activity in the older group to aid performance. The PFC is an important neural substrate underlying executive functions such as attention and working memory, it also has extensive anatomical connections with many cortical and subcortical regions (Tamraz and Comair, 2006, West, 1996).

The objective of this study is to demonstrate the relationship between structure, function, and cognition, as well as the care needed when interpreting changes in the BOLD response with age. It also highlights the added benefit that calibrated fMRI offers in terms of interpreting the underlying physiological changes that give rise to the measured BOLD response. The novelty of this study is that we collected structural, functional and cognitive information from the same participants, allowing within-subject intra-relationships between these measurements to be assessed. The aim of this thesis to determine whether, and to what extent, grey matter

density, neural activity, and/or vascular responsiveness change with age and how they impact on cognitive function.

The material, literature review and experiments, are presented in six chapters that are organised as follow:

Chapter 2 gives a brief overview of the anatomical and physiological features of the human brain focussing on the frontal cortex. This chapter describes cellular changes observed in the post-mortem literatures on development and age-related changes that likely underlie the changes observed with magnetic resonance imaging (MRI). It will then describe changes in brain structure and functional observed in brain-mapping studies with increasing age.

Chapter 3 presents a basic overview of the physical principles of MRI parameters used in this study. It includes sections about Arterial Spin Labelling (ASL) and functional MRI.

Chapter 4 explains the general design of the study. Data of the participants are presented, together with procedures employed for data acquisition (both MRI and fMRI). Neuropsychological assessment tests are also described in details.

Chapter 5 explores the primary focus of this thesis, which is the use of calibrated fMRI to determine the relative vascular and neuronal contributions to the age-related BOLD changes in response to a Stroop task. The motivation for this study arose from the fact that with increasing age the BOLD signal change is seen to increase in certain key areas such as the frontal cortex. This is often interpreted as an increase in neural activity and used to support a model of compensatory activity in the older group to aid performance. According to the compensation hypothesis (Cabeza, 2002, Cabeza et al., 1997), increased bilaterality in old adults could help counteract age-related neurocognitive deficits. However the BOLD response is a complex mix of neural and vascular factors. The first aim of this chapter is to determine whether age-related changes in the BOLD signal are neural or vascular in origin through the use of fMRI technique. We aim to understand the underlying physiology of the BOLD signal change that is seen with age. We also aim to determine regional variation in these physiological changes with age, as well as the relationship between these changes and cognition.

Chapter 6 investigates the link between grey matter density, age and sex using the new voxel-based morphometry (VBM) registration method; Diffeomorphic Anatomical Registration using Exponentiated Lie algebra (DARTEL). In addition, the effect of regional grey matter density on cognition is explored. We hypothesized that the largest age-related changes in grey matter density would be found within the frontal lobe (where we had the strongest BOLD activation in chapter 4), and that decline in cognitive performance would be particularly associated with changes in grey matter density.

Chapter 7 illustrates the link between the regional cortical thickness changes and age. The relationship between cortical thickness and cognition is also considered. We hypothesized that the largest age-related effects on cortical thickness would be found within the frontal lobe (the same grey matter regions found in chapter 5), while decline in cognitive performance tests would be particularly associated with changes in cortical thickness. We tested for regional differences in cortical thickness among all subjects and in each sex. We also tested for association between cortical thickness and brief executive assessment tests.

Chapter 8 summarises and discusses the main findings of this thesis on structural and calibrated fMRI during a cognitive Stroop task in the normal aged human brain.

Chapter 2: The Human Brain

2.1 Aim of Chapter

This chapter provides a brief overview of the basic anatomical and physiological features of the human brain focussing on the frontal cortex. Further reference can be obtained from many books on brain biochemistry and neuroanatomy textbooks(Clark et al., 2010, Crossman and Neary, 1998, Encyclopaedia Britannica, 2008, Kelley and Petersen, 1997, Kolb and Whishaw, 2003, Martin, 2003, Martini, 1998, Tamraz and Comair, 2006).

2.2 Brain Structure

2.2.1 Cellular Structure of the Brain

The brain contain several hundred billion neurons (Pakkenberg and Gundersen, 1997). Most neurons consist of: cell body (soma), nerve fibre (axons) and the receiving processes (dendrites) (Figure 2.1). The soma contains the nucleus of the cell and the essential cellular organelles, which are involved in metabolism and synthesis. Most cell bodies have branches called dendrites, which receive signals from other neurons through synaptic connection at the dendritic spines. Axons carry information from one neuron to another, and terminate at the synaptic terminals, which are attached to the dendrites or soma of another neuron. Signals are transferred across the synapse by means of a chemical neurotransmitter, whereas electrical signals transmit information from one part of a neuron to another.

The central nervous system (CNS) contains several types of neurons (sensory neurons, interneurons, motor neurons), which are adapted to the job they perform. There are also multiple glial cells for every neuron, which provide support for neurons. The microglia cells for example perform a scavenger role; and the oligodendrocytes form the myelin sheath around the axons.

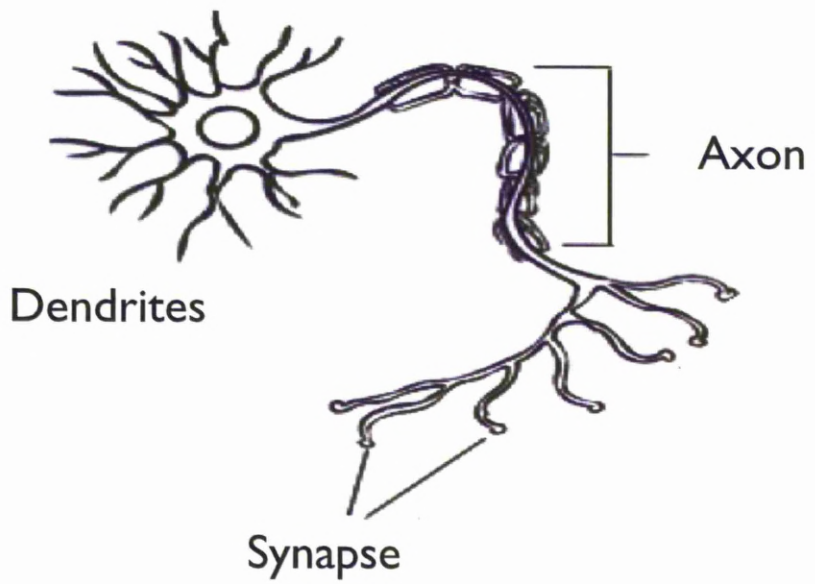

Figure 2.1: Diagram of typical motor neurone.

2.2.3 Lobes of the Brain and Function

Each cerebral hemisphere is divided into four lobes: the frontal, parietal, temporal and occipital lobes. Each lobe of them controls a different range of functions. The frontal and parietal lobes are separated by the central sulcus, and the temporal lobe separated by the lateral fissure.

Frontal Lobe

The frontal lobe (FL) is the largest of the lobes and is the most recently evolutionary parts of the brain (Tamraz and Comair, 2006). There is a strong relation between order of developmental myelination and degree of age-related volumetric atrophy, with regions developing late showing the strongest age-related atrophy (Raz, 2000). The FL occupies the anterior of the cortex and is bounded posteriorly by the central fissure and inferiorly by the lateral sulcus. It plays a major role in the planning and execution of movements (Fuster, 2002, Moscovitch and Winocur, 1995). There are four important gyri in the FL. The precentral gyrus is located approximately parallel and anterior to the central sulcus. The precentral gyrus represents the primary motor cortex. The superior frontal gyrus, the middle frontal gyrus, and the inferior frontal gyrus lie parallel to each other and approximately perpendicular to the precentral gyrus (Tamraz and Comair, 2006). The FL contains several functionally distinct regions: motor, premotor and prefrontal (Figure 2.2).

The primary motor area (M1), corresponds with Brodmann's area (BA) 4, is located in the dorsal part of the precentral gyrus and in the anterior part of the central sulcus of each cerebral hemisphere (Figure 2.2) (Tamraz and Comair, 2006). It works in association with the premotor areas to coordinate and initiate motor movements (Clark et al., 2005, Goldberg, 1985). M1 can be subdivided into two

components. M1 located along the midline controls the body below the waist; and M1 located on the lateral surface of the brain that controls the muscles of the body found above the waist (Geyer et al., 1996).

The premotor cortex (BA 6 on the lateral surface) is involved in the generation of a motor sequence from memory that requires accurate timing and also involved with visuomotor activity (Halsband et al., 1993).

The supplementary motor area (SMA) is located anterior to the M1 on the medial side of the frontal lobe along the longitudinal cerebral fissure. It corresponds approximately with BA 6 on the medial surface (Figure 2.2) (Wise et al., 1996). The SMA can be subdivided into two components. The more caudal component is associated to movement execution; and the more rostral component that function as a clearing house for cognitive and motivational information (Rizzolatti et al., 1996). SMA has also been implicated in actions that are under internal control, such as the performance of a series of movements from memory (Shima and Tanji, 1998).

The prefrontal cortex (PFC) lies anterior to the motor and premotor areas (Figure 2.2). It is connected with most other cortices a in specific manner, including sensory and high-order association areas, and subcortical structures associated with cognition, memory and emotions (Barbas, 1995, Petrides, 2000). Furthermore, there are differences in the set of connections of lateral PFC, medial PFC, and orbitofrontal cortices, consistent with their functional specialization (Barbas, 2000). PFC cortex is divided into three regions according to function: the dorsolateral region, the dorsomedial/medial region and the orbital (basal) region. The orbital and dorsomedial subdivisions of the PFC are included as part of the limbic association cortex (Kolb and Whishaw, 2003).

The dorsolateral prefrontal cortex (DLPFC) lies between longitudinal fissure superiorly and lateral fissure laterally (Figure 2.2). The DLPFC has been described as a place where past and future gather (Bonaz, 2003). It looks backward in time to construct memories from sensory input and looks forward in time to construct a motor plan of action (Fuster, 1995). DLPFC is associated with motor planning, regulation, organization and working memory (Barbas, 2000, Barbas and Zikopoulos, 2007, Goldman-Rakic, 1996, Petrides, 2000). DLPFC corresponds approximately with BA 46. Activity in this area is reported to be associated with working memory, finger movements and freely generated words (Lau et al., 2004, Petrides, 2000). Brodmann's areas 6, 8, and 9 become activated when a working memory task must be continuously updated (Wager and Smith, 2003). The more ventral dorsolateral cortex is responsible for preparation during short-term storage (Owen, 2000). The frontal eye fields are found on the dorsolateral frontal cortex and correspond with BA 8 (Figure 2.2). The frontal eye fields contribute to voluntary eye movements (Jeffrey D, 2004).

Broca's speech area occupies BA 44 and 45 on the inferior frontal gyrus (Figure 2.2). This region is specialized on the dominant side of the cortex for the production of speech (Amunts et al., 2004). Broca's area is involved in word retrieval as well as in verbal fluency (Amunts et al., 2004, Caplan et al., 2000).

The anterior cingulate cortex (ACC) is a similarly important region in cognitive control that interacts strongly with dorsolateral prefrontal areas (Barbas et al., 1999). The ACC has strongly involved in emotions and long-term memory (Allman et al., 2001, Devinsky et al., 1995). The ACC was also involved during demanding cognitive tasks and reported to have a key role in cognitive–emotional interactions (Barbas and Zikopoulos, 2007). The medial PFC in the anterior cingulate

have strong connections with medial temporal and hippocampal structures associated with long term memory, and with central autonomic structures associated with expression of emotions (Barbas and Zikopoulos, 2007).

The dorsomedial component of the prefrontal cortex (DMPFC) extends from the SMA to the orbital of the PFC, contains the anterior portion of the cingulate gyrus, medial portion of superior and middle frontal gyri. The DMPFC is involved in the combination of motor, sensory, emotional information and is important in motivation and initiation of activity (Barbas, 2000, Barbas and Zikopoulos, 2007, Owen, 2000, Petrides, 2000).

The orbitofrontal (basal) region is the most inferior region of the PFC, extending from the basal part of the frontal pole anteriorly, to the olfactory areas posteriorly. The orbitofrontal reported to be associated with emotional, social behavior, and impulse control (Bechara and Van Der Linden, 2005). Inhibitory control also arises from the orbital and medial prefrontal cortex (Fuster, 2002). Brodmann's areas included in the orbitofrontal cortex region are 11, 12, 13, and 14 (Figure 2.2) (Fuster, 2002).

Parietal Lobe

The parietal lobe (PL) is bounded anteriorly by the central sulcus, inferiorly by the lateral sulcus, and posteriorly by the parieto-occipital fissure (Figure 2.2). It has been heavily involved in the higher cognitive functions of the brain and concerned with perception of stimuli related to touch, pressure, temperature and pain (Clark et al., 2010). Moreover, the left parietal lobe might be more specialized in discriminating visual events that are important for action observation and movement control (Rushworth et al., 2001). Sensitivity to spatial information when perceiving

causality was correlated with activation of the right parietal lobe (Shulman et al., 2010).

The PL consists of the primary somatosensory (somesthetic) cortex (BA areas 1, 2, and 3), the superior parietal lobule (BA 5 and 7), and the inferior parietal lobule (BA 39 and 40) (Figure 2.2). The superior parietal lobule corresponds with BA 5 and 7. It is found on both the lateral and medial aspect of the cortex. The precuneus includes BA 7 and 31 on the medial aspect (Figure 2.2). The superior parietal lobule contains a representation of the body, limbs and a map of the space immediately surrounding the body (Colby and Goldberg, 1999, Sakata et al., 1997). The lateral interparietal area next to BA 7 are important in determining the relative behavioral importance of available visual objects and directing attention to a particularly salient object (Yantis et al., 2002).

The inferior parietal lobule corresponds with the supramarginal gyrus BA 40 and the angular gyrus BA 39 (Figure 2.2). It has been proposed that inferior parietal lobule may serve a specialized function in the expression of attention (Ciaramelli et al., 2010). The inferior parietal lobule functions to encode and retrieve a motor sequence (Rothi et al., 1985). Increased activation of dorsal posterior parietal cortex at stimulus encoding predicts success in recognition memory, whereas activation in ventral posterior parietal cortex at encoding predicts success in incidental memory and perceptual priming tests (Uncapher and Wagner, 2009, Wimber et al., 2010). The angular gyrus (BA 39) is mainly involved in transforming visual messages to the selection of a motor order (Ruby et al., 2002). The temporo-parietal junction includes portions of the inferior parietal lobule and superior temporal gyrus (Vallar et al.,

1999). This area is known to play an important role in self-other distinction processes and theory of mind (Saxe and Kanwisher, 2003).

Temporal Lobe

The temporal lobe (TL) is bounded dorsally by the lateral fissure and importantly houses the auditory cortex. The transverse gyri (Heschl's gyrus; BA 41 and 42) are located on the superior surface of the superior temporal gyrus (Figure 2.2). Brodmann's area 41 corresponds with the primary auditory cortex; and BA 42 constitutes the secondary auditory cortex. The TL also contains the superior BA 22, middle BA 21, inferior temporal gyri BA 20 and the cortex of the temporal pole BA 38 (Figure 2.2). Language is related to the posterior superior temporal gyrus and is lateralized to the left dominant side (de Guibert et al., 2011). Speech sounds are analyzed by the left TL (Binder et al., 2000). Pauses during speech, used in speech planning and word retrieval, were reported to be associated with activation of the left superior temporal sulcus BA 22 and 39 (Figure 2.2) (Kircher et al., 2004). The superior temporal sulcus BA 22 is important in social perception using visual signals such as movements of the hands, mouth and eyes (Blakemore and Decety, 2001). It has been found that the right superior temporal area plays a role in spatial awareness (Karnath et al., 2001).

The posterior portions of the middle and inferior temporal gyri next to the occipital lobe are heavily involved with visual processing (Blumberg and Kreiman, 2010). The inferior temporal area is found to be activated during sexual arousal and is related to the perception of the visual stimuli as sexual in nature (Stoleru et al., 1999). Brodmann's area 37 is the caudal portion of the middle and inferior temporal

gyri, which lie inferior to the parietal lobe (Figure 2.2). The left posterior inferior temporal area BA 37 functions to process letters and words (Buchel et al., 1998).

The fusiform gyrus is strongly activated when viewing images of human faces (Hasson et al., 2004, Haxby et al., 2001). The posterior lateral fusiform gyrus, known as the fusiform face area, is a visual area that becomes activated when viewing faces (Narumoto et al., 2001). The inferior temporal gyrus BA 20 is the last processing step for the ventral visual system to object feature analysis (Figure 2.2) (Mega et al., 1997).

The insular cortex lies deep within the lateral fissure and is located between the temporal lobe and parietal lobe. It has been suggested to be a gateway between the somatosensory areas and the limbic system and has been included as a component of the limbic integration cortex (Augustine, 1996). The insula plays a role in the appreciation of emotional aspects of pain, negative emotions, the processing of tastes, the memory of procedures, and the control of motor responses as well as interpersonal behaviour (Wicker et al., 2003, Wright et al., 2004). It is also a part of the articulatory loop, which is important in processing verbal material (Paulesu et al., 1993) and is activated during inner-speech generation (Shergill et al., 2000). The insular cortex is divided into two parts: the larger anterior insula and the smaller posterior insula. The anterior insula BA 43 is activated during sexual arousal in men (Stoleru et al., 1999). The posterior insula has been identified as the cardiac control cortex (Oppenheimer, 1993). The temporal pole, the orbital prefrontal cortex, and the insula are recognized as components of the paralimbic cortex (Flynn, 1999).

Occipital lobe

The occipital lobes (OL) form the posterior pole of the cerebral hemispheres, lying posterior to the parieto-occipital sulcus and the pre-occipital notch laterally (Figure 2.2). One of the main functions associated with the OL is simple and complex visual analysis (Sereno et al., 1995, Zeki and Moutoussis, 1997). The OL is divided into several functional visual areas. The first functional area is the primary visual cortex BA 17, which occupies a large portion of the medial aspect of the occipital lobe (Figure 2.2). Brodmann's areas 17 contains a low-level description of the local orientation, spatial-frequency and color properties (Kolb and Whishaw, 2003). Brodmann's areas 18 and 19 are the secondary and tertiary visual areas where visual processing occurs (Clark et al., 2005, Stuart, 1993, Tamraz and Comair, 2006). These areas are involved in the translation and interpretations of visual impressions transmitted from area 17 (Zeki and Moutoussis, 1997). Face recognition and identification of objects occurs here as well (Grill-Spector et al., 1998).

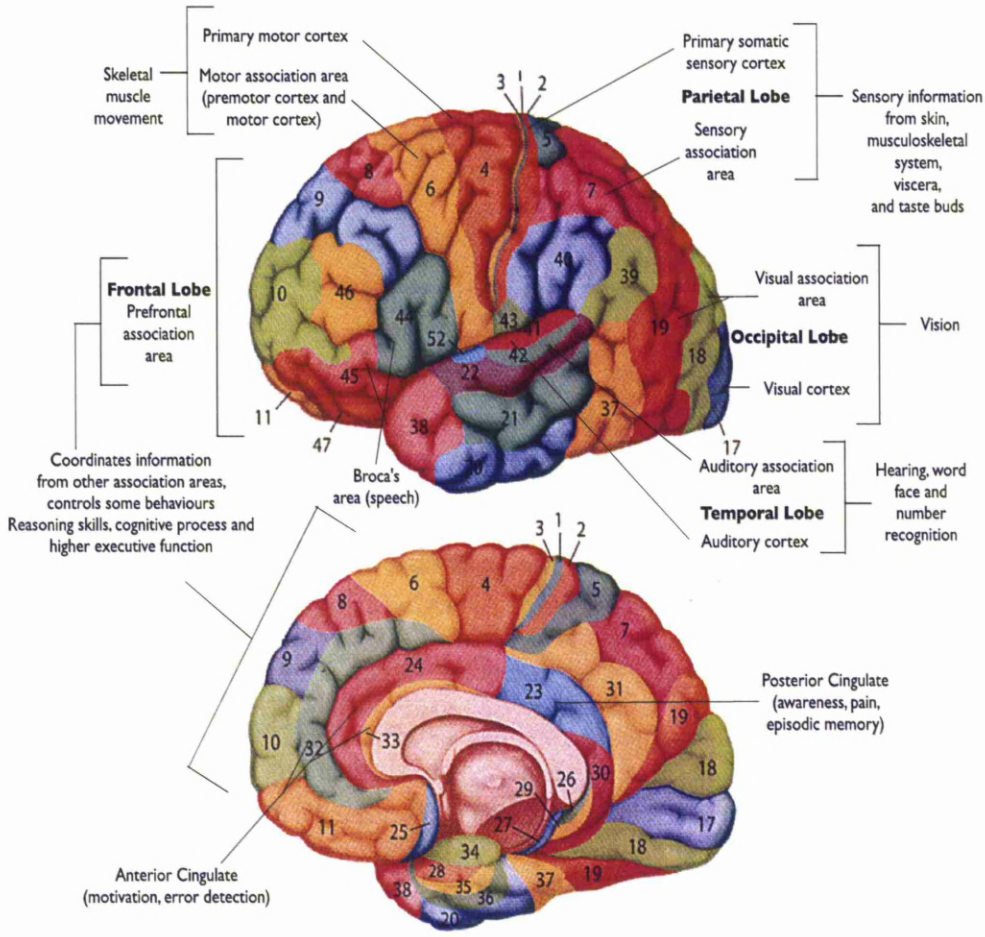

Figure 2.2: Lobes, functions and Brodmann's map of the brain cortex.

2.3 Blood supply to the brain

The brain gets blood from pairs of the common carotid and vertebral arteries. Carotid arteries and their branches supply the anterior portion of the brain; while the vertebrobasilar systems supply the posterior portion of the brain (Figure 2.4). The internal carotid artery passes up in the neck without any branches to the base of the skull where it enters the carotid canal of the Petrous bone. It runs through the

cavernous sinus (the carotid siphon), and then it continues upward to the surface of the brain. It bifurcates into the anterior cerebral artery and the larger middle cerebral artery.

The vertebral arteries join between medulla and pons to form the basilar artery. It has a number of branches supplying the cerebellum, brain stem and occipital lobe. The internal carotid and vertebrobasilar systems are joined by the posterior communicating arteries, which form the Circle of Willis (Figure 2.4). Large cerebral arteries arising from the circle of Willis branch out into smaller pial arteries and arterioles. Pial arteries give rise to penetrating arteries and arterioles that enter into the substance of the brain. Arterioles become gradually smaller, lose the smooth muscle cell layer, and become cerebral capillaries. The density of brain capillaries is regionally heterogeneous and varies according to regional metabolic demands (Ward and Lamanna, 2004). Brain endothelial cells are unique in that they are not fenestrated and are sealed by tight junctions. Endothelial cells take part in an important role in the regulation of vascular tone by releasing vasoactive factors, such as nitric oxide (NO), free radicals, prostacyclin, endothelium-derived hyperpolarizing factor, and endothelin (Faraci and Heistad, 1998).

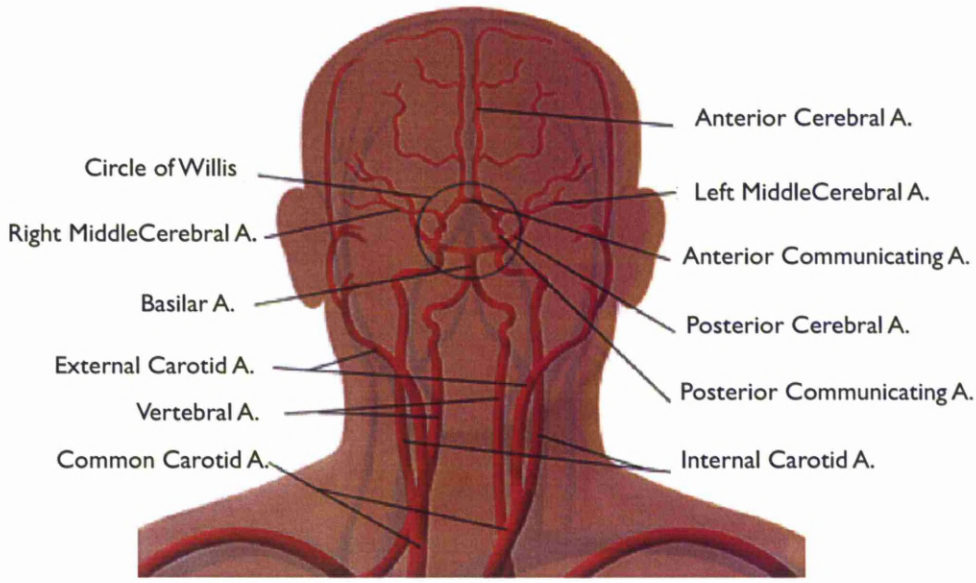

Figure 2.3: Illustration of the arterial circulation of the brain.

2.3.1 Blood flow and metabolism

Generally, the cellular biochemical processes that transmit neural information through action potentials and neurotransmitters require energy in the form of adenosine triphosphate (ATP). This energy is produced by chemical processes requiring glucose and oxygen (Gjedde et al., 2002). Thus, cerebral metabolism depends on a constant supply of both glucose and oxygen. The oxygen required by this metabolism is continuously supplied via the cerebral blood flow (CBF). When the oxygen molecule binds to the haemoglobin it is called oxyhaemoglobin, and when the oxygen is released from the haemoglobin to the neural tissue it is called deoxyhaemoglobin (Clare, 1997, Jezzard et al., 2001). The basic process of brain activation can be simply viewed as: stimuli evoke increased activity in neuronal

cells, ATP consumption increases, oxidative metabolism increases to restore ATP, and CBF increases to supply nutrients and carry away metabolic products (Buxton, 2010). However, the mechanisms involved are complex, and this simplistic picture is no longer thought to be accurate (Attwell and Iadecola, 2002). Some of these contemporary models are described in chapter 3.

2.4 Aging Brain

2.4.1 Cortical and Neuronal Changes

Neuroimaging has helped to advance our understanding of the aging process. As we age, notable changes occur in cellular metabolism (Simic et al., 1997), brain cortex (Chen et al., 2007, Courchesne et al., 2000, Cowell et al., 1994, Good et al., 2001b, Gur et al., 1991, Pfefferbaum et al., 1994, Raz et al., 2004, Resnick et al., 2003, Sowell et al., 2003, Sullivan et al., 2004, Tisserand et al., 2004, Van Laere and Dierckx, 2001) and cerebrovascular function (Leenders et al., 1990, Parkes et al., 2004). Degeneration of the cortical tissue is generally considered to be a part of the normal aging process and has been documented in all of the major lobes of the brain (Cowell et al., 1994, Raz et al., 2004, Tisserand et al., 2002). Many structural studies of the aging brain agreed that age-related differences are largest in frontal or prefrontal areas (Coffey et al., 1992, Cowell et al., 1994, Good et al., 2001b, Raz et al., 2004, Tisserand et al., 2002). The rate of reduction throughout the cortex is not uniform, but rather region specific with regions such as the PFC being very vulnerable to age-related changes (Raz et al., 2004, Sowell et al., 2003).

Grey Matter Changes:

Many volumetric imaging studies examined the effects of aging on brain tissue found notable grey matter volume changes with age (Courchesne et al., 2000, Cowell et al., 1992, Cowell et al., 2007, Cowell et al., 1994, Leonard et al., 2008, Pfefferbaum et al., 1994, Raz et al., 2004, Resnick et al., 2003, Sowell et al., 2007, Sowell et al., 2003, Sowell et al., 1999). Sowell et al. (2003) used MRI and cortical matching algorithms to map grey matter density in 176 healthy subjects (age from 7 to 87 years). They reported that cortical grey matter changes do not have the same general rate of decline throughout the cortex. The visual, auditory, and limbic regions show a general linear decline in grey matter density; while the frontal and parietal lobes show non-linear age effects on grey matter density. The posterior temporal cortices had a unique nonlinear rate of decline. It was characterized by gradual increase in grey matter density until the age of thirty, and remained stable until later years when a steep decline in grey matter density began to occur.

Raz et al. (2004) measured volumes of 13 regions of interest and cerebral hemispheres in 200 healthy subjects using MRI. They found that different segments of the brain cortex age faster than others. They stated that LPFC was the portion of the cortex that was most vulnerable to the effects of aging. The primary visual cortex, the anterior cingulate, and the inferior parietal cortices did not show any age-related differences. The hippocampus demonstrates a significant decline starting in the fifth decade of life. Another study done by Resnick et al. (2003) examined the effects of age and sex on the rates of change for regional brain volumes and ventricular volume in 92 subjects (age 59-85 years). Using images from 4 years follow-up, they revealed a significant longitudinal loss of grey matter volume in the frontal and parietal cortices, compared with temporal and occipital. Grey matter loss

was most pronounced for orbital and inferior frontal, cingulate, insular, and inferior parietal regions. Cowell et al. (1994) studied both age and sex effect in regional brain volumes in 130 subjects (age 18-80 years). They noted that the frontal and temporal lobes volume decrease with increasing age and males have greater age-related reduction than females.

White Matter Changes:

There is still disagreement regarding white matter volume decreases in ageing. Several studies have documented reduced global and regional white matter volumes with increasing age (Courchesne et al., 2000, Raz et al., 2004, Resnick et al., 2003, Sowell et al., 2003, Sullivan et al., 2004), especially in the frontal lobes (Raz et al., 1997, Salat et al., 1999). However, other imaging studies have not found evidence for global white matter volume decreases (Good et al., 2001b, Pfefferbaum et al., 2000, Raz et al., 1997, Taki et al., 2004).

It has been suggested that white matter volume shows a linear increase up to the early 20s followed by a flat period stretching into the 60s, and then a linear decline into the 70s and beyond (Courchesne et al., 2000, Pfefferbaum et al., 2000, Sullivan et al., 2004). These studies suggest that white matter volume loss accelerates in the eighth and ninth decades relative to the sixth and seventh. Sowell et al. (2003), however, found that white matter volume increased until about the age of 43 with a decline thereafter. Good et al., (Good et al., 2001b) noted trends for nonlinear age effects in global white matter volume, and regionally, cortical white matter loss was most prominent in frontal and occipital regions. Taki et al. (2004), on the other hand, found that white matter volume did not significantly correlate with age in each sex.

Cortical Thickness:

A typical interpretation of the brain cortical thinning is that degenerative processes including loss of myelinated axonal fibers (Nairn et al., 1989), shrinkage of large neurons (Terry et al., 1987), reduction in synaptic density (Morrison and Hof, 1997) and deafferentation (Bertoni-Freddari et al., 2002) causes a shrinkage of the cortical thickness. Comparable to the results of the grey matter from some volumetric studies (Raz et al., 2004, Sowell et al., 2003), age is associated with widespread thinning of the cerebral cortex (Fjell et al., 2009, Salat et al., 2004). Furthermore, similar to the results reported by some volumetric studies (Coffey et al., 1992, Cowell et al., 1994, Gur et al., 2000, Raz et al., 2004, Salat et al., 1999), cortical thickness of the frontal lobe specifically prefrontal cortex, and temporal lobe are reduced with age (Fjell et al., 2009, Salat et al., 2004, Thambisetty et al., 2010, Ziegler et al., 2010). Moreover, a relative thinning of the cerebral cortex in aging is usually associated with decreased cognitive function (Chee et al., 2009, Dickerson et al., 2008, Fjell et al., 2006).

Neuronal Changes:

As well as gross structural changes in brain volume, neuronal changes in the brain cortex have also been examined in aging. As noted earlier (Terry et al., 1987), neuronal shrinkage, rather than cell loss, accounts for the cortical volume loss observed during the normal aging process. The number of neurons in the adult brain has been shown to decrease or shrink with age and certain regions seem to be more exposed to loss than others (Uylings and de Brabander, 2002). Studies examining specific regions and different types of cells confirm that there is a significant loss of

neurons with age (Simic et al., 1997, West, 1993). The frontal cortex has been shown to be especially liable to neural degeneration (Uylings and de Brabander, 2002). Post-mortem studies of human brains have shown that a decrease in neurons corresponds to a decrease in overall cortical volume (Gur et al., 1991, Harding et al., 1998, Pakkenberg and Gundersen, 1997). Uylings and Barbander (2002) discussed whether changes in the number of cortical neurons, dendrites, and synaptic density were general or specific. The results indicated that the frontal cortex and portions of the hippocampal region are the most affected by neuronal aging. They concluded that the brain regions that are critical for learning and memory are those that have the greatest loss of neurons, dendrites, and reduction in synapse. In contrast, the visual cortex was relatively spared from neuronal degeneration. They suggested that the synapse is the portion of the neuron that is most easily affected by aging and so is likely to have the most significant impact on changes in cognition. When comparing neuronal changes in healthy subjects and those with Alzheimer's disease, Uylings and Barbander (2002) found that the association cortices are the areas most affected by both the normal aging process and Alzheimer's disease. However, the primary visual cortex and the somatosensory cortex appear essentially spared from this type of change.

Grachev et al. (2001) tested the hypothesis that brain chemical increases during normal development become reduced as part of the aging process. Their results indicated that chemical concentration was highest in the prefrontal cortex for both groups. However, compared with the younger adults, older subjects had a significant decrease in chemical concentration in the dorsolateral prefrontal, orbital frontal, and sensorimotor cortices. In contrast, brain regions such as the cingulate, insula, and thalamus showed no age related difference. Surprisingly, while there was

a marked loss of neurotransmitters in the PFC in the older subjects, the loss of neuronal volume in the PFC was relatively small. They suggested that the changes in chemical concentration might be connected with patterns of neural regression, such as a decrease in axons, dendrites, synaptic connections, neural death, and general neural atrophy.

2.4.2 Functional Changes

Functional neuroimaging studies have examined the effect of age during rest and during cognitive test performance. Studies of brain function using techniques such as positron emission tomography (PET) and functional magnetic resonance imaging (fMRI) have revealed consistent changes in the level and pattern of brain activity with age.

Some studies reported that older adults show lower levels of blood oxygenation level dependent (BOLD) activation, in a wide variety of tasks and brain regions, than younger adults (Logan et al., 2002, Madden et al., 1996). Two different interpretations have been proposed for this low BOLD activation (Logan et al., 2002). One is that aging is associated with an irreversible loss of neural resources. Another one is that resources are available but poorly recruited. Notably, however, greater frontal cortex BOLD activation has been revealed in many fMRI studies of aging, suggesting increased neural activity, (Cabeza et al., 2002, Langenecker et al., 2004, Milham et al., 2002, Zysset et al., 2007). Another common observation is that older adults show nonselective recruitment of brain regions. That is, older adults regularly show the recruitment of different brain areas in addition to those activated in the younger adults when performing the same task. This bilateral activation of

brain regions, has been classified into a model of neurocognitive aging referred to as Hemispheric Asymmetry Reduction in Older Adults (HAROLD) (Cabeza, 2002). This model suggests that, under similar condition, cortical activity tends to be less lateralized in older than younger adults. Cabeza (2002) suggested that these changes in cortical activation is not task specific but rather represents a general aging phenomenon. As the phenomenon became established, two contrasting views emerged which served to explain the mechanisms that drove HAROLD (compensation and dedifferentiation).

According to Cabeza (2001), the compensation mechanism looks at neurological changes in aging as a means to counter act cognitive deficits that often accompany aging. Examples of compensation would include increased bilateral activation and greater recruitment of the PFC for memory tasks as evident in the study Cabeza et al. (2000). The alternative view to compensation, dedifferentiation mechanism, looks at changes in neural activation as a sign of declining organization in the cortex. This view interpreters changes in activation as a reflection of older individuals difficulty in engaging and maintaining highly specialized neural pathways (Cabeza, 2002). An fMRI study done by Milham et al. (2002) investigated the changes in neural activation during the performance of the color-word Stroop task. Specifically, this involved looking at the neural components involved in attention control in younger and older subjects. The results found that older subjects had decrease responsiveness of those portions of the cortex, specifically the dorsolateral prefrontal and parietal cortices, which are associated with attentional control. The older subjects had more extensive activation in the ventral visual cortex and interior inferior PFC. The occurrence of additional neural activation in the older subjects combined with reduced attention ability lend support to the dedifferentiation

hypothesis. Milham et al. (2002) suggested that the lack of discrete activation in the cortex for the specific task resulted in reduced performance.

Cabeza (2002) discussed two contrasting views on the origin of changes in functional asymmetry, namely the psychogenic view and neurogenic view. The psychogenic view argues that changes in cortical activation result from older individuals engaging different cognitive strategies from their young counterparts, while the neurogenic view argues that the changes are a result of alterations in actual neural mechanisms (Cabeza, 2002).

HAROLD model is supported by functional neuroimaging evidence in a variety of cognitive tasks, including episodic memory retrieval (Cabeza et al., 1997, Madden et al., 1999), episodic encoding (Logan et al., 2002), working memory (Reuter-Lorenz et al., 2000), perception (Grady, 2000, Grady et al., 1994), and inhibitory control (Nielson et al., 2002).

One further observation is that the brain response in posterior regions has been found to be lower in older adults, whereas anterior regions show greater response than in younger individuals. This relative shift from posterior to anterior involvement has been termed the Posterior–Anterior Shift with Aging (PASA), which has been typically attributed to functional compensation (Dennis and Cabeza, 2008). PASA was first reported by Grady et al. (1994) in a PET study that investigated perception of faces and locations. In both conditions, older adults showed weaker activity than younger adults in occipitotemporal regions but greater activity in anterior regions, including the PFC. They suggested that older adults recruited anterior regions to compensate for sensory processing deficits in occipitotemporal regions.

Many PET and fMRI studies have found the PASA pattern across a variety of cognitive functions, including attention (Cabeza et al., 2004), visual perception (Huettel et al., 2001) visuospatial processing (Nyberg et al., 2003) working memory (Grossman et al., 2002) episodic memory encoding (Dennis et al., 2007) and episodic memory retrieval (Cabeza et al., 2004).

Previous PET and fMRI studies have found differences in frontal cortex activation between young and healthy older adults during a variety of cognitive functions. Such as, older adult showed stronger PFC activation during attentional tasks (Cabeza et al., 2004, Langenecker et al., 2004, Madden et al., 2002, Milham et al., 2002, Nielson et al., 2002). However, older adult showed weaker activity in the visual cortex but more activity in PFC (Grady, 2000, Grady et al., 1994, Huettel et al., 2001, Madden et al., 1997). In episodic memory encoding study, PFC activity was less asymmetric in older adult than in younger adult (Grady et al., 1995). During episodic memory retrieval, age-related decreases in activation were found in right PFC and right parietal regions, whereas age-related increases in activation were found in the left PFC, bilateral anterior cingulate and cuneus regions (Cabeza et al., 2004, Cabeza et al., 1997, Madden et al., 1999).

As well as looking at functional changes with age, a number of groups have considered changes in the baseline physiological properties of the brain, including CBF and cerebral metabolic rate of oxygen ($CMRO_2$). Conflicting results have been observed concerning baseline CBF and $CMRO_2$, as resting $CMRO_2$ may either remain constant (Goldstein and Reivich, 1991) or decline with age (Marchal et al., 1992, Yamaguchi et al., 1986). The observed age-related decreases in resting-state CBF, as measured with PET (Leenders et al., 1990), are consistent with the ASL

studies that have shown regionally dependent decreases in CBF with advancing age (Parkes et al., 2004).

One problem with previous fMRI studies of aging is that the magnitude of BOLD response varies across brain regions, subjects, and populations. This variability may be secondary to neural activity, and could reflect vasculature differences. Calibrated fMRI provides an opportunity to separate neural and vascular contributions to the BOLD signal, as described in Chapter 3.

Chapter 3: Functional Imaging of the Brain

3.1 Aim of Chapter

A detailed description of the nature of the MR signal and MR physics is beyond the scope of this thesis. Essentially, however, to provide essential background to help understand the basic methodological of the blood oxygenation level dependent (BOLD) response that is used in fMRI a brief basic review of MR physics is presented. Further reference can be obtained from MRI and fMRI physics texts (Buxton, 2002, Chavhan, 2007, Haacke et al., 1999, Jezzard et al., 2001, McRobbie et al., 2007, Westbrook et al., 2005).

3.2 Magnetic Resonance Imaging

3.2.1 Introduction

In 1938, Isidor Isaac Rabi documented the first observation of Nuclear Magnetic Resonance (NMR) during a molecular beam experiment (Rabi et al., 1938). Soon after that the property of (NMR) was first described by Felix Bloch and Edward Purcell in 1946 (Purcell et al., 1946, Bloch, 1946) who then were awarded the Nobel Prize in physics In 1952. Later in 1973, Lauterbur (1973) and Mansfield (1973) used the principles of NMR to establish Magnetic Resonance Imaging (MRI), for which they also received a Nobel Prize in 2003. The basis of the current MRI techniques didn't appear until 1975 when Richard Ernst proposed MR imaging using phase and frequency encoding and used the Fourier Transform for image processing. A new imaging technique, functional magnetic resonance imaging (fMRI), came about in 1990 (Kwong et al., 1992, Ogawa and Lee, 1990). This technique allows the

mapping of the function of different regions of the brain. Today MRI technology is continually improving and is used in basic science and clinical research as well as medical practice.

There are many diffusion MRI techniques, each of which are sensitive to a different property of the tissue. For example, diffusion imaging is sensitive to the microscopic diffusion of water; fMRI or blood oxygenation level dependent (BOLD) imaging is sensitive to changes in deoxyhaemoglobin concentration. They are all based on the same fundamental principles of NMR and make use of similar equipment.

3.2.2 The physical basis for MRI

The atom consists of a nucleus spinning about it own axis, electrons orbiting the nucleus and spinning on their axis. The nucleus of an atom consists of two particles: protons that have a positive charge and neutrons that have no net charge. Because the nucleus is positively charged and is spinning, it develops magnetic properties and behaves like a bar magnet (Chavhan, 2007, Haacke et al., 1999). It has a magnetic moment which means it will interact with an external magnetic field. The magnetic moment is a vector quantity having both magnitude and direction. All nuclei with an odd number of protons are magnetically active such as 1H, 13C, 19F, 31P, and 23Na (Chavhan, 2007, Haacke et al., 1999). In this thesis (and the vast majority of MRI), we only consider the MR signal arising from the hydrogen (1H) nuclei in water, which contains a single proton. Because of the spin characteristics of the hydrogen proton, if it is placed in the bore of the external magnetic field, the magnetic moment of the proton will align either parallel or anti-parallel with the direction of the magnetic field (B_0) (Chavhan, 2007, Haacke et al., 1999). In addition

to aligning with B_0, the magnetic moment of the proton will precess at some frequency around the direction of the external field (Figure 3.1) (Sands and Levitin, 2004).

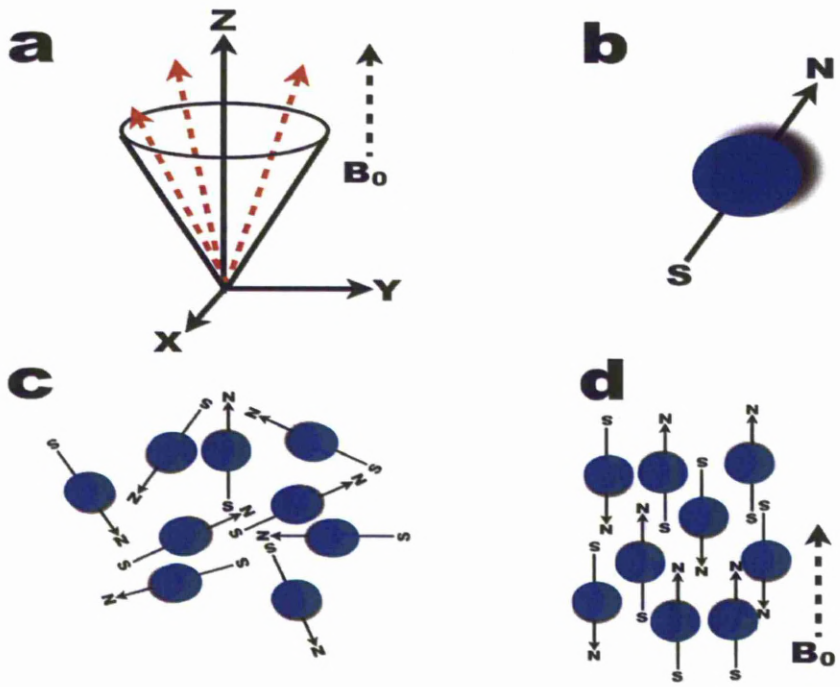

Figure 3.1: Precession of the protons and their alignments in the magnetic field. a) Precession of protons (hydrogen atom), b) Spinning proton, c) Spinning proton with no magnetic field present, d) Spinning proton if external magnetic field applied.

The precession frequency of the proton depends on the strength of the surrounding magnetic field. In particular, the precession frequency ω is directly proportional to the strength of the external magnetic field (B_0) and is defined by the Larmor Equation:

$$\omega_0 = \gamma B_0 \qquad \textbf{Equation 3.1}$$

Where w_0 is known as the precessional, Larmor or resonance frequency. The symbol γ refers to the gyromagnetic ratio, which is a constant unique to every atom. For hydrogen protons, $\gamma = 42.56$ MHz per Tesla. Therefore the precessional frequency of the hydrogen proton at 3 Tesla is $\omega_0 = 128$ MHz. Increasing magnetic fields will increase the precessional frequency (Chavhan, 2007, Haacke et al., 1999).

When placing many protons in a magnetic field, these randomly moving protons align antiparallel and a slight majority aligns parallel (Sands and Levitin, 2004). The parallel orientation has a slightly lower energy state. An increase in the strength of the magnetic field will increase the proportion of protons in the parallel direction. It is this excess of protons in the lower energy state that are accessible to us in an MRI experiment. Using an MRI system with a stronger magnetic field will allow us to gain access to more protons, so increasing the signal in our measurements (Chavhan, 2007, Haacke et al., 1999).

The magnetisation of the protons in the antiparallel direction will cancel an equal amount of magnetisation from protons in the parallel direction. The remaining magnetisation will be parallel to the direction of (B_0). This is the net magnetization vector (NMV) (Chavhan, 2007). The NMV is composed of two components of magnetization; one the magnitude of the magnetization in the direction of B_0 is referred to as the longitudinal magnetization, and the other one in the magnetization orthogonal to B_0 is known as the transverse magnetization (Haacke et al., 1999).

In an NMR experiment, a person is placed in a uniform magnetic field and an oscillating radio frequency (RF) pulse is applied into the tissue. This pulse excites nuclei away from their resting state into higher energy state. At its resonant frequency, a nucleus can absorb electromagnetic energy from the RF pulse that can affect the direction of its magnetization. As a result, if the RF pulse is applied at the

resonant frequency of the sample and in a plane orthogonal to B_0, the net magnetization of the sample will tip toward a direction orthogonal to B_0. Eventually, the magnetization recovers back to align with the direction of B_0 with a time constant T_1 (Chavhan, 2007, Westbrook et al., 2005). Throughout the recovery period, the molecules continue to rotate around the axis of the external magnetic field. Two processes with time constant T_1 and T_2 describe the relaxation back to the low energy state. The T_1 constant (longitudinal relaxation) (Figure 3.2) measures the relaxation in the direction of the B_0 magnetic field. T_1 depends upon tissue composition, structure and surrounding. T_1 relaxation is fastest when the motion of the nucleus matches that of the Larmor frequency. As a result, T_1 relaxation is dependent on the main magnetic field strength that specifies the Larmor frequency. Higher magnetic fields are associated with longer T_1 times. The T_2 (Spin – spin or spin dephasing) constant (Figure 3.2) measures the transverse relaxation of the dipole that is perpendicular to the B_0 field. When the NMV is precessing in the transverse plane it induces a signal in the receiving coil. This signal is called free induction decay (FID) signal (Chavhan, 2007, Westbrook et al., 2005). The signal decays because the protons experience slightly different magnetic fields and so begin to precess at slightly different frequencies. Thus, they move out of phase with each other and the NMV decays. The decay is exponential and is described by the time constant T_2^* (T two star) (Haacke et al., 1999).

T_2^* relaxation is the loss of transverse signal due to the dephasing of individual spins, and combines the effect of T_2 dephasing with that due to inhomogeneities in the external magnetic field (Logothetis and Wandell, 2004).. It is characterized by loss of transverse magnetization at a rate greater than T_2. In the brain, these inhomogeneities increase in the presence of deoxygenated blood, causing

faster signal decay and shorter T_2* (Logothetis and Wandell, 2004). Hence, the BOLD signal is optimised in a measurement sequence such as gradient echo-echo planar imaging (GE-EPI) which is sensitive to T2* mechanisms.

In summary, the NMR signal is a result of applying an RF pulse to tilt the sample magnetization to an angle (flip angle, angle between NMV and B_0) to the main magnetic field B_0. This causes all of the protons to precess in phase producing a NMV that precesses in the transverse plane. This induces a current in a nearby coil. The resultant signal is a function in time of the longitudinal relaxation time constant T_1 and the transverse decay constant T_2.

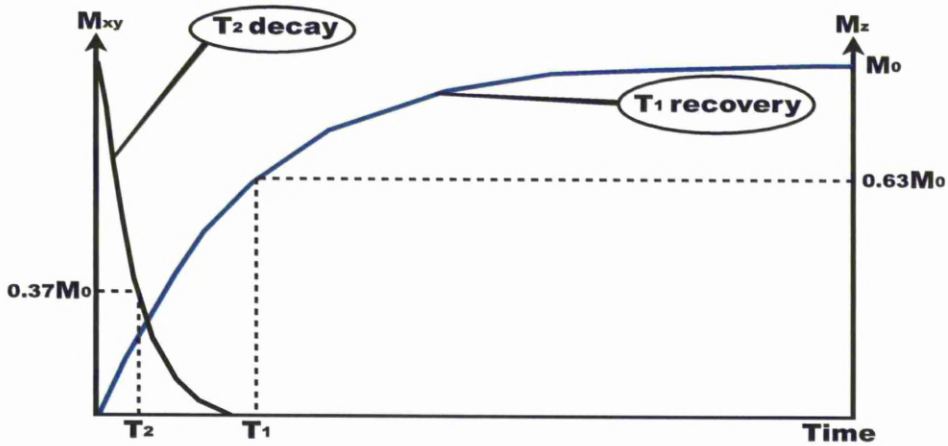

Figure 3.2: T1 relaxation time is the time constant required for 63% of NMV to recover. T2 relaxation is decay process of transverse magnetization, T2 is the time taken by transverse magnetization to reduce to 37% of its original value.

3.3 Arterial Spin Labeling Signal (ASL)

There are two techniques for measuring absolute quantification of blood flow using MRI: Arterial Spin Labeling (ASL) and dynamic contrast-enhanced (DCE) bolus tracking (the injection of an exogenous endovascular tracer). ASL is a non-invasive and non-ionising MRI technique which has provided reproducible measurements of cerebral blood flow (CBF) directly (Petersen et al., 2006). ASL utilizes the magnetic properties of the blood itself to obtain image contrast by taking the difference of two sets of images. First, the arterial blood inflowing towards the slice of interest is magnetically tagged just below the slice of interest by applying inversion pulses. After a time TI, the tagged image is acquired when the labelled blood has reached the slice of interest. Then, a second image of same slice of interest is acquired again without tagging the inflowing arterial blood to create another image (called the control image). Finally, the difference between the control image and the tag image will produce a perfusion-weighted image. This image will reflect the amount of arterial blood delivered to each voxel within the slice within the transit time.

There are mainly two approaches to ASL perfusion imaging: Continuous ASL (CASL) and Pulsed ASL (PASL). The CASL technique utilizes continuous inversion of the arterial blood by applying continuous RF pulse, whereas PASL employs a single inversion pulse. Several versions of PASL exist, including EPISTAR (echo planar imaging and signal targeting with alternating radiofrequency) (Figure 3.3) and FAIR (flow-sensitive alternating inversion recovery) (Buxton, 2002, Deibler et al., 2008, Jezzard et al., 2001, Petersen et al., 2006). The PICORE (Proximal inversion with a control for off-resonance effects) technique was used in this study (Wong et al., 1997), which is a variation of the EPISTAR technique.

For both CASL and PASL, an important source of systematic error in the quantitation of perfusion is the delay between the application of the tag and the arrival of tagged blood into the imaging slice. This error known as 'transit time effect' (Wong et al., 1998). Several modifications of PASL have been used to eliminate this effect. One such modification is the quantitative imaging of perfusion using a single subtraction version II (QUIPPS II) technique. This technique was proposed by Wong and designed to control the duration of the arterial bolus width (Wong et al., 1998). The QUIPSS II modification to PASL is to add a series of saturation pulses, after the inversion pulse and before the imaging excitation pulse, which hits the same tagging band as the inversion pulse. The difference in the magnetization between tag and control images is proportional to perfusion. The QUIPSS II modification is used to remove transit delay sensitivity. The current research used Q2TIPS to quantify perfusion. Q2TIPS is known as (QUIPSII with thin-slice TI_1 periodic saturation). It is a variation on the QUIPSSII, which offers improved accuracy of CBF measurement (Luh et al., 1999). In Q2TIPS the saturation pulse, which is applied to the tagging region at time TI_1 in QUIPSSII, is replaced with a train of thin slice saturation pulses at the distal end of the tagging region.

As the ASL technique relies on biophysical models to quantify the physiologic parameters from measured MR signals, several fundamental assumptions have been used in these techniques to simplify the quantification procedures. Single-compartment models had been employed in ASL assuming an instant water exchange between blood and brain tissue and constant cerebral blood volume (CBV) in both steady and dynamic states (Buxton et al., 1998, Detre et al., 1992). Other studies have attempted to improve quantification of CBF by using a two-compartment model and assuming limited permeability (Parkes and Tofts, 2002,

Zhou et al., 2001). For this study, the perfusion-weighted images were converted into quantitative CBF maps using a single blood compartment model described by Parkes and Tofts (2002). This model assumes that the labelled water does not cross the capillary wall or leave the voxel during the inversion time. This model requires only one inversion time, and does not depend on arrival time or vessel wall permeability. Parkes and Tofts (2002) reported a high level of accuracy (<10% error) in CBF estimates in grey matter using this model, in comparison to a full two-compartment model.

The ASL method measures a physiological quantity, CBF, which is tightly linked to neural activity, and can be used to significantly enhance the interpretation of fMRI experiments. As compared to BOLD, ASL measures also have the potential for providing better localization of the sites of neural activity (Duong et al., 2001, Luh et al., 2000), due to the fact that ASL measures come from the capillary bed, whereas BOLD measures come from the veins. ASL measures CBF, and provides measurements of both the baseline value and the changes with activation value, whereas BOLD is a complex signal giving only a non-quantitative marker of changes in neural activity. ASL has the potential to better reflect neural activity as compared to BOLD. One ASL study suggest that the relation between CBF changes and neural activity may be more linear than the relation between BOLD and neural activity (Miller et al., 2001). Several studies have shown that ASL measures can exhibit decreased inter-subject and inter-session variability as compared to BOLD, possibly reflecting a more direct link between CBF and neural activity (Aguirre et al., 2002, Tjandra et al., 2005, Wang et al., 2003). However, ASL techniques have been limited in use for the reason that they have a low signal-to-noise (SNR); because the inflowing blood magnetization is typically only about 1 percent of the tissue,

therefore sensitivity to weak activations is better with BOLD imaging (Liu and Brown, 2007).

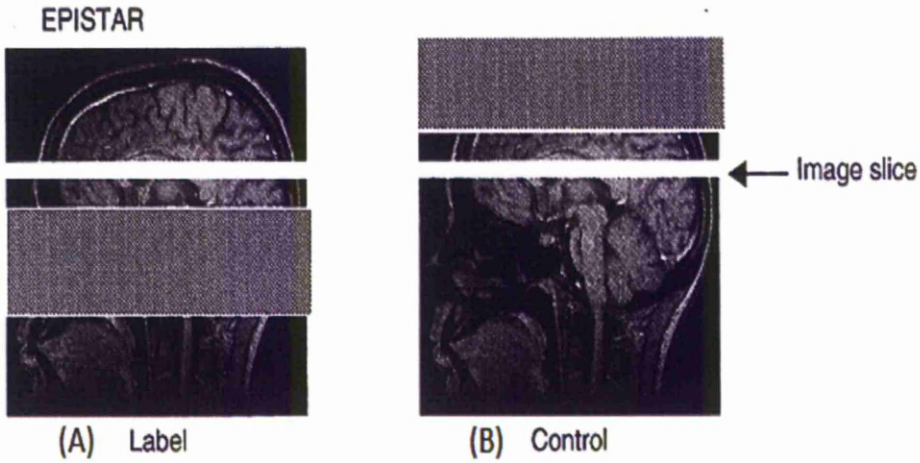

Figure 3.3: The tagging sequence produces a tagged image in (A), and the control pulse sequence generates a control image in (B) (modified from (Tofts, 2003)).

3.4 Functional MRI

3.2.1 Introduction

Functional MRI is based on the discovery of Dr. Seiji Ogawa in the early 1990's, that MRI can be used to obtain signals depending on the level of blood oxygenation (Ogawa et al., 1990a). They found that the MR signal around a blood vessel decreased when the oxygen content of the inspired air was reduced, and the effect was inverted when the oxygen was returned to normal values. This is because of the presence of deoxyhaemoglobin in a blood vessel that gives the blood vessel a different magnetic susceptibility to the surrounding tissue. Such susceptibility

differences cause dephasing of the MR proton signal (Thulborn et al., 1982), leading to a reduction in the value of T_2* and consequent reduction in the MR signal, by creating microscopic field gradients within and around those voxels containing the blood vessels (Ogawa and Lee, 1990, Ogawa et al., 1990b). While oxyhaemoglobin is diamagnetic and does not produce the same dephasing, changes in oxygenation of the blood can be observed as the signal changes in T_2* weighted images (Jezzard et al., 1994, Ogawa et al., 1990a, Turner et al., 1991). Regionally increased neuronal activity leads to increased local CBF, CBV and metabolic rate of oxygen consumption ($CMRO_2$). These all contribute to changes in local blood oxygenation and so alter the BOLD signal (T_2* weighted signal) (Kwong et al., 1992, Ogawa et al., 1993).

During neural activity it would be expected that while oxygen consumption is increased, the level of deoxyhaemoglobin in the blood would also increase, and the MR signal would decrease. However what is detected is an increase in MR signal, implying a decrease in deoxyhaemoglobin due to the decreases in oxygen extraction fraction (OEF) and a much larger increase in CBF, which bring with it more oxyhaemoglobin, and in turn leads to an increase of the MR signal (Kwong et al., 1992, Ogawa et al., 1992). These are all supported by a previous PET study (Fox et al., 1988) which showed that changes in CBF and CBV upon activation are not accompanied by any significant increase in tissue oxygen consumption. Moreover, Villringer et al. (1993), using near infrared spectroscopy (NIRS), reported an increase in oxyhaemoglobin, and a decrease deoxyhaemoglobin upon activation. The $CMRO_2$ is increased by only ~15% whereas the CBF is increased ~50% (Raichle et al., 2006). An increase in the total amount of haemoglobin is also observed, reflecting the increase in blood volume upon activation (Villringer et al., 1993).

Therefore the net effect during increased neural activity is a regional decrease in paramagnetic deoxyhaemoglobin and a consequent increase in BOLD signal.

The BOLD signal intensity change in hemoglobin oxygenation can be measured by a variety of pulse sequences using a fast GE sequence, such as EPI (Stippich et al., 2002). EPI is an imaging sequence that allows the collection of a complete two-dimensional image, following a single excitation pulse. GE sequences usually achieve higher BOLD-signals predominantly from venous origin; whereas spin echo (SE) sequences measure lower BOLD-signals predominantly arising from the capillary bed in brain parenchyma (Hulvershorn et al., 2005b, Hulvershorn et al., 2005a).

3.4.2 Neural correlates of BOLD

fMRI relies on the BOLD signal which is the result of a complex relationship between changes in CBF, CBV, and $CMRO_2$ accompanying neural activity (Kwong et al., 1992, Ogawa et al., 1993). In brief, the basic idea of brain activation when stimuli evoke increased activity in neuronal cells, adenosine triphospate (ATP) consumption increases, oxidative metabolism increases to restore ATP, and CBF increases to supply nutrients and carry away metabolic products. However, the mechanisms involved are very complex. Many studies have identified a coupling between blood flow and metabolic rate; specifically, the blood supply is tightly regulated in space and time to provide the nutrients for brain metabolism. Present data indicate that local field potentials (LFP's, an index of integrated electrical activity), form a better coupling with blood flow than the action potentials that are most directly associated with neural communication (Logothetis et al., 2001). A

recent review by Iadecola (2004) summarizes the role of activity-induced signalling mechanisms that not only involve neurons but also astrocytes and vascular cells. One view originated by Roy and Sherrington (1890) stated that functional activity increased blood flow, which is controlled directly by energy demand. This relationship between local neural activity and subsequent changes in CBF is known as neurovascular coupling (*n*). Regional blood flow is sensitive to variations in the concentrations of ionic and molecular metabolic vasoactive factors (Roy and Sherrington, 1890). Attwell and Iadecola (2002) suggested that a glutamate induced Calcium ($Ca2^{+}$) influx in postsynaptic neurons activates the production of vasoactive factors. These vasoactive factors, such as potassium (K^{+}), nitric oxide (NO), ATP, carbon dioxide (CO_2) and arachidonic acid metabolites, may directly or indirectly alter blood flow by either dilation or constriction of the blood vessels (Attwell and Iadecola, 2002). An alternative view suggested that local blood flow is controlled directly by neuronal signalling via neurotransmitters (Attwell and Iadecola, 2002). This mechanism suggests that astrocytes play a role in detecting synaptic activity and modulating blood flow (Harder et al., 1998, Iadecola and Nedergaard, 2007, Koehler et al., 2009). A number of chemical processes within the astrocyte link the rate of glutamate cycling to the production of vasoactive chemical factors (Raichle and Mintun, 2006).

Interpretation of BOLD measurements is greatly enhanced with the application of ASL techniques used to image the CBF response to neural activity. Taken together, the ASL and BOLD signals provide an added insight into the dynamics and composition of the hemodynamics response to neural activity.

3.4.3 The calibrated-BOLD method

Davis et al. (1998) introduced the calibrated-BOLD method which determines the $CMRO_2$ response as well as the CBF response with activation by combining the ASL and BOLD techniques. The combination of ASL and BOLD can provide much more information than either one alone, and it has become a primary tool for investigating the physiological mechanisms that underlie the BOLD response (Brown et al., 2007b, Chiarelli et al., 2007a, Davis et al., 1998, Hyder, 2004, Hyder et al., 2001, Leontiev and Buxton, 2007, Leontiev et al., 2007, Restom et al., 2008). Recently, a new approach to calibration using hyperoxia has been introduced which offers a number of possible benefits, including increased comfort for the participant, and no reliance on the noisy ASL signal for calibration (Chiarelli et al., 2007c).

3.4.3.1 Quantification of oxygen metabolism change

The BOLD technique is sensitive to changes in blood oxygenation, which depends on the changes in CBF, CBV, and $CMRO_2$. The BOLD signal change correlates strongly with changes in CBF, but it does not provide a direct quantitative measurement of CBF (Detre and Wang, 2002). The BOLD response associated with brain activation depends on three physiological factors: (1) the CBF response (the CBF during activation normalized to the CBF in the baseline state); (2) the fractional change in $CMRO_2$; and (3) a local calibration factor M that depends on the amount of deoxyhaemoglobin present in the baseline state.

The parameter M was first described by Davis, et al. (1998). Because the parameter M may vary regionally, and also depends on the echo time used in gradient-echo or spin-echo fMRI experiments, the parameter M must be measured for each brain region for the particular experimental acquisition (Chiarelli et al.,

2007c, Leontiev et al., 2007). To measure M, the CO_2 inhalation (hypercapnia), breath holding or O_2 inhalation (hyperoxia) experiment can be performed.

The hypercapnia approach relies on the stimulated increase in CBF to generate a measurable change in BOLD signal. The hypercapnia method produces large potential inconsistency in the calculated calibration parameter M (Hoge et al., 1999a), due to the use of ASL imaging for CBF measurement, which is a low signal-to-noise ratio (SNR) technique (Chiarelli et al., 2007a, Chiarelli et al., 2007b). Breath holding has been used as a technique for causing short periods of mild hypercapnia (Kastrup et al., 1999b) and demonstrated the potential to reduce inconsistency in fMRI studies (Kastrup et al., 1999a, Thomason et al., 2007). The hyperoxia calibration method involves inhalation of pure oxygen air as an isometabolic stimulus (Chiarelli et al., 2007b). Hyperoxia generates an increase in BOLD response by the reduction in deoxyhaemoglobin resulting from the saturation of venous blood with oxygen (Chiarelli et al., 2007b). Chiarelli et al. (2007b) demonstrated that variability in M has a large impact on the measured $CMRO_2$–CBF coupling constant from a neural activation task, as well as an impact on the linearity of the relationship between these two variables. Importantly, parameter M keeps the same meaning in the hyperoxia as for the hypercapnia-calibrated approach. Therefore, calibration can be performed using hyperoxia, which was used in the current work, to obtain M. M can be estimated using the Chiarelli et al. model (2007c), as given in Equation 3.2.

$$\frac{\Delta BOLD_{HO}}{BOLD_0} = M\left[1-\left(\frac{CBF_{HO}}{CBF_0}\right)^{\alpha}\left(\frac{[dHb]_{HO}}{[dHb]_0}+\frac{CBF_0}{CBF_{HO}}-1\right)^{\beta}\right] \qquad \textbf{Equation 3.2}$$

Where $\Delta BOLD_{HO}$ is the change in the BOLD signal during hyperoxia, CBF_{HO} is the CBF during hyperoxia, and $[dHb]_{HO}$ is the concentration of deoxygenated haemoglobin in the venous vasculature during hyperoxia. The subscript 0 refers to these parameters at baseline.

With determination of M it is possible then to calculate $CMRO_2$ changes with a functional paradigm. Under the assumption that $CMRO_2$ does not change during the calibration procedure, a theoretical model developed by Hoge et al. (1999b) describing how deoxyhaemoglobin affects the BOLD signal, has led to a relatively simple expression describing the change in BOLD signal in relation to the change in CBF and $CMRO_2$ and stating that the fractional BOLD signal change ($\Delta BOLD/BOLD_0$) can be modelled as a function of the relative changes in CBF and $CMRO_2$ according to Equation 3.3.

$$\frac{\Delta BOLD}{BOLD_0} = M\left(1 - \frac{CBF}{CBF_0}^{\alpha-\beta} \frac{CMRO_2}{CMRO_{20}}^{\beta}\right)$$

Equation 3.3

Where $\Delta BOLD$ refers to the change in BOLD signal during activation and CBF and $CMRO_2$ are the values for these parameters during activation. The subscript 0 denotes the baseline values. In steady-state, the parameter α is the Grubb constant (assumed to be 0.38, accounting for an assumed fixed relationship between changes in CBV and CBF (Grubb et al., 1974). β describes the oxygenation and field strength dependence of the BOLD effect and was assumed to be 1.5 (Boxerman et al., 1995, Davis et al., 1998). The parameters α and β are assumed to be global properties with the same values in each subject (Brown et al., 2007a). The parameter

M is the calibration constant, which corresponds to the maximum BOLD change for complete removal of deoxyhaemoglobin in the voxel.

In conclusion, imaging sequences based on BOLD contrast are currently the predominant method for fMRI of the brain (Liu and Brown, 2007). The use of simultaneous measurements of CBF and BOLD responses to a stimulus (i.e. hyperoxia) can provide information that is then used to calibrate the BOLD response and estimate functional changes in $CMRO_2$ (Davis et al., 1998). Simultaneous measures of CBF and BOLD with ASL are also important for understanding the mechanisms underlying the BOLD response (Obata et al., 2004). Chapter 5 in this thesis describes the first use of hyperoxia-calibrated fMRI in aging during a cognitively demanding Stroop task.

CHPTER 4: Subjects and Methods

4.1 Aim of Chapter

This chapter presents the general design of the study. Demographic data of the participants are presented, together with procedures employed for data acquisition (both MRI and fMRI). Neuropsychological assessment tests are described. Detailed description of image analysis methods and statistical analyses are presented within each chapter of the results (fMRI in chapter 5, Voxel Based Morphometry in chapter 6 and FreeSurfer in chapter 7).

4.2 Participants

Fifty-five healthy, right-handed volunteers (twenty-six male, twenty-nine female, mean age 41 years, SD 16 years, age range 18-71 years) were recruited from the Liverpool University as well as the Liverpool metropolitan area via advertisements specifically for this study posted locally. This study was approved by the University of Liverpool research ethics committee. All subjects were right handed and had English as a first language. Years of education were recorded, as most of the participants were university's student or staff members.

At the screening visit, following informed consent, all participants underwent a standard screening. Subjects were excluded based on the following criteria: evidence of significant medical disease (e.g., cancer, cardiovascular disease, diabetes, lung or kidney disease), neurologic disease (e.g., epilepsy, significant head trauma), psychiatric illness (e.g., depression, substance abuse); evidence of cognitive impairment by clinical evaluation; colour blindness or contraindication to MRI. A

brief cognitive assessment test (O'Sullivan et al., 2005) was administered to further screen out subjects with any cognitive deficits. Tests comprised: digit symbol, verbal fluency, trail-making (B-A) and digit span backwards from which a composite score was calculated. Subjects performing below 0.57 on the composite score (see table 2 of (O'Sullivan et al., 2005)) were excluded.

4.3 Neuropsychological assessment

Series of executive tasks to assess frontal lobe functions were administered (O'Sullivan et al., 2005). The battery of tests included: the trail making test, verbal fluency, digit span, and the digit symbol substitution task. The trail making and digit symbol tests are timed executive tasks, so that these tests are sensitive to executive function and the speed of mental processing (O'Sullivan et al., 2005). Normal aging is known to lead to a reduction of the cortical volume of the frontal lobes (Raz et al., 2004, Tisserand et al., 2002). This regional loss is taken to support the view that 'executive' or 'frontal' abilities decline relatively more with increasing age than other cognitive functions (O'Sullivan et al., 2005, Rabbitt, 2005, West, 1996).

In brief, the trail making test had two parts (A and B). In part A the subject was asked to draw a line to join numbered points scattered randomly over a sheet of paper in numerical order. In part B, the test sheet contains points marked by both numbers (1-26) and letters (A-Z). The subject was asked to join the points with a line, alternating between numerical and alphabetical order (i.e., in the sequence 1,A,2,B,3,C….). The timing was recorded by a stopwatch by the experimenter. Part B of the trail making test differs from part A in having an executive component, however, also shares similar non-executive aspects (visualizing of the paper and

motor function in joining between numeric and alphabetic) (O'Sullivan et al., 2005). Part B of the trail making test requires shifting between different mental rules, which is described as cognitive set shifting, and is an aspect of executive function (Lezak, 1995). Subtracting the time for part A from that for part B corrects for differences some of the non-executive aspects, so that this B-A score is considered more specific for executive performance (Lezak, 1995).

In the verbal fluency test, subjects are generally given 60 seconds to retrieve as many words as they can beginning with specific letters (F, A, and S). The subjects was asked to say as many words as they can think of that begin with the given letter of the alphabet, excluding country names, numbers, same word with different suffix and avoid repetitions. After the experimenter explained the task, asked the subject to begin and start timing on the stopwatch. The score is the sum of all acceptable words produced in the three one-minute trails (Lezak, 1995). Successful performance of the verbal fluency test involves the formation of appropriate strategies for word retrieval, this test is "best" neuropsychological measure of executive function (Salthouse et al., 2003).

The digit span test included both forwards and backwards conditions where a subject was given a number sequence and was asked either to repeat it (forward), or to repeat it in backward order. Presentation begins with tree digits for the forward condition and two digits backward condition. The test is usually discontinued after two failures at the same level. The score for both longest correct span and the longest span of correct but out-of- sequence digits. Digit span forward measures are more closely related to the efficiency of attention, whereas, the digit span backwards condition is heavily dependent on working memory and therefore provides a measure of working memory performance (Lezak, 1995).

In the digit symbol task, each digit (1–9) was assigned to a unique symbol that is presented in the form of a key. In this test, the subject was presented with a series of digits and was asked to fill in the matching symbols in a space below. Subjects were given 90 seconds to complete as many substitutions of symbols as possible according to symbols provided on the top of the sheet. The score is the number of squares filled in correctly (Lezak, 1995). The digit symbol task is a measure that reflects both performance IQ and executive functioning (Wechsler, 1981). This test requires subjects to switch between rules for each digit and therefore requires mental flexibility and has parallels to other set shifting tasks (Lezak, 1995).

4.4 fMRI Image Acquisition

Imaging was carried out on a 3 Tesla whole-body Siemens Trio system (Siemens, Erlangen, Germany). An eight-channel radiofrequency (RF) head coil was used with foam padding to comfortably restrict head motion. For the functional ASL acquisitions, we recorded control and tagged images using a Proximal Inversion with a Control for off-Resonance Effects (PICORE) tagging scheme with the Quantitative Imaging of Perfusion using a Single Subtraction II with Thin-Slice TI_1 Periodic Saturation (QUIPSS II modification) (Wong et al., 1998) that enables simultaneous collection of BOLD signal and quantitative CBF data (Wong et al., 1998). The sequence parameters were: TR = 2.13 s, TE = 25 ms, tag-saturation time (TI_1) = 0.7 s, tag-saturation end-time (TI_{1stop}) = 1.3s, time between label and readout (TI_2) = 1.4 s, 10-cm tag width, a 10-mm tag-slice gap and crusher gradients with b=5 mms^{-1}. Control and label acquisitions were interleaved, such that the labelling was applied every two TR. We acquired a total of twelve slices of 3.5-mm thickness and 0.35

gap that covered the frontal, motor and parietal cortices (Figure 4.1). Prospective motion correction (PACE) (Thesen et al., 2000) was included in the pulse sequence. In order to avoid T_1 relaxation effects, we discarded two 'dummy' scans at the start of each functional run. To produce quantitative CBF maps we collected a calibration image at the end of each functional run, using the identical QUIPSS II sequence with labelling switched off and a TR of 10 s. In addition to these scans, 1mm isotropic structural 3D magnetization-prepared rapid gradient echo (MPRAGE) image was also collected (Mugler and Brookeman, 1990).

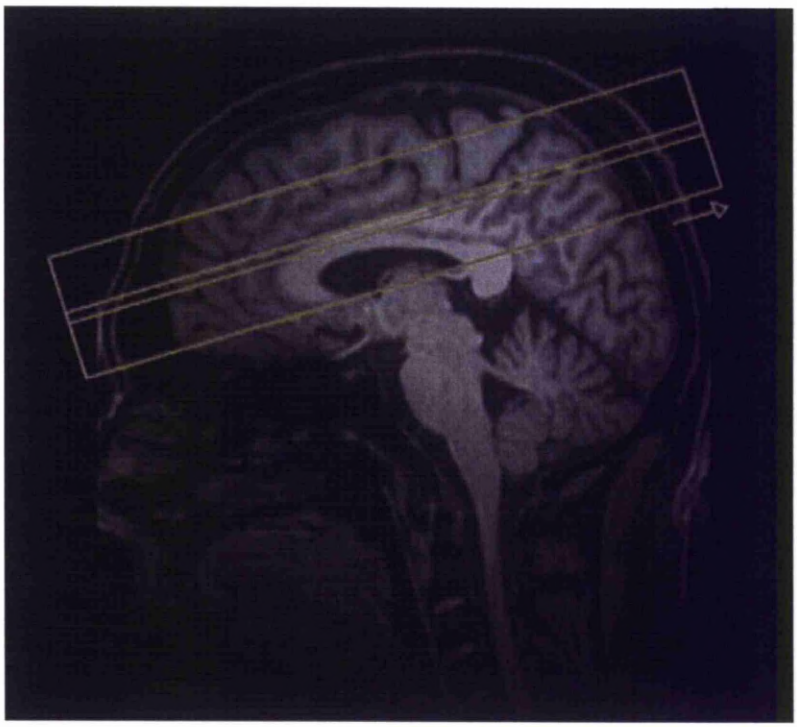

Figure 4.1: Slice coverage. Limited coverage of the ASL sequence restricted our acquisition to cover frontal, motor and parietal regions.

4.5 MRI Image Acquisition:

All subjects were scanned using a 3-Tesla Trio whole-body scanner (Siemens, Erlangen, Germany). An eight-channel radiofrequency (RF) head coil was used with foam padding to comfortably restrict head motion. Three-dimensional high resolution T_1-weighted structural MRI brain images were obtained using the optimized MPRAGE (Magnetization-Prepared Rapid Gradient-Echo imaging) sequences (Mugler and Brookeman, 1990). The imaging parameters were: repetition time TR = 2040 ms, echo time 5.57 ms, inversion time TI = 1100 ms, flip angle = 8°, bandwidth = 130 Hz/pixel, number of excitations = 1, a FOV of 256 mm with an acquisition matrix of 256 X 208 producing 176 contiguous sagittal slices with slice thickness of 1 mm. Acquired images were of voxel size 1.0 X 1.0 X 1.0 mm, the acquisition time was 4 minutes and 14 seconds using GRAPPA (Gene-Ralized Autocalibrating Partially Parallel Acquisition) parallel imaging techniques.

CHAPTER 5: Calibrated fMRI during a cognitive Stroop task.

5.1 Aim of Chapter

This chapter explores the primary focus of this thesis, which is the use of calibrated fMRI to determine the relative vascular and neuronal contributions to the age-related blood oxygenation level dependent (BOLD) changes in response to a Stroop task.

5.2 Introduction

Neuroimaging has helped to advance our understanding of the aging process, in particular the relationship between cognitive decline and physiological changes. As a person ages, notable changes occur in cellular metabolism (Simic et al., 1997), cortical density (Good et al., 2001b, Sowell et al., 2003, Tisserand et al., 2004, Van Laere and Dierckx, 2001) and cerebrovascular function (Leenders et al., 1990, Parkes et al., 2004). Structural studies of the aging brain indicate that the frontal lobe cortices experience a high degree of age-related atrophy (Coffey et al., 1992, Cowell et al., 1994, Good et al., 2001b). However, even with the susceptibility of the frontal cortex to aging, greater frontal cortex blood-oxygenation-level-dependent (BOLD) activation with increasing age, suggesting increased neural activity, has been revealed in many fMRI studies of aging (Cabeza et al., 2002, Langenecker et al., 2004, Milham et al., 2002, Zysset et al., 2007).

fMRI has been used widely to map brain activation in response to functional tasks and to measure brain changes with aging. fMRI relies on the detection of hemodynamic changes that accompany neural activity. As such, the BOLD signal is

an indirect measure of neural activity and may also reflect changes in the cerebrovascular system due to age (D'Esposito et al., 2003, Lu et al., 2010, Restom et al., 2007). Therefore, it is difficult to conclude if age-related differences in the BOLD signal develop from age-related neural plasticity or age-related cerebrovascular changes. We aimed to address this question through the use of calibrated fMRI during a cognitive Stroop task. Ances et al. (2009) used a similar approach to investigate the age-related decline in BOLD response in the visual cortex. Using calibrated fMRI they were able to quantify the component parts of the BOLD response, concluding that the reduced BOLD response in the visual cortex with ageing does not reflect lower neural activity, but rather differences in neurovascular properties.

Calibrated fMRI is a non-invasive approach that allows quantification of the component parts of the BOLD signal, namely changes in the cerebral metabolic rate of oxygen ($CMRO_2$) and cerebral blood flow (CBF) (Davis et al., 1998, Hoge et al., 1999b). A calibration constant, M, reflecting baseline vascular properties is also determined. Estimates of $\Delta CMRO_2$ may be particularly useful as it is reported to have a closer link with changes in neural activity than the BOLD signal (Davis et al., 1998, Hyder, 2004). Calibrated fMRI uses an arterial spin labelled (ASL) pulse sequence, which allows simultaneous measurements of the BOLD and CBF response. Addition of either a hypercapnic (Ances et al., 2009, Kastrup et al., 2002, Rostrup et al., 2000, Thomason et al., 2007) or hyperoxic (Chiarelli et al., 2007c, Goodwin et al., 2009) gas challenge allows additional quantification of the change in $CMRO_2$. In our study, hyperoxia calibration was chosen over hypercapnia, as it is more comfortable and better tolerated, important when studying an older population.

In addition, hyperoxia calibration does not rely on noisy ASL-derived CBF measurements, which are required for hypercapnic calibration.

In this study, a form of the Stroop task was used as the cognitive challenge, as it has been proven to be a powerful, simple task, which can examine age-related changes in the neural substrates of executive function (Banich et al., 2000, Bench et al., 1993, Pardo et al., 1990). The Stroop Colour Word Interference task has been a classic paradigm to study cognitive control (Derrfuss et al., 2004) and also to measure frontal lobe functions (MacLeod, 1991). It requires a focus of attention on the task relevant processes for a successful performance. The Stroop task is thought to be a useful tool for the investigation of executive aspects of attentional control, this is because reading a word is more practiced and more automatic skill than naming of colours, therefore attentional control is required to respond to the colour instead of to the word (MacLeod, 1991).

A number of studies have used the Stroop task and modified it to investigate aging processes (Langenecker et al., 2004, Milham et al., 2002, Zysset et al., 2007). Most fMRI studies of the Stroop task have found greater BOLD activation in anterior cingulate cortex, frontal cortex, and parietal cortex (Langenecker et al., 2004, Milham et al., 2002, Zysset et al., 2007) with increasing age. Langenecker et al. (2004) compared 13 younger and 13 older adults who completed a Stroop test during fMRI. They found that with increasing age, several regions showed greater activations, including the left inferior frontal gyrus. In another study, Milham et al. (2002) used fMRI to measures neural activity during performance of Stroop task to compare the neural substrates of attentional control in younger (21-27 years) and older participants (60-75 years). They reported activation differences between young and older adults mainly in frontal regions, but the differences occurred in both

congruent and incongruent conditions. Additionally, they found that younger adults had greater activation than older adults during Stroop interference in left middle frontal gyrus, anterior cingulate, and superior parietal lobule, while older adults had greater activation than young adults in bilateral inferior frontal gyri. Finally Zysset et al. (2007) investigated the effects of aging (22-75 years) on Stroop task performance and on the hemodynamic response. They reported that middle-aged adults showed increased activation in several task-related regions, mainly in the inferior frontal junction area bilaterally and the pre-supplementary motor area. Older adults seemed to use multiple frontal regions to a greater degree than young adults. These increased activations of multiple frontal regions in response to a cognitive Stroop task has been interpreted as increased neural activity (Langenecker et al., 2004, Milham et al., 2002, Zysset et al., 2007); compensatory activity in the older group to aid performance.

The Stroop task is easy when the colour and the word are congruent (the word ''red'' in red letters); but when the colour and the word are incongruent (the word ''blue'' in red letters), people experience interference (MacLeod, 1991). In our study, BOLD activation during an incongruent Stroop task was compared to rest (rather than a congruent task) in order to robustly activate large regions of the brain, allowing individual analysis and regional comparison of the calibrated fMRI measurements. A comparison of incongruent and congruent (or neutral) conditions would have been of additional interest, allowing the isolation of the inhibitory executive function. However, the differences in BOLD signal between these conditions (Zysset et al., 2007) are likely to be too small to provide reliable estimates of the change in oxygen metabolism (Goodwin et al., 2009). In addition, previous work (Zysset et al., 2007) shows an age-related increase in BOLD response to the

incongruous condition compared to rest, which is attributed to increased neural processing.

We measured ΔBOLD, ΔCBF, and estimated $\Delta CMRO_2$ and M in regions activated by the Stroop task and considered whether these parameters are affected by age. M can be considered as a 'baseline' parameter that is expected to be independent of cognitive task (Hyder, 2004), reflecting the general physiological state of the brain. We aimed to replicate previous findings of an age-related increased BOLD response in the frontal cortex and determined whether this is due primarily to alterations in the metabolic ($CMRO_2$) or the vascular (CBF) response to neural activity. Finally, we aimed to determine which of the parameters are most related to performance change with increasing age.

5.3 Methods

5.3.1 Stroop Task

An incongruent color-word Stroop task was used as a functional stimulus, similar to the one used in the studies by Zysset et al. (2007) and Goodwin et al. (2009). Participants had to decide (with a choice of two buttons using the right hand), if the meaning of the bottom word matched the print color of the top word (Figure 5.1). Subjects were instructed to respond as quickly and accurately as possible. Fifteen stimuli were presented in each block. Stimuli were self-paced but with a minimum of 2 seconds between each stimulus, during which a fixation cross was presented. Eight active blocks of approximately 30 seconds were interspersed with a 30 seconds fixation cross on a black screen. To become familiar with the task all

participants first practiced the task for 4 minutes outside of the scanner prior to scanning. For each participant we calculated mean response time and accuracy of responses recorded during the scanning session.

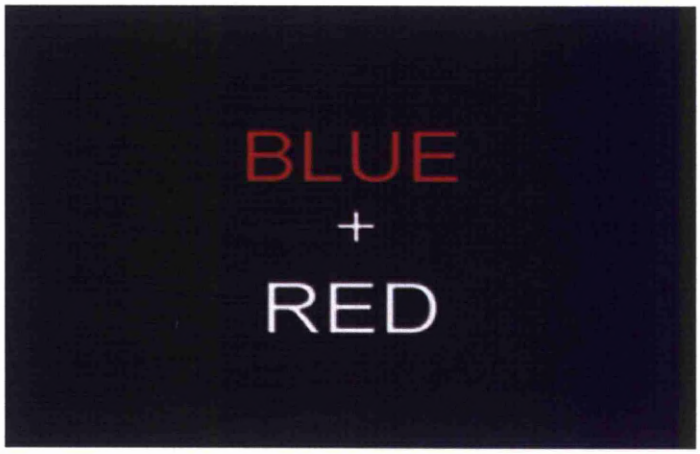

Figure 5.1: Stimulus Paradigm: The incongruent Stroop task.
Subjects had to decide if the meaning of the bottom word matched the color of the top word (red in this case).

5.3.2 Hyperoxia Calibration

Hyperoxia was induced by breathing 100% oxygen delivered through an open mask over the mouth and nose at a flow-rate of 15 L/min, following the same procedure as described in Goodwin et al. (2009). The protocol comprised 2 minutes of air, 3 minutes of oxygen, 3 minutes of air and 3 minutes of oxygen (Figure 5.2). Respiratory composition was continuously monitored using an oxygen analyser (Model S-3A) (AEI Technologies, Pittsburgh, PA, USA), which was calibrated prior to each scan against an oxygen depletion monitor (GasMonitor4) situated in the scanner room. Respiratory data logging was performed at intervals of 1 ms using Powerlab software (ADInstruments, Colorado Springs, USA). End-tidal values were

extracted from the data using code created in Matlab (The MathWorks Inc, Massachusetts, USA).

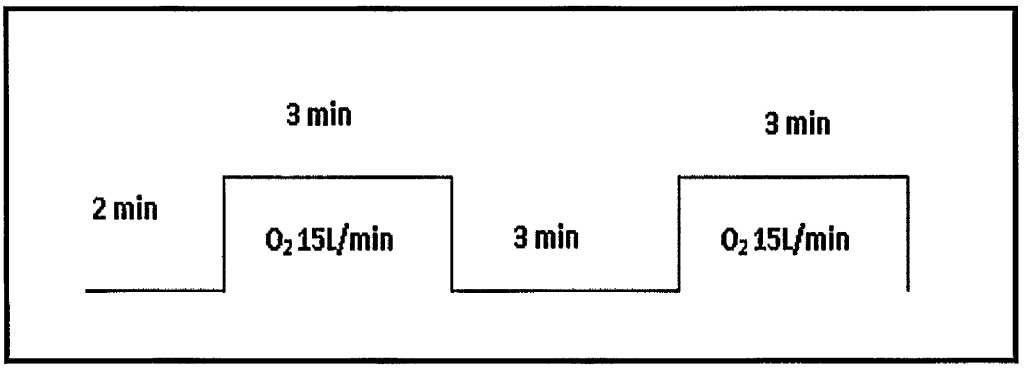

Figure 5.2: The hyperoxia paradigm.

5.3.3 Data analysis

Matlab software (The MathWorks Inc., Massachusetts, USA) was first used to process the ASL data for the Stroop and hyperoxia runs in order to extract BOLD and CBF time-courses. Label and control images were added to produce a time-course of BOLD images; or subtracted to produce a time-course of perfusion-weighted images. Perfusion-weighted images were converted into quantitative CBF maps using a single blood compartment model described by Parkes and Tofts (2002).

BOLD and CBF time-course data were analyzed using BrainVoyager QX software. Pre-processing included spatial full-width at half-maximum (FWHM 6 mm) and temporal (10 s FWHM) smoothing and linear trend removal. Temporal smoothing was applied to increase the signal to noise ratio in the exported time-courses, to allow more precise estimates of BOLD and CBF change. The BOLD and CBF images were then co-registered to the structural T_1-weighted image and

transformed into Talairach space. The regressor for the Stroop task was generated by convolving the timing of the Stroop blocks (using subject-specific onset and offset times for the whole block) with the haemodynamic response function as implemented in BrainVoyager. A group-wise analysis was then performed using both the BOLD and CBF time-courses from all individuals to determine regions where the model accounted for significant variance in the data at a threshold of $p<0.05$ (corrected for false-discovery rate (FDR)), i.e. regions that are responsive to the Stroop task.

The estimation of $\Delta CMRO_2$ requires precise measurements of BOLD and CBF signal change, and so is usually done on a regional rather than a voxel-wise basis (Leontiev et al., 2007) in order to increase the signal to noise ratio. Hence, when considering age-related effects we performed analysis on a regional basis, using signal time-courses from those regions defined as significantly active during the Stroop task in the group analysis (FDR $p<0.05$). These regions are then employed for the analyses of both the Stroop and the hyperoxia runs.

Within each region, a volume of $1cm^3$ was defined, composed of the voxels with the most significant activity (derived from a general linear model using both BOLD and CBF data as described above). BOLD and CBF signal time-courses were recorded for both the Stroop and hyperoxia runs, averaged over all the voxels within each region for each individual. For hyperoxia, the percentage change in the BOLD signal was found in each region by comparing the mean signal over the last minute of each hyperoxia period compared to 1 minute prior to hyperoxia. For the Stroop activation, the BOLD and CBF time-courses were averaged over the 8 activation blocks and the percentage change in BOLD and CBF between the maximum and minimum response was found.

Quantification of oxygen metabolism change

The analysis procedure to extract the calibration constant M and the change in $CMRO_2$ followed the same approach as in Goodwin et al. (2009), where a more detailed description can be found. In brief, the fractional BOLD signal change ($\Delta BOLD/BOLD_0$) can be modelled as a function of the relative changes in CBF and $CMRO_2$ according to Equation 5.1.

$$\frac{\Delta BOLD}{BOLD_0} = M\left(1 - \frac{CBF}{CBF_0}^{\alpha-\beta} \frac{CMRO_2}{CMRO_{20}}^{\beta}\right) \qquad \textbf{Equation 5.1}$$

Where ΔBOLD refers to the change in BOLD signal during activation and CBF and $CMRO_2$ are the values for these parameters during activation. The subscript 0 denotes the baseline values. In steady-state, the parameter α is the Grubb constant (assumed to be 0.38, accounting for an assumed fixed relationship between changes in cerebral blood volume (CBV) and CBF) (Grubb et al., 1974). β describes the oxygenation and field strength dependence of the BOLD effect and was assumed to be 1.5 (Boxerman et al., 1995, Davis et al., 1998). The parameter M is the calibration constant, which corresponds to the maximum BOLD change for complete removal of deoxyhemoglobin in the voxel. *M* was estimated using the Chiarelli and Bulte model (Chiarelli et al., 2007c), as given in Equation 5.2.

$$\frac{\Delta BOLD_{HO}}{BOLD_0} = M\left[1 - \left(\frac{CBF_{HO}}{CBF_0}\right)^{\alpha}\left(\frac{[dHb]_{HO}}{[dHb]_0} + \frac{CBF_0}{CBF_{HO}} - 1\right)^{\beta}\right] \qquad \textbf{Equation 5.2}$$

Where $\Delta BOLD_{HO}$ is the change in the BOLD signal during hyperoxia, CBF_{HO} is the CBF during hyperoxia, and $[dHb]_{HO}$ is the concentration of deoxygenated haemoglobin in the venous vasculature during hyperoxia. The subscript 0 refers to these parameters at baseline. Values for $[dHb]_{HO}/[dHb]_0$ were calculated from the end-tidal measurements (averaged over the same time-periods as for the BOLD response) following the procedure described in (Chiarelli et al., 2007c). We assumed a baseline oxygen extraction fraction of 0.4 based on previous data (Raichle et al., 2001), and a reduction in CBF of 5% during hyperoxia (Chiarelli et al., 2007c). Note that an assumed reduction in CBF was used as the ASL signal is too noisy to allow reliable estimates of such a small change in CBF. On a regional basis, values for M, $\Delta BOLD$ and ΔCBF are substituted into equation 5.1 and $\Delta CMRO_2$ is found.

Statistical analysis

We first rejected any regional data where M or $\Delta CMRO_2$ were negative, as this was deemed physiologically implausible (4% of data rejected). We then considered the global response from all of the activated regions. The estimated ΔCBF, $\Delta BOLD$, $\Delta CMRO_2$, and M values were correlated with age using bivariate correlation, with significance accepted at $p<0.05$. The benefit of looking first for a global effect is that the signal to noise of the measurements will be increased such that an age effect is more likely to become apparent. In addition, the numbers of statistical comparisons are kept low.

We then considered regional differences, as it is predicted that any age-related effects will be largest in the frontal cortices. We first determined the magnitude of any BOLD increase with age in each of the identified regions. In

regions showing a significant BOLD age-effect we consider age-related changes in ΔCBF, $\Delta CMRO_2$, and M.

The final aim was to establish whether there is a relationship between the physiological parameters and performance change with age. We found the variance in performance levels was greater with older participants (aged over 40 years), such that we could define two older groups with the same age distribution but with one group perform at the same level as those subjects in their twenties (the 'high' performers) and the other group having a much lower performance (the 'low' performers). We have selected those participants in their twenties, and then those participants aged over forty, split into two groups of the highest and lowest performance (Table 5.1). There was no significant difference in age between the older high and low performing groups (p=0.57, unpaired two-tailed t-test). There was no statistically significant difference in performance accuracy (p=0.89, unpaired two-tailed t-test) or reaction times (p=0.28, unpaired two-tailed t-test) between the twenty year old and high performing groups. Performance accuracy was significantly better for the high performers compared to the low performers (p=0.0006, unpaired two-tailed t-test), with a trend towards lower reaction times (p=0.07, unpaired two-tailed t-test). Within the regions showing a significant change in BOLD response with increasing age, we compared the measured/estimated parameters between the younger and the low performing groups and the younger and high performing groups. This determined which of the parameters are related to the drop in performance with age. A further comparison between the two older groups determined whether the changes could be attributed to a difference in performance per-se.

Group	Number	Mean age (years)	Mean end-tidal O_2 (% ± SE)	Mean accuracy (% ± SE)	Mean reaction time (s ± SE)
Young	15	21 (18-29)	60 ± 2.0	98.9 ± 0.2	910 ± 50
Old high performers	15	55 (42-67)	65 ± 2.0	98.9 ± 0.2	1010 ± 40
Old low performers	14	55 (43-71)	63 ± 2.0	95.7 ± 0.7	1220 ± 100

Table 5.1: Age, end-tidal O_2 values and Stroop task performance accuracy for the three groups.

Effect of Aging between Sexes:

We investigated sex differences using repeated measures GLM analyses, with the mean average of the physiological parameters for the 10 regions as within subject variables, sex and age factors as between subject factors. There were no significant differences between sexes ($F_{1,49}$=0.14, p=0.91) and no significant age by sex interaction ($F_{1,49}$=2.36, p=0.13). As no "Sex by Age" interaction was found, age-related effects on physiological parameter are presented for the entire sample of 55 subjects.

5.4 Results

The data from three subjects were excluded: one subject did not complete the experiment (due to claustrophobia), in another the images were too severely degraded by artifact, and one performed very badly on the Stroop task (accuracy more than 3 standard deviations from the mean) and reported falling asleep during the scan. Thus, 26 male subjects (mean age 40.5 years, SD 15 years) and 29 female subjects (mean age 42 years, SD 17 years) were included in the analyses. The mean years of education was 17 years (most of the subjects were recruited from the Liverpool university), SD 3.2 years with no significant effect of age (r=-0.02, p=0.9, Pearson correlation). No subjects were excluded on the basis of their performance on the cognitive assessment tests. Mean performances on these tests are given in table 5.2, along with age-related regression coefficients.

Test	Mean	SD	Correlation Coefficient	Significance (p-value)
Trail making B-A	20	12	-0.11	0.4
Verbal fluency total	53	14	0.17	0.2
Digit span back	8.5	2.6	-0.15	0.3
Digit symbol	67	11	-0.54	<0.0001

Table 5.2: Performance on the cognitive assessment tests and relation to age.

5.4.1 Behavioural data

All participants performed the Stroop task correctly with mean accuracy of 98% and standard deviation of 2%. Mean response time was 1040 ms with a standard deviation of 278 ms. The behavioural results showed a trend towards lower accuracy (p=0.07) (Figure 5.3a) and longer response times (p=0.09) with increasing age

(Figure 5.3b). Mean duration of each Stroop block was 30.7s with a standard deviation of 0.7s. There was no significant correlation between block duration and age (p=0.5).

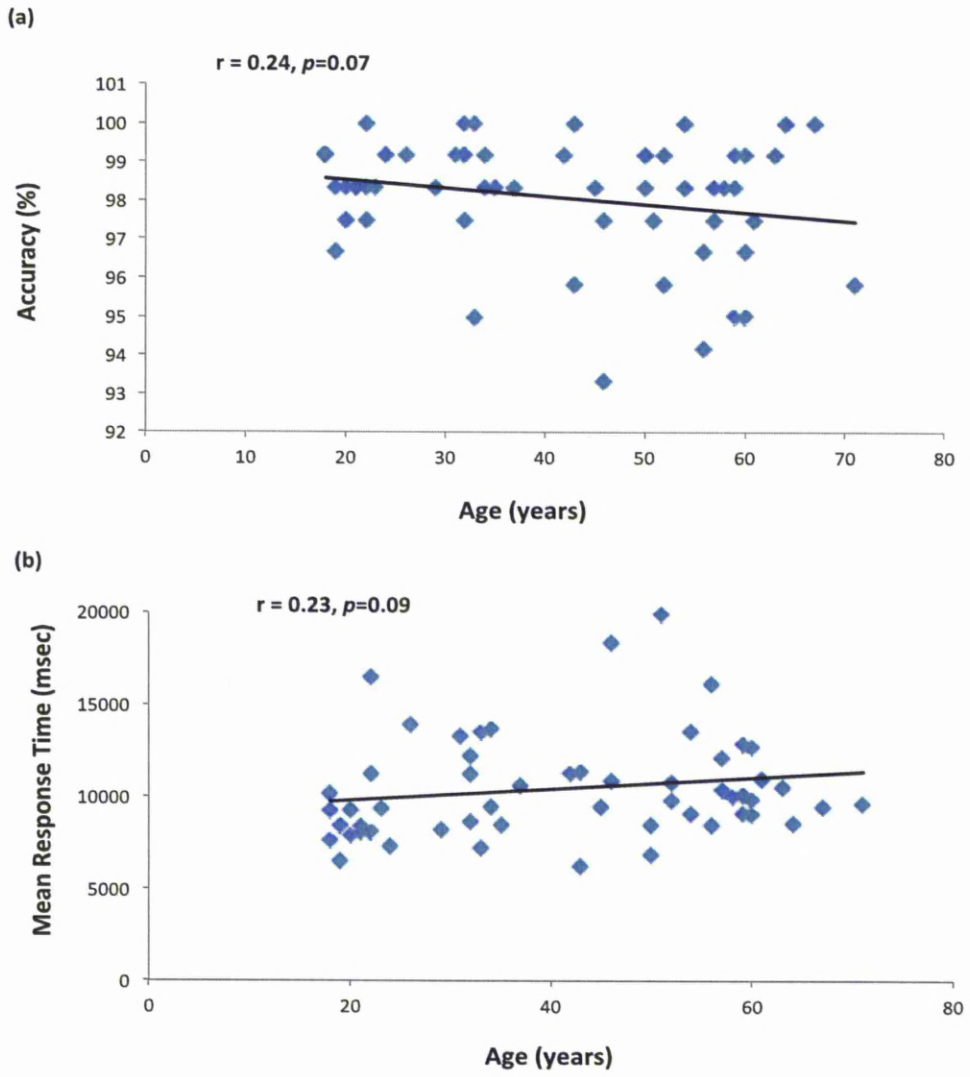

Figure 5.3: Stroop task performance with age for a) accuracy and b) response time.

5.4.2 Gas data

To determine whether there were any age-related differences in the end-tidal O_2 levels, we performed regression analysis of the mean end-tidal values (averaged over both periods of O_2 administration) against age. Figure 5.4 shows an unexpected increase in end-tidal O_2 with increasing age (r=0.37, p=0.01). Theoretically the estimate of the calibration constant M is independent of the level of end-tidal O_2, as the venous haemoglobin deoxygenation is calculated directly from the O_2 measurements (Chiarelli et al., 2007c). As such, this age-dependence should not affect our results. This assumes that the arterial tension of oxygen can be inferred directly from the end-tidal O_2 measurements (Chiarelli et al., 2007c), which in general appears valid as the measures are very tightly correlated in normoxia (Bengtsson et al., 2001).

One possible contributory reason for the increase in end-tidal O_2 is a reduction in pulmonary function with increasing age. This could increase the dead-space in the lung, resulting in a reduction in oxygen transfer and hence increased end-tidal O_2 (Bengtsson et al., 2001). This would lead to an overestimation of arterial tension of oxygen with increasing age, leading to an underestimation of M with increasing age.

To further assess the effect of the age-dependence of end-tidal O_2, the analysis was repeated using data within a narrower range of end-tidal O_2 values from 47 to 77 %, centered on the mean value of 62 %. This excluded 3 subjects and removed the age-dependence of end-tidal O_2 values (r=0.25, p=0.1). Additional analysis was not performed for the group-wise data as there was found to be no significant difference in end-tidal O_2 values between the groups (Table 5.1).

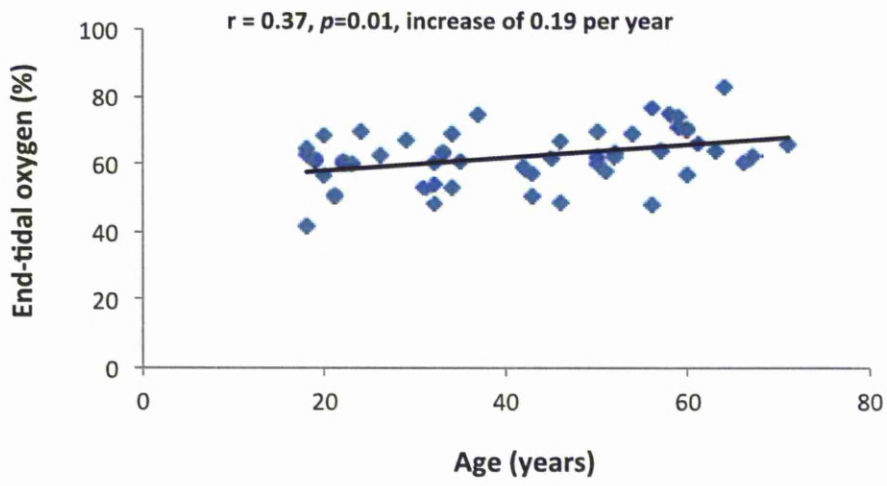

Figure 5.4: Effect of age on end-tidal O_2. Mean end-tidal O_2 (averaged over two periods of O_2 administration) measurements for each individual are plotted against age.

5.4.3 fMRI data

Mean response over all activated regions

Group analysis over all subjects revealed ten regions to be significantly activated at $p<0.05$ (corrected for False Detection Rate), as shown in Figure 5.5 with Talairach coordinates for the 10 regions shown in table 5.3. Anatomical locations were determined using the Talairach daemon (www.talairach.org) (Sakata et al., 1997), choosing the closest grey matter region if the peak activation fell in white matter.

Averaged over all regions the BOLD response increased significantly (r=0.30, p= 0.03) with increasing age (Figure 5.6a). There was a significant reduction in the $CMRO_2$ response with increasing age (r=-0.31, p= 0.03) (Figure 5.6b), the calibration constant M decreased significantly with increasing age (r=-0.29, p= 0.04)

(Figure 5.6c) but CBF did not change with age (Figure 5.6d). Re-analysis using the data within the restricted end-tidal O_2 range showed similar results for BOLD response (r=0.35, p=0.01), $CMRO_2$ response (r=-0.34, p=0.02) and CBF response (no change with age), but the age-dependence of M was no longer present (r=-0.23, p=0.1). As a further check for the influence of end-tidal O_2 differences, a regression of end-tidal measurements against $CMRO_2$ response was performed (using the full dataset). This showed no significant relationship (r=-0.14, p=0.3).

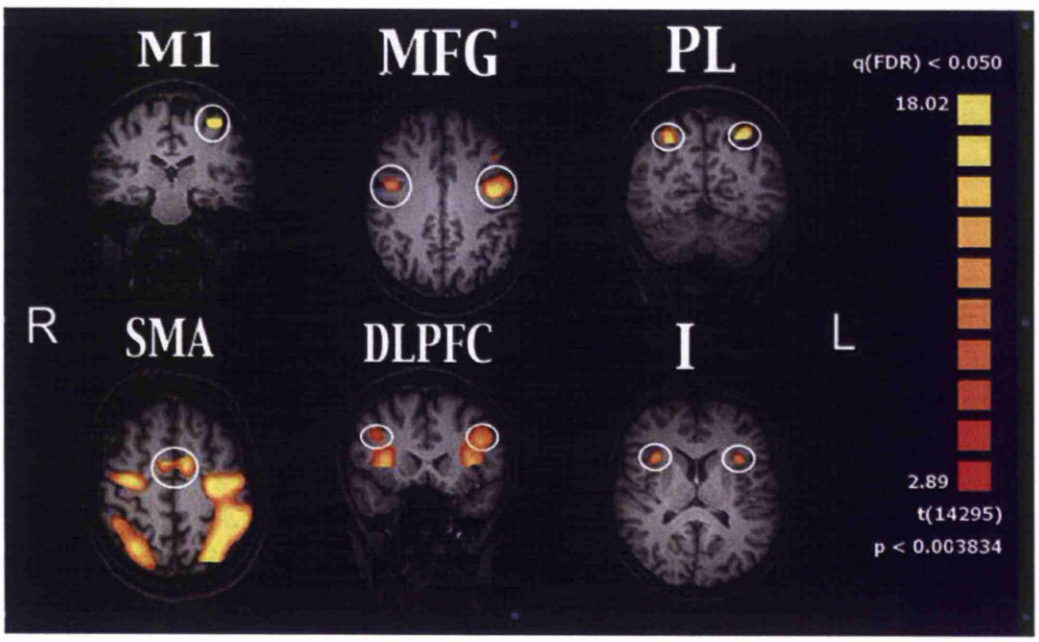

Figure 5.5: Regions of activation during the Stroop task. Results from the group analysis at FDR p<0.05, using a general linear model incorporating both BOLD and CBF data. Ten regions were identified, as indicated by the white circles. M1 = primary motor cortex (BA 4), SMA = supplementary motor area (BA 6), MFG = middle frontal gyrus (BA 6), DLPFC = dorsolateral pre-frontal cortex frontal cortex (BA 9), PL= parietal Lobe (BA 7), I = Insula (BA 13 & 14).

Anatomical Region	Tal. Coordinates
Left Pre-central gyrus	-35 -23 54
BA4 Primary Motor cortex (M1)	
Medial Frontal Gyrus	-3 -5 53
BA 6 Supplementary motor area (SMA)	
Left parietal lobe	-24 -61 45
BA7 (LPL)	
Right parietal lobe	31 -57 45
BA7 (RPL)	
Left Middle Frontal Gyrus	-40 1 40
BA6 (LMFG)	
Right Middle Frontal Gyrus	44 8 38
BA6 (RMFG)	
Left Middle Frontal Gyrus	-40 18 26
BA9 dorsolateral pre-frontal cortex (LDLPFC)	
Right Middle Frontal Gyrus	36 18 30
BA9 dorsolateral pre-frontal cortex (RDLPFC)	
BA 13 & 14 Left Insula (LI)	-33 14 11
BA 13 & 14 Right Insula (RI)	30 16 11

Table 5.3: Talairach coordinates of the active regions shown in Figure 5.5.

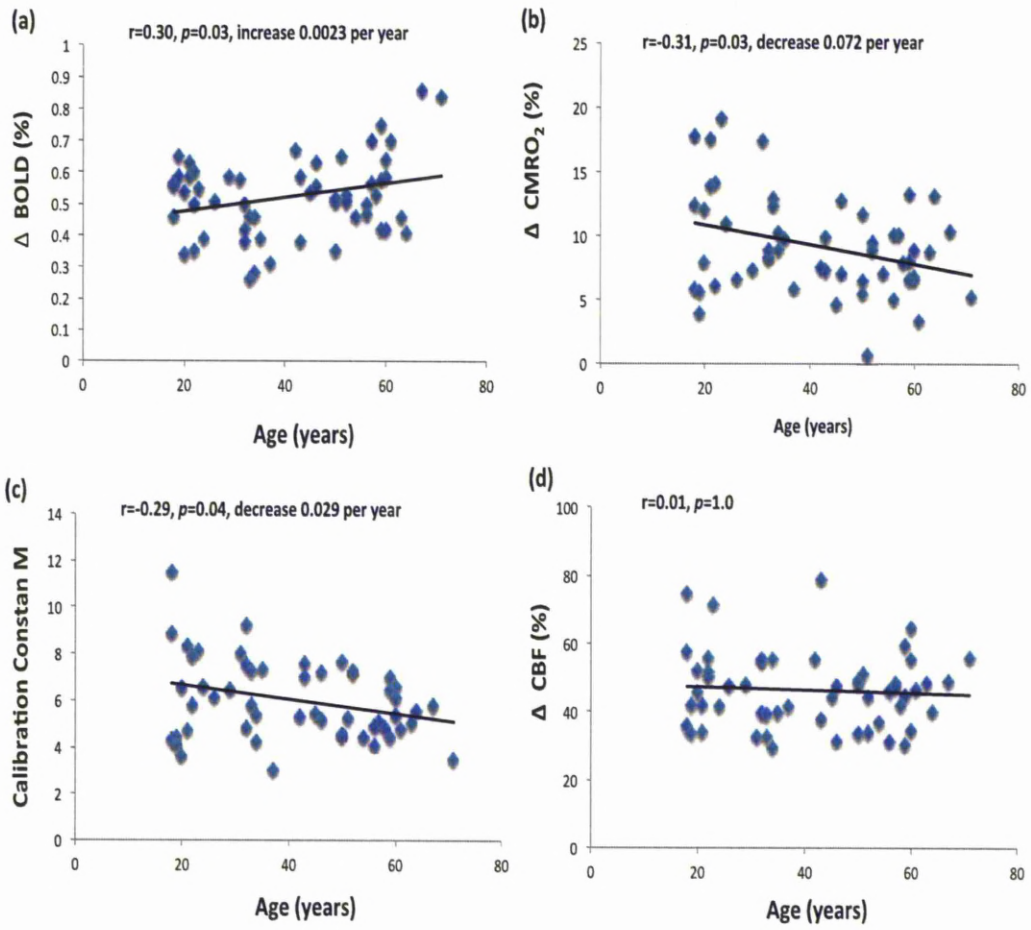

Figure 5. 6: The age-related change in the measured/estimated parameters ((a) ΔBOLD, (b) $\Delta CMRO_2$, (c) *M* and (d) ΔCBF), averaged over the ten activated regions. Each point shows the average value for an individual over the ten activated regions.

Regional Differences

Regression results of all four parameters within each of the ten regions are shown in Table 5.4. We first considered the magnitude of the BOLD increase with age in the ten individual regions. The greatest BOLD increase with age was found in M1, LMFG and RMFG (Table 5.4) and, indeed, the increase was significant in these regions: M1 (p=0.003), LMFG (p=0.02) and RMFG (p=0.02). Further regression

tests on the other 3 parameters within these 3 regions show no significant change for ΔCBF and *M*, but a significant reduction in $\Delta CMRO_2$ within M1 and LMFG (Table 5.4). Regions showing the largest change in calibration constant *M* were the left insula, left DLPFC and right DLPFC.

Re-analysis using the data within the restricted end-tidal O_2 range showed very similar results to Table 5.4, identifying the same three regions with the largest, and significant, age-related increase in BOLD response. None of the results in Table 5.4 changed in terms of their significance (i.e. results remained above or below the p=0.05 threshold), except for *M* within the right DLPFC where p increased from 0.01 to 0.06.

Region	**ΔBOLD**			**M**			**ΔCBF**			**$\Delta CMRO_2$**		
	Slope x 10^{-3}	r	*p*	Slope	r	*p*	Slope	r	*p*	Slope	r	*p*
M1	4.9	0.40	0.003	-0.02	-0.26	0.06	-0.03	-0.06	0.7	-0.13	-0.42	0.004
SMA	1.0	0.06	0.7	-0.03	-0.17	0.2	-0.14	-0.20	0.1	-0.13	-0.30	0.03
LPL	1.5	0.10	0.4	-0.03	-0.20	0.2	0.09	0.16	0.2	0.008	0.02	0.9
RPL	1.4	0.09	0.5	-0.02	-0.12	0.4	0.09	0.20	0.1	-0.03	-0.10	0.5
LMFG	4.8	0.31	0.02	-0.02	-0.22	0.1	-0.04	-0.07	0.6	-0.12	-0.34	0.03
RMFG	5.1	0.31	0.02	-0.01	-0.14	0.4	0.09	0.16	0.2	-0.05	-0.15	0.3
LDLPFC	-1.3	-0.10	0.4	-0.05	-0.37	0.008	-0.11	-0.16	0.2	-0.15	-0.38	0.01
RDLPFC	-1.7	-0.19	0.1	-0.04	-0.35	0.01	0.06	0.01	0.9	-0.03	-0.09	0.5
LI	-0.02	0.00	1.0	-0.05	-0.31	0.03	0.05	0.08	0.5	-0.07	-0.19	0.2
RI	0.08	0.01	0.9	0.001	0.01	0.9	0.02	0.04	0.8	-0.07	-0.28	0.06

Table 5.4: Regression of the measured/estimated parameters with age in the 10 activated regions. Slope represents the change in the measured/estimated value per year. Significant values are shaded.

Relationship with Performance

We determined the relationship between the measured/estimated parameters and performance accuracy in the 3 regions showing an age-related effect (L and R MFG and M1) in the BOLD response. We split the subjects into 3 groups as

described in the methods (Table 5.1): young, old high performers and old low performers. Table 5.5 shows the mean parameter estimates across each of these groups in each of the regions. It can be seen that in LMFG and M1, the BOLD and $\Delta CMRO_2$ responses are significantly different for the low performing old group in comparison to the young group. In LMFG the BOLD response (but not the $\Delta CMRO_2$ response) is significantly different for the low performing old group in comparison to the high performing old group. None of the parameters showed any significant difference between the high performing old group and the young group.

	M	ΔBOLD (%)	ΔCBF (%)	$\Delta CMRO_2$ (%)
LMFG				
Young	5.6 ± 0.7	0.63 ± 0.04*	27.6 ± 3.1	10.4 ± 2.0*
Old high	5.1 ± 0.3	0.65 ± 0.04†	23.4 ± 2.5	7.1 ± 1.0
Old low	4.6 ± 0.4	0.85 ± 0.07*†	24.7 ± 2.3	4.2 ± 1.0*
RMFG				
Young	6.0 ± 0.6	0.55 ± 0.04	24.1 ± 2.2	8.7 ± 1.8
Old high	5.9 ± 0.3	0.54 ± 0.04	24.7 ± 2.5	9.3 ± 0.9
Old low	4.9 ± 0.5	0.67 ± 0.11	27.9 ± 2.6	6.7 ± 1.2
M1				
Young	5.7 ± 0.5	0.49 ± 0.06*	25.2 ± 1.7	11.9 ± 1.3**
Old high	4.9 ± 0.3	0.59 ± 0.06	22.9 ± 1.0	8.2 ± 1.1
Old low	4.9 ± 0.4	0.64 ± 0.03*	21.7 ± 2.0	5.3 ± 1.2**

Table 5.5: Mean (±SE) values for the measured/estimated parameters in the young, old high performers and old low performers in the three regions showing an age-related response.

* and † indicates pairs of values that are significantly different at $p<0.05$

** indicates pairs of values that are significantly different at $p<0.005$

5.5 Discussion

5.5.1 Mean response over all activated regions

Initially, the estimated calibration constant *M* was found to decline with increasing age (Figure 5.6c), consistent with a previous study considering age-related alterations in the response of the visual cortex (Ances et al., 2009). However, on re-analysis within a narrow range of end-tidal values, this age-dependence is no longer present, suggesting that the age-related differences in end-tidal O_2 were driving the changes seen in *M*. *M* reflects the amount of deoxyhaemoglobin present in the baseline state. As such, *M* depends on a number of physiological parameters including baseline CBV, resting oxygen extraction fraction (OEF), the constant β, and the hematocrit, all of which could potentially change with age. There is evidence that CBV declines with age (Leenders et al., 1990), which would predict a reduction in *M* with age. Hematocrit remains fairly stable up to the age of 65 and then declines (Arbeev et al., 2011), so is unlikely to affect *M* over the age range we have studied. OEF has been found to remain stable (Leenders et al., 1990, Pantano et al., 1984, Yamaguchi et al., 1986) or increase with age (Lu et al., 2010), predicting an increase in *M* with age.

The BOLD response to the Stroop task was found to increase with age (figure 5.6a), in agreement with previous work (Langenecker et al., 2004, Milham et al., 2002, Zysset et al., 2007). However, we found a reduction in the estimated $\Delta CMRO_2$ with increasing age (Figure 5.6b), that would be consistent with neurodegeneration (Uylings and de Brabander, 2002), which could be attributed to age-related brain atrophy (Cowell et al., 2007, Good et al., 2001b). ΔCBF did not change with age, suggesting that the increased BOLD response with age is due primarily to a

reduction in $CMRO_2$ response with age. Hence caution should be exercised in interpreting the BOLD signal increase with age as increased neural activity. Previous studies using combined ASL and BOLD in ageing have focussed on other brain regions. One study (Ances et al., 2009) found reduced BOLD response in the visual cortex with increasing age, but no significant alteration in $\Delta CMRO_2$. Another study (Restom et al., 2007) found increased BOLD and CBF response with increasing age in the medial temporal lobe during memory encoding, consistent with increased $\Delta CMRO_2$ with age. However a calibration scan was not included and so baseline effects could not be accounted for. These two studies consider responses in different brain regions and to different tasks and so would not necessarily be expected to show the same age-related changes as in our present study.

5.5.2 Regional differences

Considering regional changes, we found the age-related BOLD increase to be greatest in the left and right (MFG, BA6) and in the primary motor cortex (M1, BA4) (Table 5.4), in broad agreement with previous studies (Cabeza et al., 2002, Cabeza et al., 2003, Langenecker et al., 2004, Milham et al., 2002, Nielson et al., 2002, Zysset et al., 2007) using similar tasks. Langenecker et al. (2004) reported that older adults exhibited greater BOLD response in many frontal areas during a Stroop task, including the left inferior frontal gyrus (IFG). Milham et al. (2002) showed greater BOLD response to a Stroop task for younger subjects compared to elderly subjects across a number of brain regions including frontal and parietal lobes. However, older adults had greater BOLD response compared to young adults in the inferior frontal gyrus (IFG). Finally, in a recent study by Zysset et al. (2007) middle-aged adults

showed increased BOLD response to a Stroop task in several task-related regions, mainly in the inferior frontal junction (IFJ) area (bilaterally) and the pre-supplementary motor area. The Talairach coordinates of the IFJ and IFG given in the studies by Langenecker and Zysset are within 1 cm of the regions we identify as L and RMFG (Table 5.3). The significant BOLD activation that was seen in M1 was primarily due to responses made during the Stroop task with the right index or middle finger (Pardo et al., 1990).

Considering the other parameters (Table 5.5), only $\Delta CMRO_2$ is found to have an age dependence in LMFG and M1. This supports the findings from the global analysis (Figure 5.6) that the increased BOLD response with increasing age is due to a reduction in $\Delta CMRO_2$. Increased BOLD response in the frontal cortex is interpreted in previous studies as increased neural activity (Langenecker et al., 2004, Zysset et al., 2007); compensatory activity in the older group to aid performance. Our results suggest caution in this interpretation, suggesting instead that increased BOLD response is related to a reduction in neural processing in this context.

The regions showing the largest decline in M with age were the left insular and left and right DLPFC. The insular and frontal cortex have also been found to show the largest decline in CBV with age (Leenders et al., 1990), consistent with the view that regional alterations in M are due to CBV changes.

5.5.3 Relationship with Performance

Despite the very high performance of all participants in this study (Table 5.1 and Figure 5.3), we were able to define two groups of older adults, those with high performance and those with 'low' performance (Table 5.1). We found that the low performers showed a significant difference in the measured/estimated parameters

compared to the young group (Table 5.5), whereas the older group of high performers had values indistinguishable from the young group (Table 5.6). The low performers group showed increased BOLD response and reduced $CMRO_2$ response in LMFG and M1 compared to the young group. This suggests that reduced neural processing in these regions is impacting negatively on performance. Thus, rather than compensatory activity, increased BOLD response in these regions could be interpreted as an indication of neurodegeneration, associated with lower performance. The comparison of the two old groups indicated increased BOLD response in LMFG for the low performers, but no difference in $CMRO_2$ response, suggesting it is age-related differences in performance (not performance alone) that is leading to the altered $CMRO_2$ responses between young and old.

5.6 Methodological Considerations

In terms of probing the interference Stroop effect, it would have been beneficial to look at, for example, incongruent verses congruent Stroop conditions. However, the contrast to noise ratio of this measure would have been insufficient to extract the quantitative BOLD parameters (Goodwin et al., 2009, Zysset et al., 2007). Using Stroop/rest paradigm boosted the SNR and enabled the interference Stroop effect (Zysset et al., 2007). Besides, the well known increase in reaction time during the incongruent as compared to the congruent condition (Pardo et al., 1990).

The end-tidal O_2 values showed an unexpected increase with age, which could influence our findings of reduced M and $\Delta CMRO_2$ with increasing age. Re-analysis using data within a restricted range of end-tidal O_2 values did remove the

apparent age-dependence of M, but not $\Delta CMRO_2$. We find an increase in % end-tidal O_2 of 0.19 per year. Calculations show that this would lead to a reduction in M of 0.03 per year and a decline in $\Delta CMRO_2$ of 0.07 per year. Hence, this could be responsible for the reduction in M that we see (decline of 0.03 per year averaged over all regions, maximum regional decline of 0.05 per year in left DLPFC). However, the reduction in % $\Delta CMRO_2$ per year is much greater (0.07 per year averaged over all regions, maximum regional decline of 0.15 in left DLPFC), which cannot be entirely accounted for by errors in the arterial tension of oxygen.

The hyperoxia calibration model assumes fixed values for a number of physiological parameters, including Grubb's constant α, the field-dependent parameter β and the baseline OEF. It is possible that all 3 of these parameters could change with age, thus affecting our conclusions. To address this problem, we have performed simulations using plausible age-related changes in these parameters. For the simulations we have taken average values of end-tidal O_2 (17% during rest and 62% during hyperoxia), BOLD response (0.52%) and CBF response (24%) from our data, along with values of OEF=0.4, $\alpha = 0.38$ and $\beta = 1.5$. We calculate values for M and $\Delta CMRO_2$ using equation [5.2] along with the equations in (Chiarelli et al., 2007c) for calculating $[dHb]_{HO}/[dHb]_0$, while altering one parameter at a time as described below. Results of the simulations are shown in Figure 5.7.

First, considering OEF, a number of previous studies revealed no significant age-related changes in OEF (Leenders et al., 1990, Pantano et al., 1984, Yamaguchi et al., 1986). However, one recent study of a large sample size (232 subjects) revealed an increase in OEF with age (Lu et al., 2010) from 0.35 at 20 years up to approximately 0.40 at 60 years (from (Lu et al., 2010) figure 5.1). Substituting these values into the model, produces an increase in M of 0.02 per year and an increase in

$\Delta CMRO_2$ of 0.03 per year (Figure 5.7). Thus, assuming a fixed value of OEF of 0.4 for all ages, as we have done, would tend to overestimate M and $\Delta CMRO_2$ at the younger age, producing an apparent decline in M and $\Delta CMRO_2$.

The relaxation parameter R_2* depends on the concentration of deoxygenated haemoglobin raised to the power of β (Davis et al., 1998). β is dependent on the composition of vessel sizes and increases as the proportion of smaller vessels increases (Buxton et al., 2004). With increasing age, it might be expected that the relative proportion of smaller vessels reduces, due to sub-clinical vascular disease, leading to a reduction in β. It is difficult to estimate by how much β might decline with age. It is known that grey matter perfusion declines by approximately 0.5% per year (Parkes et al., 2004), hence a similar reduction in β seems reasonable (i.e. from β=1.5 at 20 years to β=1.2 at 60 years). Substituting these values into the model, produces an increase in M of 0.03 per year and a decrease in $\Delta CMRO_2$ of 0.04 per year (Figure 5.7). Thus, assuming a fixed value of β of 1.5 for all ages, as we have done, would tend to underestimate M and overestimate $\Delta CMRO_2$ at the older age, producing an apparent decline in M and an apparent increase in $\Delta CMRO_2$.

The relationship between changes in CBV and CBF (from baseline to a new steady state) is governed by the Grubb constant, α (Grubb et al., 1974), according to $\Delta CBV=\Delta CBF^{\alpha}$. Following an increase in neural activity the venous vessels are thought to expand passively due to increased pressure, producing an increase in CBV. It is difficult to predict how and by how much α might change with increasing age, but it seems likely that α would increase due to loss of elasticity in the vessel walls, i.e. there would be a larger change in CBV for a given change in CBF. Again we assume an increase in α of 0.5% per year (from 0.32 at 20 years to 0.38 at 60 years). Substituting these values into the model, produces a decline in M of 0.002 per

year (negligible) and a decrease in $\Delta CMRO_2$ of 0.03 per year (Figure 5.7). Thus, assuming a fixed value of α of 0.38 for all ages, as we have done, would tend to underestimate M and $\Delta CMRO_2$ at the younger age, producing an apparent increase in M and $\Delta CMRO_2$.

Our data shows a decline in M of 0.03 per year averaged over all regions, with a maximum regional decline of 0.05 per year in the left DLPFC. Given the above simulations, it seems entirely possible that this decline is artifactual and due instead to the incorrect assumption that OEF and β are fixed across the lifespan.

However, our data also shows a much larger decline in $\Delta CMRO_2$ of 0.07 per year averaged over all regions, with a maximum regional decline of 0.15 in left DLPFC. This decline is two to five-fold larger than what would be expected if the assumption of fixed OEF is incorrect. In fact, the simulations show that the age-related decline in $\Delta CMRO_2$ we find is probably conservative due to our assumptions of fixed α and β.

In our application of the hyperoxia calibration model, a fixed value for CBF reduction in response to hyperoxia is used. However, there is evidence that this CBF reduction may reduce with increasing age (Watson et al., 2000), which would lead to overestimated values for M and $\Delta CMRO_2$ in the older subjects. If true this would suggest the age related decline in M and $\Delta CMRO_2$ that we found, may in fact be conservative.

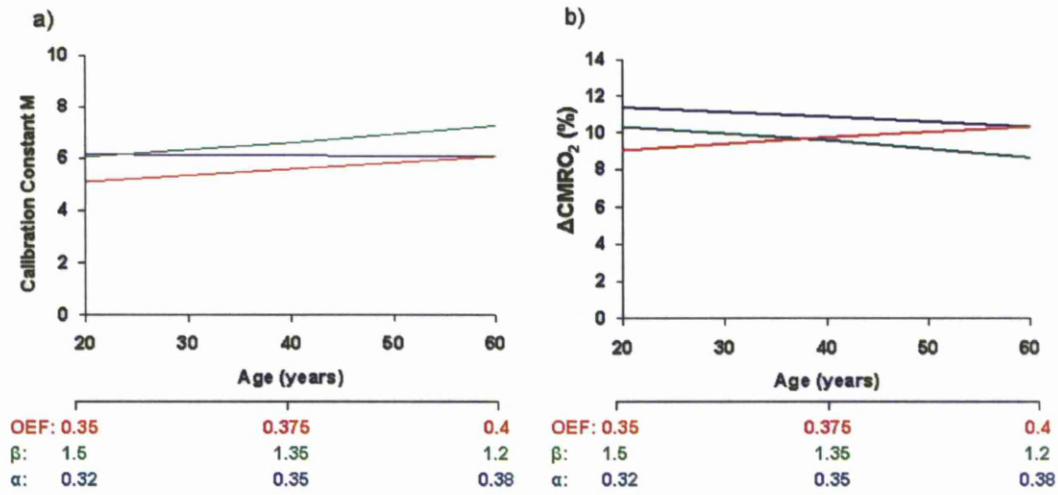

Figure 5.7: Sensitivity of the calculated parameters M and $\Delta CMRO_2$ to the assumed values for OEF, α and β as they would be estimated to vary across an age span from 20 to 60 years.

In conclusion, this study demonstrates the need to take into account alterations in vascular-metabolic coupling and resting blood volume when interpreting changes in the BOLD response with aging. It also highlights the added benefit that calibrated fMRI offers in terms of interpreting the underlying physiological changes that give rise to the measured BOLD response.

CHAPTER 6: Effects of age and sex on regional brain grey matter density and relation to cognitive performance: VBM-DARTEL study.

6.1 Aim of Chapter

This chapter investigated the link between grey matter (GM) density, age and sex using the new voxel-based morphometry (VBM) registration method: Diffeomorphic Anatomical Registration using Exponentiated Lie algebra (DARTEL). The relationships between regional GM density and brief cognitive assessment scores are also investigated.

6.2 INTRODUCTION

There is strong evidence from previous post-mortem (Ankney, 1992, Pakkenberg and Gundersen, 1997, Uylings and de Brabander, 2002) and structural neuroimaging studies (Coffey et al., 1992, Courchesne et al., 2000, Cowell et al., 1994, Filipek et al., 1994, Goldstein et al., 2001, Good et al., 2001b, Gur et al., 1999, Lemaitre et al., 2005, Luders et al., 2005, Raz et al., 1997, Resnick et al., 2000, Sullivan et al., 2004, Tisserand et al., 2000) that the human brain shrinks with ageing, and the brain shrinkage is not uniform but is, rather, region specific.

The associations between sex and grey matter (GM) changes with age have been widely observed using MRI. Generally, the total brain volume of males is 10% larger than that of females, as reported by post-mortem (Ankney, 1992) and in vivo imaging research (Filipek et al., 1994, Gur et al., 1999, Leonard et al., 2008). Some studies showed larger GM volume in females compared to males (Goldstein et al., 2001, Gur et al., 1999, Lemaitre et al., 2005, Luders et al., 2005, Leonard et al.,

2008). Other studies show larger GM volume in males (Good et al., 2001a), or no sex differences in GM volume (Nopoulos et al., 2000). Some studies reported decreased GM volume in females comparative to males (Resnick et al., 2000, Sullivan et al., 2004). Females reported to have larger dorsolateral prefrontal cortex (Schlaepfer et al., 1995), thalamus (Murphy et al., 1996, Xu et al., 2000), hippocampal regions (Filipek et al., 1994, Murphy et al., 1996), anterior cingulate gyrus (Brun et al., 2009), and parietal lobes (Nopoulos et al., 2000) as compared with males. On the other hand, males have a larger volume of cortical gray matter in the cerebellum (Raz et al., 2001, Xu et al., 2000) and the limbic region (Good et al., 2001a).

The effects of aging clearly differ among regions of the brain and to some degree between the sexes. Several studies suggested that with increasing age, male's brains aged earlier than female's brains (Cowell et al., 1994), while other studies revealed the opposite result (Hubbard and Anderson, 1983). But findings from these studies have not been in agreement regarding the GM volumes changes; with some reporting that males exhibited greater GM volumetric decreases with age (Coffey et al., 1992, Raz et al., 2004), and few others have reported the same volumetric decreases between sexes (Raz et al., 2005, Tisserand et al., 2002).

In regards to regional age-related GM volume changes, Cowell et al. suggested that the pattern of change is region and sex-specific (2007). Males have a larger of cortical GM in the limbic region (Good et al., 2001b), whereas, females have an increased GM volume compared with males in the frontal lobe cortices. A greater reduction in GM volume occurred in males than in females in the frontal and temporal lobe regions (Cowell et al., 1994).

This was supported by the findings of Murphy et al. (1996), who suggested an earlier or faster volume loss with ageing in the frontal lobe and temporal lobe in males, and in the parietal lobes and hippocampus region in females. Also Raz et al. (1997) demonstrated a steeper trend of age-related changes in the inferior temporal cortex in males. Some studies indicated that the regional GM volume decreased linearly with age; Coffey et al. (1992) for example found that both frontal lobe and temporal lobe volumes decreased with age, but the frontal lobe exhibited a greater decrement than the temporal lobe. Likewise, Cowell et al. (1994) revealed that the FL exhibits greater decrements in brain volume than the temporal lobe.

These results suggest that the frontal lobe and temporal lobe are more sensitive to the aging-related changes than other brain lobes. Specifically, the prefrontal cortex (PFC), which has been reported to be more sensitive to aging process (Cowell et al., 1994, Gur et al., 2000, Raz et al., 2004, Salat et al., 1999). Raz (2000), suggested that volume decreases in PFC regions are a characteristic of normal aging.

With respect to cognitive functioning, it is still not clear yet whether a direct relation exists between age-related volumetric changes and performance in cognitive tests. The PFC region is frequently reported to show volume losses during the aging process (Cowell et al., 1994, Gur et al., 2000, Raz et al., 2004, Salat et al., 1999). A weak relation was noted between PFC and working memory performance (Raz et al., 1998). Reduced performances in attention and executive function in elderly have been linked with decreased global cortical volumes and reduced volumes of lateral PFC (Zimmerman et al., 2006). Some studies reported an association between regional brain volume decrement and cognitive functioning, such as hippocampal volume and memory performance (Golomb et al., 1994), between the PFC volume

and mental imagery (Raz et al., 1999), between the limbic structures and memory (Raz et al., 1998), and between medial prefrontal cortex and fluid intelligence (Gong et al., 2005). However, other studies have not found any evidence for such a relation between brain volume and cognitive performance with age (Raz et al., 1998, Tisserand et al., 2000, Tisserand and Jolles, 2003).

Other possible factors associated with discrepancies in these results would be most likely due to the variation in age range, sample sizes, and differences in neuroimaging protocols and processing techniques. Most of these previous studies have been based on manual or semi-automated region of interest-guided measurements. In this study the voxel-based morphometry (VBM) was used, which is a computational quantitative fully automated analysis technique (Ashburner and Friston, 2000), that allows an objective analysis of the differences of the brain tissue composition between groups. It involves a voxel-wise comparison of the tissue concentration throughout the whole brain between groups (Ashburner and Friston, 2000). VBM requires that voxels are classified according to different tissue types, usually GM, white matter (WM) and cerebrospinal fluid (CSF). To allow comparison across subjects, images are non-linearly aligned to a standard brain, where a common coordinate system can be defined, and volumes are corrected for local shrinkages and expansions (Good et al., 2001b). VBM allows for the quantification of the GM volumes, globally and regionally, using either the voxels directly or regions of interest.

The advantage of VBM includes greater sensitivity for localizing small size regional differences in grey or white matter. However, an important limitation of VBM is that the poorly registered MR images to a common template can lead to false estimates (Bookstein, 2001). The major doubt is that VBM is very sensitive to

systematic shape differences attributable to misregistration from the spatial normalization step (Ashburner and Friston, 2001). To solve this problem, Ashburner (2007) proposed new preprocessing steps for VBM in statistical parametric mapping (SPM); as an alternative to SPM's traditional registration approaches. These run as a toolbox in SPM8, the "Diffeomorphic Anatomical Registration Through Exponentiated Lie Algebra" (DARTEL) registration method.

This improved analysis technique can achieve more accurate inter-subject registration of brain images and it can improve the realignment of small inner structures over the standard VBM method (Yassa and Stark, 2009). The key result estimated by this method is called local tissue ''density'', where reduction in this density is hypothesised to indicate atrophy (Raz and Rodrigue, 2006).

Several studies have used the standard VBM technique to assess age-related changes in normal healthy volunteers (Good et al., 2001b, Smith et al., 2007, Tisserand et al., 2002, Van Laere and Dierckx, 2001). Good et al. (2001b) were able to assess a large sample of 465 healthy subjects aged 17-79 years; whereas, Van Laere and Dierckx (2001) recrutied 81 subjects (age range between 20-81 years), Tisserand et al. (2002) studied 57 normal subjects aged 21-81 years, and finally, Smith et al. (2007) analysed the scans of 122 healthy subjects (aged between ages 58-95 years). Their findings are below. Global GM volume significantly declined with age (Good et al., 2001b), with regional patterns of GM density reduction in the middle frontal (Good et al., 2001b, Tisserand et al., 2002), inferior frontal (Good et al., 2001b), orbital frontal (Tisserand et al., 2002), superior parietal(Good et al., 2001b), inferior parietal (Good et al., 2001b, Van Laere and Dierckx, 2001), superior temporal (Good et al., 2001b, Van Laere and Dierckx, 2001), anterior cingulate (Good et al., 2001b, Tisserand et al., 2002), and insular cortices (Good et al., 2001b),

and the cerebellum (Good et al., 2001b, Van Laere and Dierckx, 2001). However, Smith et al. (2007) found that with age, regional differences in GM volume occurred more focally in the frontal, parietal and temporal lobes, but not in medial or anterolateral temporal lobes, or in posterior cingulate. Generally, these VBM results are in agreement with those volumetric studies in which parietal and frontal regions may have more prominent GM volume loss with age. More recently, a VBM study of 662 healthy older adults (age between 63-75 years) also revealed a similar pattern of reduction as the one suggested by the volumetric studies (Lemaitre et al., 2005).

A VBM study with regard to sex differences carried out a strict age-matched gender comparison in 441 healthy subjects (aged 44–48 years) and found that males have more GM density in the midbrain, left inferior temporal gyrus, right occipital lingual gyrus, right middle temporal cortex and in both cerebellar hemispheres. Females showed greater GM density in the cingulate cortices and right inferior parietal lobule (Chen et al., 2007) . Good et al. (2001a) found that males had significantly increased GM density bilaterally and symmetrically in the amygdala /hippocampal complexes, and the left anterior temporal pole. In contrast, females had increased GM density in the posterior temporal lobes, right orbital gyri, inferior frontal gyri bilaterally and in the left angular gyrus (Good et al., 2001a). The other VBM gender comparison study, using a larger age range (58–95 years) failed to detect any gender differences (Smith et al., 2007).

VBM studies with regard sex differences in aging; Taki et al. (2004) reported reduction in GM density bilaterally in the superior temporal gyri in males, and in the left superior temporal gyrus and the left precentral gyrus in females. However, Smith et al. (2007) did not find any significant sex effects.

VBM and volumetric studies often are not directly comparable (Allen et al., 2005). However, a direct comparison between VBM and the volumetric methods in an investigation of aging effects reveals some significant areas of agreement in which parietal and frontal regions may have more prominent GM changes with age. Still, there are some discrepancies reported between the two approaches that were seen in many brain regions (i.e. the anterior cingulate cortex and DLPFC) when these approaches were compared (Tisserand et al., 2002).

In this study, main goal was to apply the new VBM-DARTEL method to investigate the range of age-related changes in GM density and correlate these with performance on brief executive assessment tests in healthy subjects. We hypothesized that the largest age-related changes in GM density would be found within the frontal lobe, and that decline in cognitive performance would be particularly associated with changes in GM density in this region.

6.3 METHODS

6.3.1 Data Analysis:

Image Preprocessing

DARTEL-VBM analysis of MRI data was performed using SPM8 software (Statistical Parametric Mapping, Wellcome Department of Imaging Neuroscience, University College London, UK; available at http://www.fil.ion.ucl.ac.uk/spm) implemented in MATLAB & SIMULINK, version 7.9.0.529 - R2009b., The MathWorks, Inc., Natick, MA, USA. The VBM-DARTEL preprocessing included several steps: (1) all T1-weighted MR images were segmented using a segmentation

algorithm developed in SPM8 described by Ashburner and Friston (2000) to produce GM and WM images in the native space of the T1-weighted MRI scans. The remaining steps used the DARTEL toolbox (Ashburner, 2007); (2) GM/WM images were aligned by a rigid transformation (with the tissue probability map) using the normalization parameter developed from the segmentation step; (3) The group-specific templates were created by the aligned images from all subjects. The procedure of creating a template was an iterative procedure that began with the generation of an original template computing the average of all the aligned data. Deformations from the initial template to each of the GM/WM images were computed, and the inverse deformation was applied to each of the GM/WM images. A second template was created as the mean of the deformed GM/WM images, and this procedure was repeated six times, and the template was generated, which was the average of the DARTEL registered data; (4) The flow field computed for each subject in step 3, warping rigidly aligned GM/WM to the common DARTEL space, was composed with an affine transformation that transforms DARTEL to MNI space; (5) All these images were smoothed with an 10-mm full-width at half-maximum Gaussian kernel.

The VBM-DARTEL method was used to investigate the effects of age and sex on the global GM density and to study the relation between GM density and decline in performance on brief executive assessment tests. The full factorial model of analysis of variance was used to address the differences in GM/WM with age. For all VBM analyses, to adjust for inter sex variation in brain volume, and to estimate global effects, total intracranial volume (TIV) for each subject was computed and set as a vector of global values. Participants were categories into two groups of under and over 50 years of age, based on the findings that hemisphere volumes remained

stable in both sexes up to the age of 50 years (Ge et al., 2002, Luft et al., 1999, Miller et al., 1980). First, regional GM alterations with aging were examined in each gender. Second, we tested the regional differences in GM density between: males above 50 years and males under 50 years; females above 50 years and females less than 50 year.

Multiple regression and correlation between age and GM density were examined for all subjects and within each sex. To control for multiple comparisons, p values were thresholded at $p < 0.05$ (false discovery rate correction (FDR)) at the voxel level and $p < 0.05$ (family wise error (FEW)) at the cluster level. Significant anatomical localizations were determined by the anatomy SPM toolbox (Eickhoff et al., 2005).

Multiple regression and correlation analyses were also performed to characterize the extent to which age was associated with the cognitive measures. All results of SPM image analysis were superimposed on structural MR images on sagittal, coronal and axial slices, which were the average images of all subject's normalized T_1-weighted images, to facilitate correlation with anatomy.

6.4 RESULTS

6.4.1 Association between Intracranial Volumes, Ages and Sexes:

All variable distributions were normal when tested with Kolmogrov-Smirnov test of normality (p>0.05). From the segmented images, the relative GM, WM and CSF volumes normalized to each individual's intracranial volume were extracted. TIV was the addition of total GM, WM, and CSF volumes. Person correlations

between these volumes and age were calculated (Table 6.1) by using bivariate correlation analysis (PASW Statistics v18.0), with significance accepted at $p < 0.05$. Although age was matched between females and males (females 41.8 ± 17.2 years, males 40.5 ± 15.1 years, t=-0.02, df=53 p=0.98), males had greater mean average of GM (639.5 ± 55.6 mm^3), WM (609.9 ± 68.2 mm^3), CSF (251.6 ± 27.6 mm^3), and TIV (1501.1 ± 135.9 mm^3) than females GM (598.9 ± 49.8 mm^3), WM (527.6 ± 45.6 mm^3), CSF (222.3 ± 26.8 mm^3), and TIV (1348.9 ± 92.5 mm^3) (Table 6.2). Independent samples t-test of variances between sexes showed significant differences between males and females in the GM (t=2.86, df=53, p=0.01), WM (t=5.31, df=53, p =0.00), CSF (t=3.99, df=53, p=0.00) and TIV (t=4.90, df=53, p=0.00), suggesting that there is a difference in tissue compartment volumes between males and females.

Among all subjects, the correlation between age and TIV indicated no significant age related differences in head size (r=-0.09, p=0.53). However, a significant negative correlation was seen for GM volume with age (r=-0.45, p=0.00) (Table 6.1, Figure 6.1). This correlation (Table 6.2) was significantly higher in females (r =-0.59, p=0.00) than in males (r=-0.37, p=0.06) (Figure 6.2). On the other hand, the WM, CSF and TIV did not show any significant correlation with age in females or males (Table 6.2).

		Age	Mean ± SD
	N	55	
Grey Matter (GM)	Pearson Correlation	-.45	
	Sig. (2-tailed)	.00	617.9 ± 55.7
White Matter (WM)	Pearson Correlation	.11	
	Sig. (2-tailed)	.40	564.9 ± 66.6
Cerebrospinal Fluid (CSF)	Pearson Correlation	.18	
	Sig. (2-tailed)	.20	235.1 ± 28.4
Total Intracranial	Pearson Correlation	-.09	
Volume (TIV)	Sig. (2-tailed)	.53	1417.9 ± 130.9

Table 6.1: Results of all subjects mean average (±S.D.) of GM, WM, CSF, TIV, and correlation with age. Yellow shaded cells indicate significant correlations.

	Sex	N	Person Correlation	Sig. (2-tailed)
GM	**M**	26	-.37	.06
	F	29	-.59	.00
WM	**M**	26	.22	.28
	F	29	.08	.69
CSF	**M**	26	.12	.56
	F	29	.27	.16
TIV	**M**	26	-.02	.93
	F	29	-.20	.29

Table 6.2: Sexes mean averages and S.D. of the GM, WM, CSF, and TIV volumes and correlation with age. Yellow shaded cells indicate significant correlations.

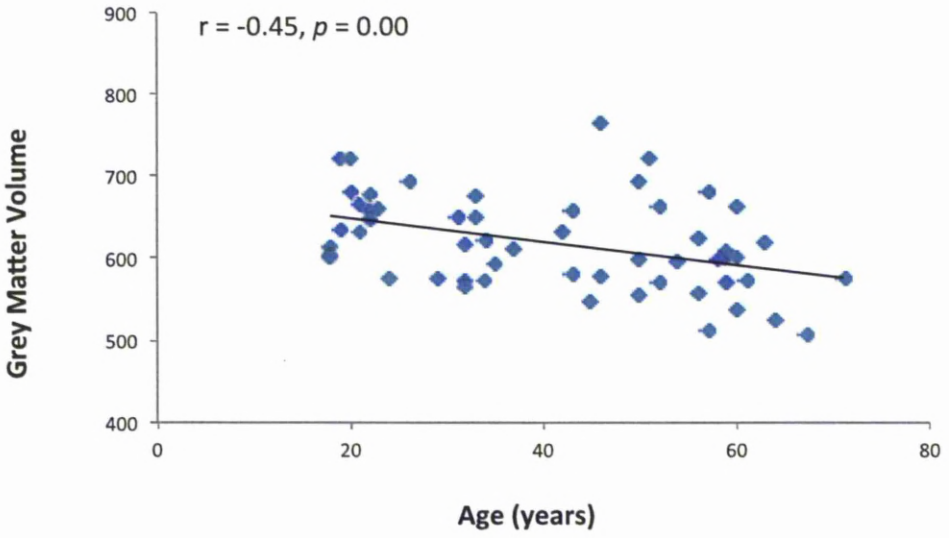

Figure 6.1: Correlation between grey matter volume and age among all subjects.

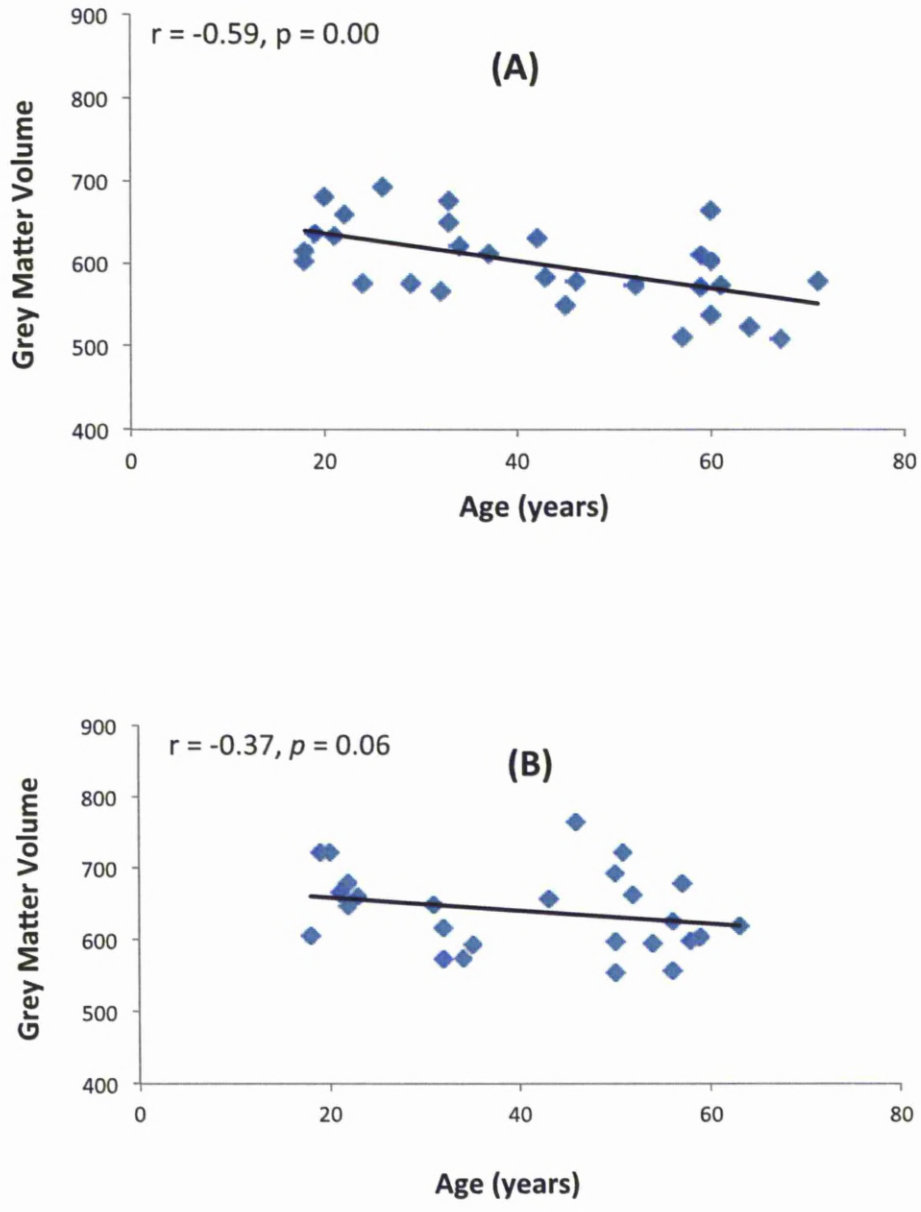

Figure 6.2: Correlation between grey matter volume and age in (A) females and (B) in males.

6.4.2 Cognitive Assessment Data:

Independent samples t-test of variances between sexes showed significant differences between males and females in the digit span forward (t=-2.15, df=53, p=0.04) and digit symbol (t=-2.52, df=53, p=0.02). Data were then tested for correlation with age using (PASW Statistics v18.0), the results of Pearson product moment correlation is presented in (Table 6.3). Bonferroni multiple comparisons corrections were performed, with alpha (corrected) = 0.007. The mean level of education for all subjects was 17 years, SD 3.2 years with no significant effect of age (r=-0.02, p=0.9). No subjects were excluded on the basis of their performance on the cognitive assessment tests. The digit symbol test showed a significant correlation with age among all subjects (r=-0.54, p=0.00) (Figure 6.3 and Table 6.3). This correlation was larger in females (r=-0.58, p=0.00) than males (r=-0.50, p=0.01) (Figure 6.4 and Table 6.4). Results of Fisher's Z transformations showed no significant difference in these correlations (Z=-0.4, p=0.69). Interestingly, the digit span backward test was significantly negative correlated with age in females (r=-0.40, p=0.03) but not in males (r=0.19, p=0.35) (Figure 6.5 and Table 6.4). Fisher's Z transformations showed significant difference in these correlations (Z=-2.15, p=0.03). Conversely, the digit span forward test was significantly positively correlated with age in males (r=0.40, p=0.05) but not in females (r=-0.26, p=0.17) (Figure 6.6 and Table 6.4). The Fisher's Z results also showed significant difference in these correlations (Z=-2.41, p=0.02).

		Age	Mean ± SD
	N	55	
Trail Making A	Pearson Correlation	.23	
	Sig. (2-tailed)	.1	21.2 ± 7.2 seconds
Trail Making B	Pearson Correlation	-.01	
	Sig. (2-tailed)	.92	41.7 ± 17.7 seconds
Trail Making B-A	Pearson Correlation	-.10	
	Sig. (2-tailed)	.46	20.5 ± 14.1 seconds
Digit Span Forward	Pearson Correlation	.04	
	Sig. (2-tailed)	.78	9.7 ± 2.4
Digit Span	Pearson Correlation	-.15	
Backward	Sig. (2-tailed)	.27	8.6 ± 2.7
Digit Symbol	Pearson Correlation	**-.54**	
	Sig. (2-tailed)	**.00**	64.8 ± 13.0
Verbal Fluency	Pearson Correlation	.17	
Total	Sig. (2-tailed)	.22	52.4 ± 13.6

Table 6.3: Results of the cognitive assessment tests mean average, (±S.D.), and correlation with age among all subjects. Yellow Shaded cells indicate significant correlations after correcting for alpha = 0.007.

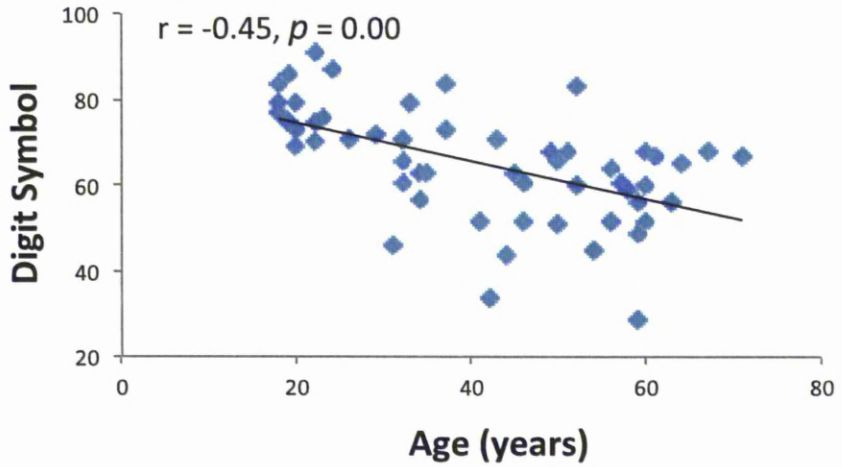

Figure 6.3: Correlation between digit symbol test and age among all subjects.

	Sex	N	Mean	Std. Deviation	Correlation	Sig. (2-tailed)
Trail Making A	M	26	21.73	6.53	.16	.44
	F	29	20.72	7.95	.28	.15
Trail Making B	M	26	44.80	21.45	-.13	.54
	F	29	38.93	13.51	.18	.36
Trail Making A-B	M	26	23.08	17.95	-.21	.31
	F	29	18.21	9.17	0.02	.91
Digit Span Forward	M	26	9.04	2.49	**.40**	**.05**
	F	29	10.38	2.14	-.26	.17
Digit Span	M	26	8.15	2.71	.19	.35
Backward	F	29	9.03	2.81	**-.40**	**.03**
Verbal Fluency Total	M	26	50.54	14.19	.01	.95
	F	29	54.69	12.96	.30	.11
Digit Symbol	M	26	60.34	10.65	**-.50**	**.01**
	F	29	68.83	13.85	**-.58**	**.00**

Table 6.4: Mean averages and S.D. of the cognitive assessment tests and correlation with age. Yellow shaded cells indicate significant correlations. Gray shaded cells are borderline after correcting for alpha = 0.007.

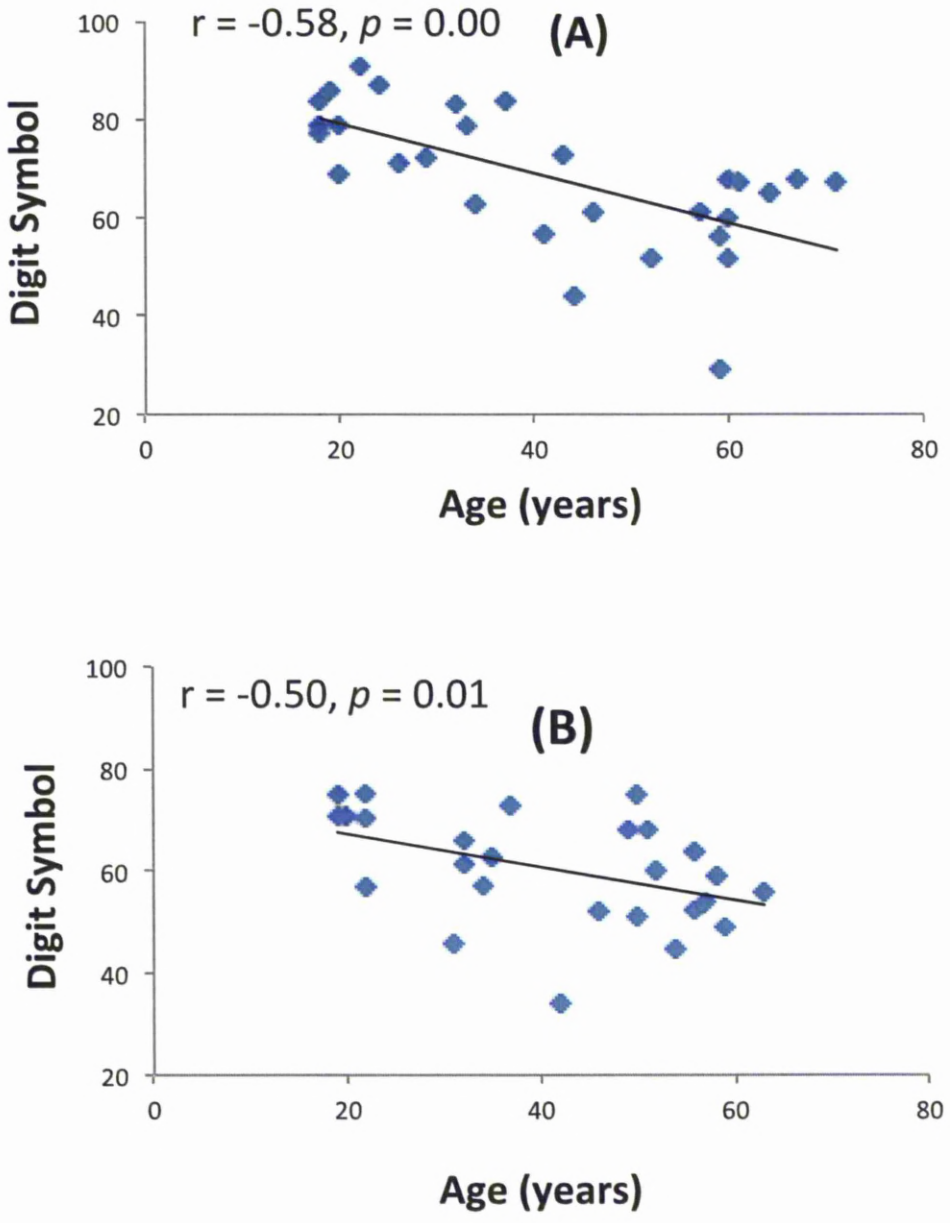

Figure 6.4: Correlation between digit symbol test and age in (A) females and (B) in males.

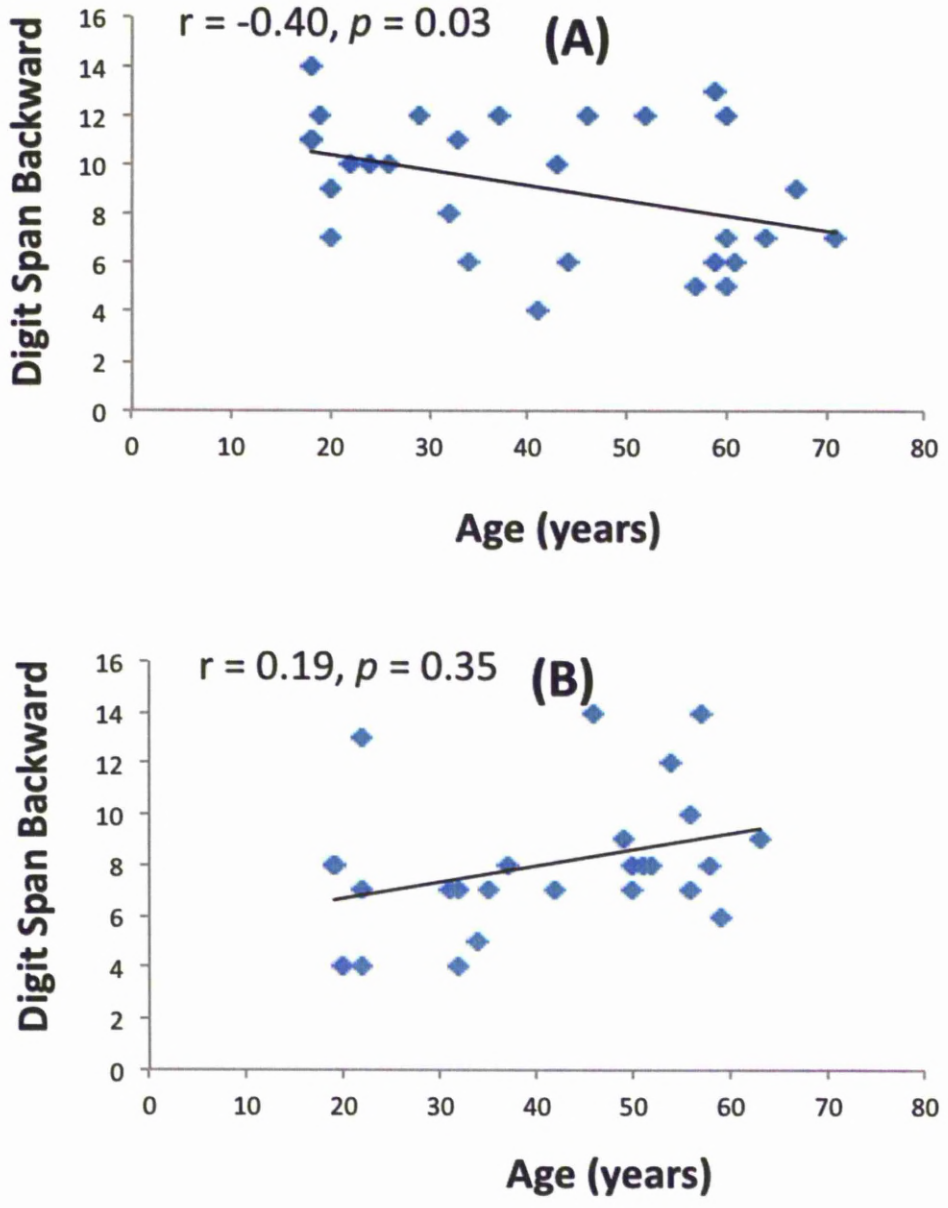

Figure 6.5: Correlation between digit span backward test and age in (A) females and (B) in males.

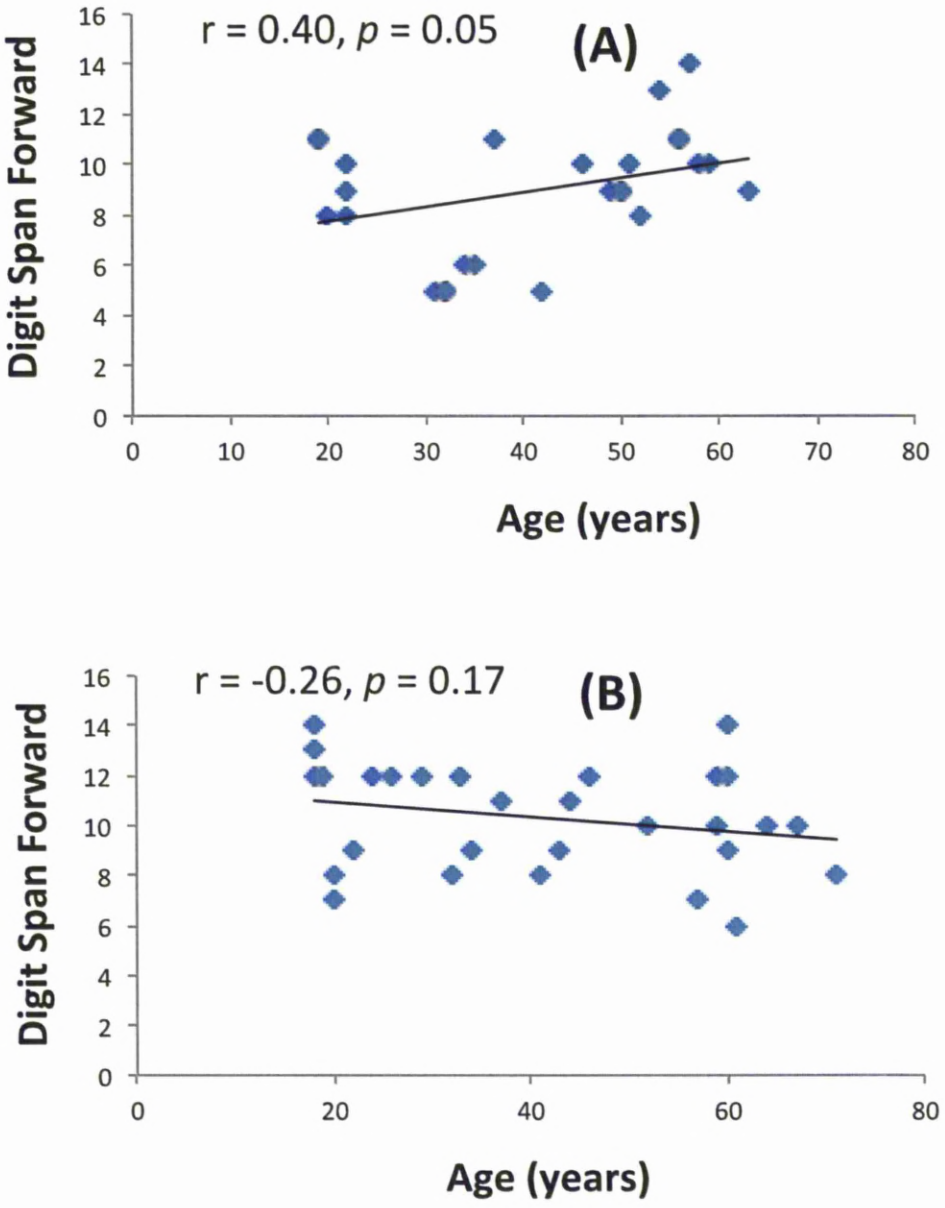

Figure 6.6: Correlation between digit span forward test and age in (A) males and (B) in females.

6.4.3 VOXEL BASED MORPHMETRY RESULTS

Grey Matter

Global Effect of Aging Among all Subjects:

We investigated the age-related changes in GM density among all subjects *with a voxel-based multiple regression analysis tool SPM8, resulting in a 3D t-statistic map.* There were no positive correlations between GM density and age; the negative correlations are shown in (Figure 6.7). Table 6.5 illustrates the Talairach coordinates, and anatomical regions for significant clusters for GM regions.

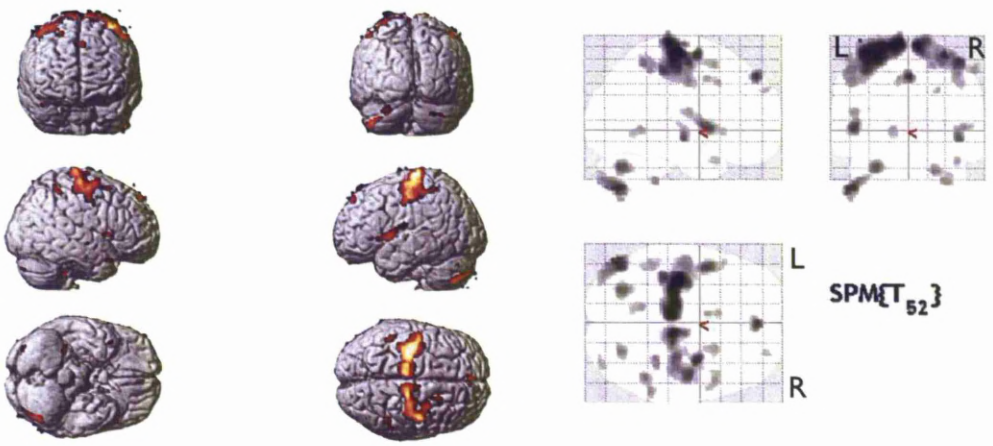

Figure 6.7: Statistical parametric maps, in sagittal, coronal and axial projections showing significant clusters (height threshold p=0.05, corrected, extent threshold, p=0.05) with statistically significant negative correlation with grey matter density in all subjects.

Region	BA	Talairach Coordinates X	Y	Z
Left paracentral lobule	4a & 6	-8	-25	75
Left superior medial frontal gyrus	6	2	50	46
Left insula lobe		-46	8	1
Left SMA	6	-8	8	45
Left inferior frontal gyrus	44, 45, 46	-51	21	-2
Left inferior partial lobule	40	-50	-42	57
Left lingual gyrus	17 & 18	-14	-51	0
Left Heschl's gyrus	41 & 42	-44	-16	6
Right paracentral lobule	4a & 6	9	-24	73
Right superior frontal gyrus	6	21	14	57
Right inferior frontal gyrus	44 & 45	48	14	3
Right superior temporal gyrus	22	45	-13	-6
Right temporal pole		44	15	-26
Right inferior partial lobule	40	46	-48	57

Table 6.5: Regional grey matter negative correlated with age in all subjects (p=0.05). BA= Broadmann's *areas*.

Group Sexes Differences:

The full factorial model of analysis of variance was used to address the differences in GM density. For all VBM-DARTEL analyses, TIV was used as a vector of global values for estimating global effects. We first investigated sex by age interactions. Three areas of GM density showed significant interaction (including right superior medial frontal gyrus, left inferior frontal gyrus, and left inferior temporal gyrus) had significantly greater density reduction in male than female with increasing age (Figure 6.8) (Table 6.6). Therefore, we investigated the correlations between aging and GM density losses within age groups were examined in both males and females. Additionally, two-sample t-test was computed for age-based analyses within each sex, males and females were subdivided into two groups (above 50 years and under 50 years). In each analysis, two contrasts were examined: 1) identifying local increases in GM density between males above 50 years and under

50 years old; 2) identifying local increases in GM density between females above 50 years and less than 50 years old.

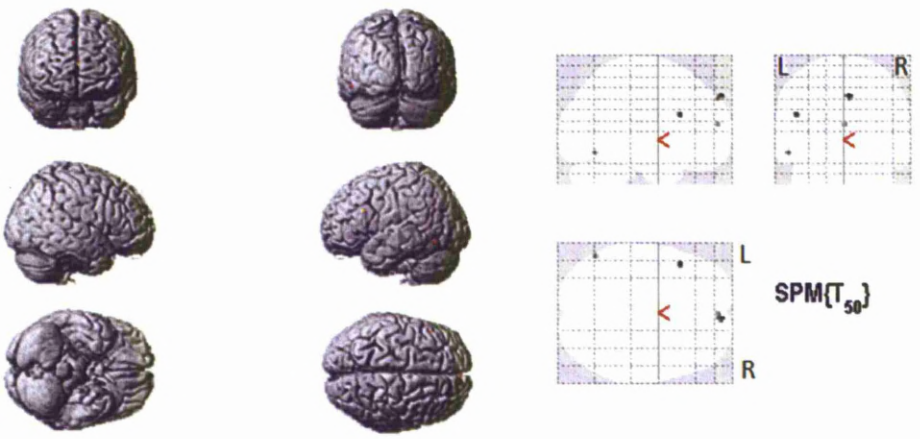

Figure 6.8: Statistical parametric maps, in sagittal, coronal and axial projections showing significant clusters (height threshold p=0.001, uncorrected) of GM density age by sex interaction.

Region	BA	Talairach Coordinates X	Y	Z
Left inferior frontal gyrus	45	-47	21	25
Left inferior temporal gyrus	20	-54	-63	-11
Right superior medial frontal gyrus	6	2	59	16

Table 6.6: Regional grey matter density age by sex interaction. BA= Broadmann's *areas.*

Global Effect of Aging between Sexes:

The association between age and GM density was investigated in each sex with a voxel-based multiple regression analysis tool SPM8, resulting in a 3D *t*-statistic map.

Male

There were no positive correlations between GM density and age in males. The negative correlations are shown in (Figure 6.9). Table 6.7 illustrates the Talairach coordinates, and anatomical regions for significant clusters for GM regions.

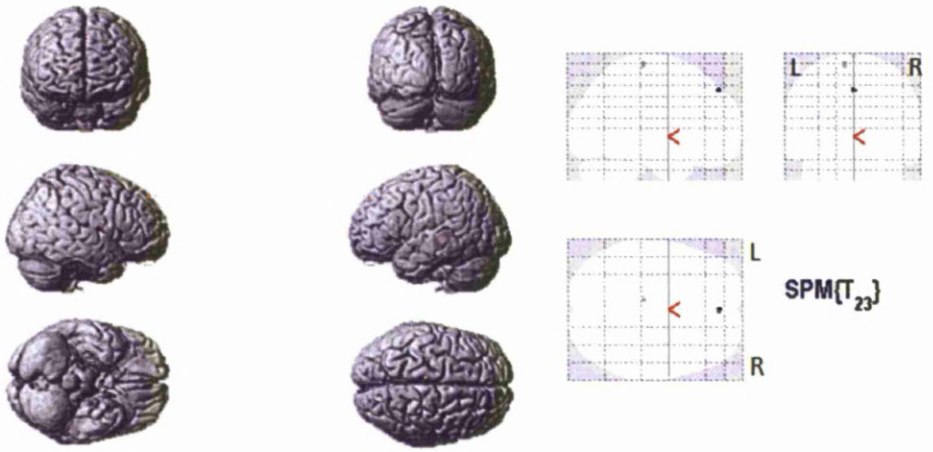

Figure 6.9: Statistical parametric maps, in sagittal, coronal and axial projections showing significant clusters (height threshold p=0.05, corrected, extent threshold, p=0.05) with statistically significant negative correlation with grey matter density in Male subjects.

Region	BA	Talairach Coordinates X	Y	Z
Left superior medial frontal gyrus	6	0	50	46
Left paracentral lobule	4a & 6	-9	-24	72

Table 6.7: Regional grey matter negative correlated with age in males (p = 0.05). BA=*Brodmann's areas.*

Female

There were no positive correlations between GM density and age in females. The negative correlations are shown in (Figure 6.10). Table 6.8 illustrates the Talairach coordinates, and anatomical regions for significant clusters for GM regions.

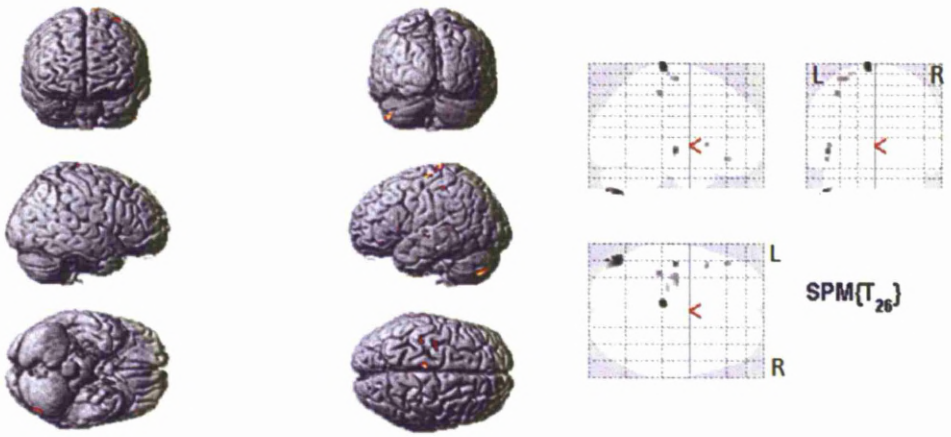

Figure 6.10: Statistical parametric maps, in sagittal, coronal and axial projections showing significant clusters (height threshold p=0.05, corrected, extent threshold, p=0.05) with statistically significant negative correlation with grey matter density in Female subjects.

Region	BA	Talairach Coordinates X	Y	Z
Left paracentral lobule	4a & 6	-6	-27	78
Left superior temporal gyrus	22	-47	-15	-5
Left precentral gyrus (M1)	4	-29	-13	67
Left postcentral gyrus	1,2,3	-38	-30	52
Left frontal gyrus	44 & 45	-48	36	-12

Table 6.8: Regional grey matter negative correlated with age in females (p =0.05). BA =*Brodmann's areas.*

Males above 50 years old greater than Males under 50 years old

There were no regions of increased GM density identified in males above 50 years old in comparison to males under 50 years old.

Males under 50 years old greater than Males above 50 years old

Figure 6.11 shows the regions of increased GM density identified in males under 50 years old in comparison to males above 50 years old. The Talairach coordinates, and anatomical regions for significant clusters for GM regions are illustrated in (Table 6.9).

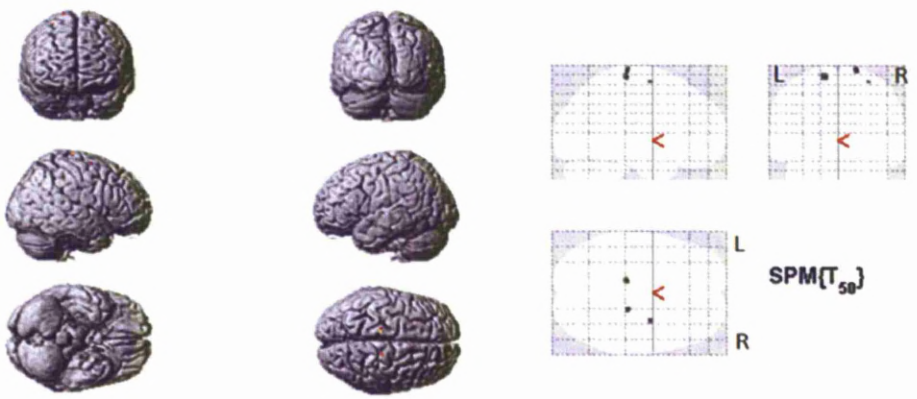

Figure 6.11: Statistical parametric maps, in sagittal, coronal and axial projections showing significant clusters (height threshold p=0.05, corrected, extent threshold, p=0.05) with statistically significant regions of increased grey matter density in male subjects less than 50 years old.

Region	BA	Talairach Coordinates X	Y	Z
Left paracentral lobule	4a, 6	-12	-25	70
Right precentral gyrus	4a, 6	18	-25	76
Right superior frontal gyrus	6	30	-3	64

Table 6.9: Regional grey matter increased in males under 50 years old (p=0.05). BA = *Brodmann's areas.*

Females above 50 years old greater than Females under 50 years old

There were no regions of increased GM density identified in females above 50 years old in comparison to females under 50 years old.

Females under 50 years old greater than Females above 50 years old

There were regions of increased GM density identified in females under 50 years old in comparison to females above 50 years old (Figure 6.12). Table 6.10 illustrates the Talairach coordinates, and anatomical regions for significant clusters for GM regions.

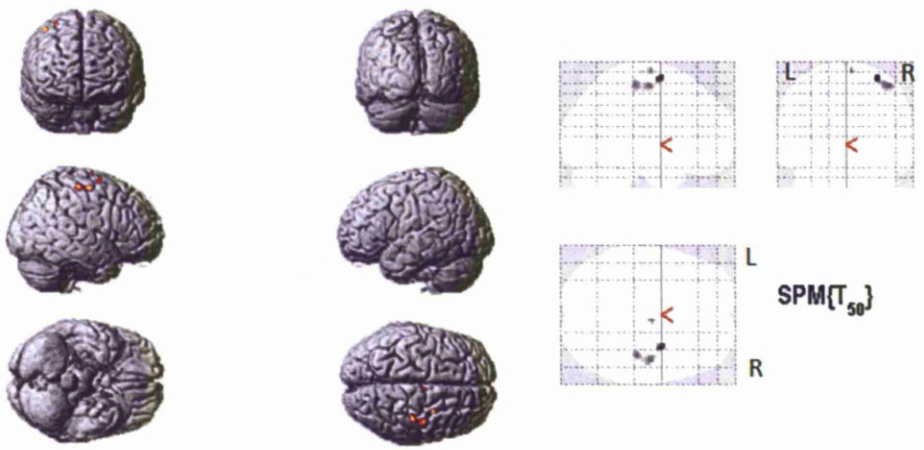

Figure 6.12: Statistical parametric maps, in sagittal, coronal and axial projections showing significant clusters (height threshold $p<0.05$, corrected, extent threshold, $p=0.05$) with statistically significant regions of increased grey matter density in female subjects less than 50 years.

Region	BA	Talairach Coordinates X	Y	Z
Left precentral gyrus	4a, 6	-24	-25	63
Right precentral gyrus	4a, 6	44	-12	58
Right SMA	6	6	-10	73
Right superior frontal gyrus	6	32	-1	66

Table 6.10: Regional grey matter increased in females under 50 years old ($p=0.05$). BA=*Brodmann's areas.*

In summary, regions of GM density that showed significant negative correlation with age were found in the bilateral paracentral lobule, superior medial frontal gyrus, inferior frontal gyrus, inferior partial lobule, right superior temporal gyrus, right temporal pole, left insula lobe, left SMA, left, left lingual gyrus and left Heschl's gyrus.

Grey Matter Correlations with Cognitive Performance among all Subjects

We investigated the age-related changes in GM density and cognitive assessment scores that showed significant correlation with age among all subjects (Table 6.3) and in each sex (Table 6.4).

Digit span forward

There were no GM regions in male that were significantly correlated (either positively or negatively) with digit span forward test among the male subjects.

Digit span backward

There were no GM regions in males that were significantly correlated (either positively or negatively) with Digit span backward test.

Digit symbol

In this analysis, the correlation between GM density and digit symbol performance was investigated among all subjects using the multiple regression analysis tool SPM8. There were no negative correlations between GM density and digit symbol test among all subjects. The positive correlations are shown in (Figure

6.13). The Talairach coordinates, and anatomical regions for significant clusters for GM regions are illustrated in (Table 6.11).

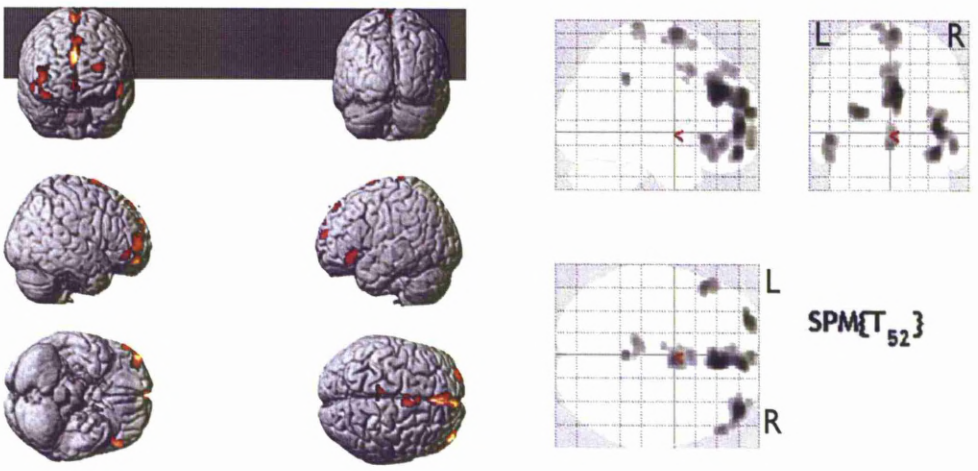

Figure 6.13: Statistical parametric maps, in sagittal, coronal and axial projections showing significant clusters (height threshold p=0.001, uncorrected, extent threshold, p=0.05) with statistically significant positive correlation with grey matter density in all subjects.

Region	BA	Talairach Coordinates		
		X	Y	Z
Left superior frontal gyrus	6	-26	63	15
Left superior medial frontal gyrus	6	-4	50	45
Left paracentral lobule	4a, 6	-10	-33	78
Left SMA	6	0	14	45
Left inferior frontal gyrus	45	-51	26	-5
Left middle cingulate cortex	6	0	-40	40
Right middle orbital gyrus	11	2	65	-9
Right superior medial frontal gyrus	6	6	75	25
Right middle cingulate cortex	6	6	36	30
Right inferior frontal gyrus	45	54	41	-9
Right middle frontal gyrus	6	41	56	4

Table 6.11: Regional grey matter positive correlated with digit symbol test in all subjects (p=0.05).

BA =*Brodmann's areas.*

Grey Matter Correlations with Cognitive Performance Within Sexes

In this analysis correlations between GM density and cognitive test performance, that showed strong correlation with age, were investigated using multiple regression analysis tool SPM8.

Male

Digit span forward

There were no GM regions in male that were significantly correlated (either positively or negatively) with digit span forward test among the male subjects.

Digit span backward

There were no GM regions in males that were significantly correlated (either positively or negatively) with Digit span backward test.

Digit symbol

There were no negative correlation between GM density and digit symbol test among the male subjects. However, the positive correlations are shown in (Figure 6.14). The Talairach coordinates, and anatomical regions for significant clusters for GM regions are illustrated in (Table 6.12).

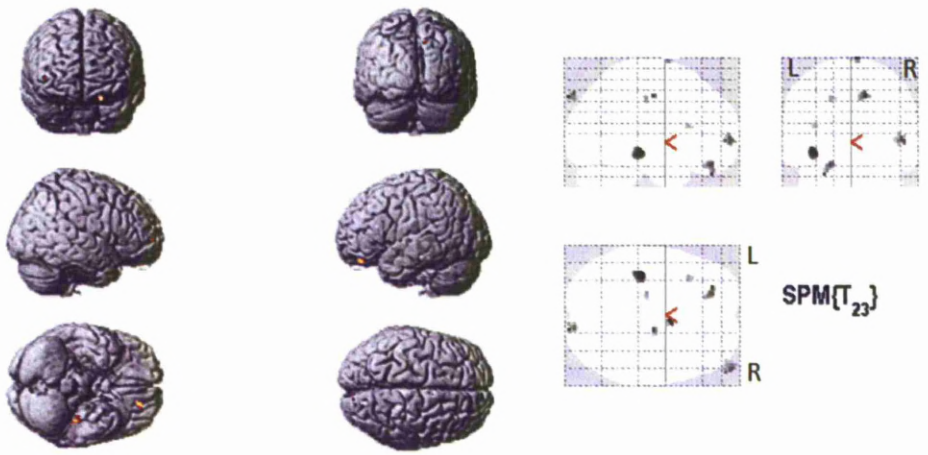

Figure 6.14: Statistical parametric maps, in sagittal, coronal and axial projections showing significant clusters (height threshold p=0.001, uncorrected, extent threshold, p=0.05) with statistically significant positive correlation with grey matter density in Male subjects.

Region	BA	Talairach Coordinates X	Y	Z
Left Hippocampus		-36	-25	-8
Left superior orbital gyrus	47	-20	45	-20
Left inferior frontal gyrus	44	-35	23	16
Right middle cingulate cortex	6	14	-12	46

Table 6.12: Regional grey matter positive correlated with digit symbol test in males (p=0.05). BA =*Brodmann's areas.*

Female

Digit span forward

There were no GM regions in female that were significantly correlated (either positively or negatively) with Digit span forward test.

Digit span backward

There were no GM regions in female that were significantly correlated (either positively or negatively) with Digit span backward test.

Digit symbol

There were no negative correlation between GM density and digit symbol test among the female subjects. The positive correlations are shown in (Figure 6.15). The Talairach coordinates, and anatomical regions for significant clusters for GM regions are illustrated in (Table 6.13).

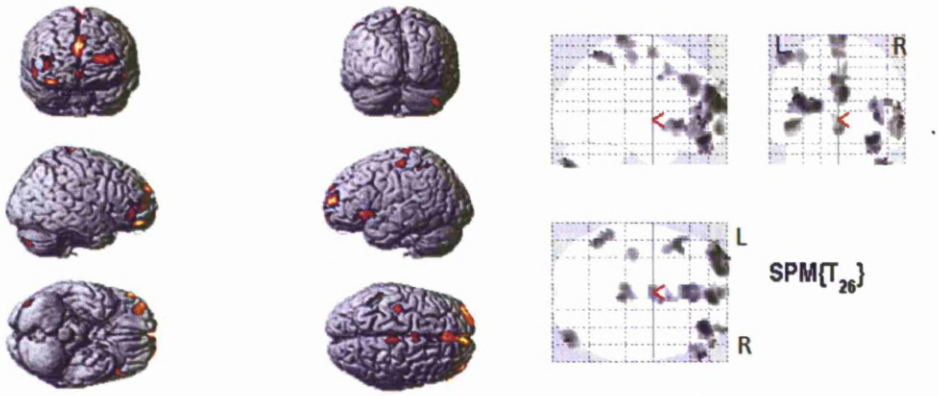

Figure 6.15: Statistical parametric maps, in sagittal, coronal and axial projections showing significant clusters (height threshold p=0.001, uncorrected, extent threshold, p=0.05) with statistically significant positive correlation with grey matter density in Female subjects.

Region	BA	Talairach Coordinates X	Y	Z
Left superior frontal gyrus	6	-21	65	15
Left superior medial gyrus	6	-3	32	39
Left paracentral lobule	4a, 6	-5	-27	78
Left SMA	6	-2	-1	64
Left precentral gyrus	4a, 6	-38	-19	61
Right middle orbital gyrus	11	35	50	-18
Right superior medial frontal gyrus	6	6	57	27
Right middle cingulate cortex	6	6	41	30
Right paracentral lobule	6	5	-30	81
Right middle frontal gyrus	10	39	56	4

Table 6.13: Regional grey matter positive correlated with digit symbol test in females (p=0.05). BA =Brodmann's areas.

In summary, regions of GM density that showed significant positive correlation with performance on digit symbol test were found in the bilateral superior medial, inferior, middle frontal gyrus, paracentral lobule, middle cingulate cortex, middle orbital gyrus, right middle orbital gyrus, left SMA, left Hippocampus left superior orbital gyrus and left precentral gyrus. No other correlations were found between GM density and performance on other cognitive tests.

White Matter

We investigated the age-related changes in WM density among all subjects and each sex with a voxel-based multiple regressions analysis tool SPM8. No correlations were found between WM density and age among all subjects or in each sex. The full factorial model of analysis of variance was used to address the differences in WM between the groups in each sex. For all VBM analyses, TIV was used as a vector of global values for estimating global effects. There were no areas of increased WM density between the groups in males or females.

6.5 DISCUSSION AND CONCLUSION

This study explored sex-related differences in regional GM density in a representative healthy population (age ranged 18-71 years), by applying VBM-DARTEL analysis. To our knowledge, this is the first study that shows the correlations of the tissue density of GM/WM with age, sex and several cognitive tests using the DARTEL-VBM analysis in healthy subjects aged 18-71 years. The objectives of this study were to evaluate the global volume change of the GM and

WM with age, sex and to evaluate the correlations of the tissue probabilities of the GM with performance on brief cognitive tests by a VBM-DARTEL analysis.

6.5.1 Volumetric analysis of correlation of GM, WM & TIV with age:

In our study comparisons of brain volumes showed sex differences in correlation with age, similar to what has been reported by some studies (Cowell et al., 1994, Good et al., 2001b, Gur et al., 1999, Murphy et al., 1996, Raz et al., 1997). The total brain volume ($p = 0.00$), GM ($p = 0.02$) and WM ($p = 0.00$) partitions were larger in males (see Table 6.2) compared with females in accordance with previous literature (Coffey et al., 1998, Good et al., 2001b, Gur et al., 1991, Gur et al., 1999, Murphy et al., 1996, Raz et al., 1997, Smith et al., 2007). Among all subjects, there was a significant decline of global GM volume with age ($r = -0.41$, $p = 0.00$) (see Figure 6.1) (Good et al., 2001b, Smith et al., 2007). Females had a significantly steeper decline ($r = -0.58$, $p = 0.00$) in GM volume with age than males ($r = -0.34$, $p = 0.09$) (see Figure 6.2) (Good et al., 2001a). We did not observe any WM, CSF or TIV correlation with age in both males and females (Taki et al., 2004). Similar to the previous findings, these results clearly indicate that the main factor contributing to brain atrophy with ageing is the volume reduction of the GM.

6.5.2 Voxel-based morphometry of grey matter:

Among all subjects, the regional changes of GM density with aging were most prominent in the frontal cortices, the strongest correlation with age was seen in the paracentral gyrus (BA 4 and 6), supplementary motor area (SMA) (B6), superior frontal gyrus (BA 6), inferior frontal gyrus (BA 44 and 45) (Table 6.14). Figure 6.7

shows the regions in which GM density significantly and negatively correlated with age among all subjects.

Significantly greater GM density reductions in male than female with increasing age (age by sex interaction) were found in the right superior medial frontal gyrus (BA 6), left inferior frontal gyrus (BA 45), and left inferior temporal gyrus (BA 20). In both sexes correlations were found in the left paracentral lobule (BA 6, 4a) (Table 6.14). In males, these correlations were found in the left superior medial frontal gyrus (BA 6) (Table 6.14). In females, the strong correlations were found in left superior temporal gyrus (BA 22), left precentral gyrus which also called primary motor cortex (M1) (BA 4), left postcentral gyrus (BA 1, 2 and 3) and left frontal gyrus (BA 44 and 45) (Table 6.14). These findings are in agreement with some previous standard VBM studies (Table 6.15).

Comparison	Regions	BA	Talairach Coordinates X	Y	Z
All subjects age related regression (negative)	Left paracentral lobule	4a & 6	-8	-25	75
	Left superior medial frontal gyrus	6	2	50	46
	Left insula lobe		-46	8	1
	Left SMA	6	-8	8	45
	Left inferior frontal gyrus	44, 45, 46	-51	21	-2
	Left inferior partial lobule	40	-50	-42	57
	Left lingual gyrus	17 & 18	-14	-51	0
	Left Heschl's gyrus	41 & 42	-44	-16	6
	Right paracentral lobule	4a & 6	9	-24	73
	Right superior frontal gyrus	6	21	14	57
	Right inferior frontal gyrus	44 & 45	48	14	3
	Right superior temporal gyrus	22	45	-13	-6
	Right temporal pole		44	15	-26
	Right inferior partial lobule	40	46	-48	57
Male group age related regression (negative)	Left superior medial frontal gyrus	6	0	50	46
	Left paracentral lobule	4a & 6	-9	-24	72
Female group age related regression (negative)	Left paracentral lobule	4a & 6	-6	-27	78
	Left superior temporal gyrus	22	-47	-15	-5
	Left precentral gyrus	4	-29	-13	67
	Left postcentral gyrus	1, 2, 3	-38	-30	52
	Left frontal gyrus	44 & 45	-48	36	-12
Males Above 50 > Males Under 50	No significant regions				
Females Above 50 > Females Under 50	No significant regions				
Males Under 50 > Males Above 50	Left paracentral lobule	4a & 6	-12	-25	70
	Right precentral gyrus	4a & 6	18	-25	76
	Right superior frontal gyrus	6	30	-3	64
Females Under 50 > Females Above 50	Left precentral gyrus	4a & 6	-24	-25	63
	Right precentral gyrus	4a & 6	44	-12	58
	Right SMA	6	6	-10	73
	Right superior frontal gyrus	6	32	-1	66

Table 6.14: Summery of voxel-based morphometry analyses. BA =*Brodmann's areas.*

Lobe	Region of Grey Matter Reduction	Study by
Frontal	Left Precentral gyrus (present study)	(Good et al., 2001b, Lemaitre et al., 2005, Taki et al., 2004)
	Left Postcentral gyrus (present study)	(Good et al., 2001b, Lemaitre et al., 2005)
	Left Superior frontal gyrus (present study)	(Tisserand et al., 2002)
	Left Inferior frontal gyrus (present study)	(Good et al., 2001b, Tisserand et al., 2002, Van Laere and Dierckx, 2001)
	Left Orbital frontal	(Lemaitre et al., 2005, Tisserand et al., 2002)
	Left Middle frontal gyrus (present study)	(Good et al., 2001b, Lemaitre et al., 2005, Tisserand et al., 2002, Van Laere and Dierckx, 2001)
	Left Frontal pole (present study)	(Tisserand et al., 2002)
	Right Precentral gyrus (present study)	(Good et al., 2001b)
	Right Superior frontal gyrus (present study)	(Tisserand et al., 2002)
	Right Inferior frontal gyrus (present study)	(Good et al., 2001b, Tisserand et al., 2002, Van Laere and Dierckx, 2001)
	Right Orbital frontal	(Lemaitre et al., 2005, Tisserand et al., 2002)
	Right Middle frontal gyrus	(Good et al., 2001b, Lemaitre et al., 2005, Tisserand et al., 2002, Van Laere and Dierckx, 2001)
Temporal	Left Heschl's gyrus (present study)	(Good et al., 2001b, Lemaitre et al., 2005)
	Left Superior temporal gyrus (present study)	(Good et al., 2001b, Taki et al., 2004, Van Laere and Dierckx, 2001)
	Left Hippocampus	(Lemaitre et al., 2005, Van Laere and Dierckx, 2001)
	Right Heschl's gyrus	(Good et al., 2001b, Lemaitre et al., 2005)
	Right Superior temporal gyrus (present study)	(Good et al., 2001b, Taki et al., 2004, Van Laere and Dierckx, 2001)
	Right Hippocampus	(Van Laere and Dierckx, 2001)
Parietal	Left Inferior parietal gyrus (present study)	(Good et al., 2001b, Van Laere and Dierckx, 2001)
	Left Superior parietal gyrus	(Lemaitre et al., 2005)
	Left Angular gyrus	(Good et al., 2001b)
	Right Postcentral gyrus	(Good et al., 2001b, Lemaitre et al., 2005)
	Right Angular gyrus	(Good et al., 2001b)
Occipital	Left Occipital	(Van Laere and Dierckx, 2001)
	Right Occipital	(Van Laere and Dierckx, 2001)
Cingulate	Anterior cingulate sulcus	(Good et al., 2001b, Tisserand et al., 2002)
	Middle Cingulate gyrus	(Van Laere and Dierckx, 2001)
Insular	Left Insula (present study)	(Good et al., 2001b, Van Laere and Dierckx, 2001)
	Right Insula	(Good et al., 2001b, Van Laere and Dierckx, 2001)

Table 6.15: Results of previous VBM studies, shown regions of GM negatively correlated with age.

No regions of increased GM density were found in groups above 50 years old when compared to groups less than 50 years old in both sexes (Table 6.14). However, Figure 6.11 shows the regions in which GM density were significant increased in males less than 50 years when compared to males above 50 years old. These regions were identified in left paracentral lobule (BA 6 and 4a), right precentral gyrus (BA 6 and 4a) and right superior frontal gyrus (BA 6). Significant regions of increased GM density were also found in females less than 50 years when compared to females above 50 years old. These regions were identified (see Figure 6.12) in bilateral precentral gyrus (BA 6 and 4), right superior frontal gyrus (BA 6), and right SMA (BA 6).

Previous VBM studies have found age-related GM reduction bilaterally in the superior parietal gyri, pre- and postcentral gyri, insula/ frontal operculum, and anterior cingulate (Good et al., 2001b). Other VBM studies have suggested sex differences in regional GM volume. For example, Good et al. (2001b), found that males have a larger volume of cortical GM in the limbic region. Whereas, females have an increased GM volume compared with males in the FL. Chen et al. (2007) revealed that males have more GM density in the midbrain, left inferior temporal gyrus, right occipital lingual gyrus, right middle temporal and in both cerebellar hemispheres, while females showed greater GM density in the cingulate cortices and right inferior parietal lobule.

Few VBM studies have reported sex by age differences in regional GM volume. Taki et al. (2004) reported reduction in GM density bilaterally in the superior temporal gyri in males, and in the left superior temporal gyrus and the left precentral gyrus in females. More recently however, Smith et al. (2007) did not observe any significant sex differences in GM with age.

Non-VBM studies have also suggested GM regional sex differences with age. Cowell et al. (1994), for instance, observed more reduction in GM volume occurred in males than in females in FL and TL regions. Murphy et al. (1996) suggested an earlier or faster volume loss in the FL and TL in males, and in the PL and hippocampus region in females. Raz et al. (1997) demonstrated a steeper trend of age-related changes in the inferior temporal cortex in males. Overall, and despite methodological differences, our results agree with these studies in which the frontal cortices experience the most age-related effects.

6.5.3 Voxel-based morphometry: correlation of GM with Cognitive Performance:

In this study the hypothesis was tested that age-related decline in cognitive functioning would be associated with changes in GM density. It was expected that reductions in GM brain density would be related to a decline in performance on cognitive tests designed to assess frontal lobe functions. We investigated the relation between GM density, digit span forward, digit span backward and digit symbol tests which were significantly correlated with age in each sex (West, 1996). A significant positive correlation could be established between GM density and the digit symbol test among all subjects (Figure 6.13) in the left superior frontal gyrus (BA 6), left paracentral lobule (BA 4 and 6), left SMA (BA 6), bilateral superior medial frontal gyrus (BA 6), bilateral inferior frontal gyrus (BA 45), bilateral middle cingulate cortex (BA 6), right middle orbital gyrus (BA 11) and right middle frontal gyrus (BA 6).

This VBM result showed similar positive correlations between GM density and digit symbol performance in both sexes. In males, the correlations with age were found in the left hippocampus, left superior orbital gyrus (BA 47), left inferior frontal gyrus (BA 44) and right middle cingulate cortex (BA 6) (Figure 6.14). While, in females the correlations with age were found in bilateral frontal gyrus, (BA 6) bilateral paracentral lobule (BA 4and and 6), left SMA (BA 6), left precentral gyrus (BA 6, 4a), right middle orbital gyrus (BA 11), and right middle cingulate cortex (BA 6) (Figure 6.15). These regions could be highly associated with improved performance on the specific cognitive test.

Prefrontal cortex volumes has been found to be associated with performance on executive tasks such as Wisconsin Card Sorting Test (Gunning-Dixon and Raz,

2003, Raz et al., 1998) as well as with performance in visuospatial skills (Raz et al., 1999), episodic memory performance (Head et al., 2008) and fluid intelligence (Raz et al., 2008). Larger hippocampal volumes were observed in younger adults who showed better spatial memory performance than the older adult (Driscoll et al., 2003). The association between performance on cognitive tests and changes in regional GM volumes remains inconclusive (Raz and Rodrigue, 2006). Van Petten et al. (2004) gave an overview of many studies of healthy participants and concluded that it has been difficult to determine strong associations between neuropsychological functioning and brain morphometry. When structure cognition relations are found, they are not easily replicated and appear sensitive to the choice of cognitive tests (Raz and Rodrigue, 2006).

6.5.4 Voxel-based morphometry of white matter

There were no significant correlation between age and WM density among all subjects or in each sex in accordance with previous findings (Taki et al., 2004). These findings clearly indicate that the main factor contributing to brain atrophy with age is the density reduction of the GM, but not WM.

6.6 Methodological Considerations

A limitation of the present study was the relatively small sample size of the study group. A larger group would have been needed to provide adequate statistical power to examine whether there are sex differences. A final limitation was that the signal to noise ratio (SNR) of the images was suboptimal due to MRI scans being acquired with the use of parallel imaging (Madore and Pelc, 2001). In summary, we

evaluated the change in GM and WM densities in sexes with age, and identified the regions of the GM that are affected by age and several cognitive tests. As a result, we also found a significant negative correlation between GM volume and age in each sex, while white matter volume did not significantly correlate with age in each sex. This study showed a consistent GM density difference in the older groups of subjects. We identified regions of increased GM density in groups less than 50 years old in comparison to above 50 years old in each sex. We also found that the digit symbol test was positively correlated with local GM density in both sexes. However, density or volume decreases within the GM structures have not been found to be predictive of deterioration in specific cognitive tests. In this study, the use of DARTEL analysis has produced the same findings as reported by many previous standard VBM studies. Finally, it is important to consider individual variability due to sex differences and age-extrinsic biomedical factors (i.e. blood pressure, diabetes mellitus, chronic respiratory disease, and hormones) when interpreting age effect on brain structure (for review see (Tisserand and Jolles, 2003)).

CHAPTER 7: Effects of age and sex on the brain cortical thickness and relation to cognition.

7.1 Aim of Chapter

This chapter aims to investigate any association between the regional cortical thickness and age for all subjects and within each sex; it also investigates associations between cortical thickness and brief cognitive assessment test performances.

7.2 INTRODUCTION

Changes in cortical thickness are pivotal for the study of age-related changes as they provide a regional measure of variations in grey matter (GM) morphology that can be made continuously across the cortical surface. Age-related changes in cortical brain structure has been explored previously using a variety of methods, including a post-mortem (Kemper, 1994) and in vivo volumetric studies of regional cortical thickness (Fjell et al., 2009, Salat et al., 2004, Thambisetty et al., 2010, Ziegler et al., 2010). Comparable to the results of the GM changes from some volumetric studies (Raz et al., 2004, Sowell et al., 2003), age was found to be associated with widespread thinning of the cerebral cortex (Fjell et al., 2009, Salat et al., 2004, Sowell et al., 2007). Furthermore, similar to the results reported by some volumetric studies (Coffey et al., 1992, Cowell et al., 1994, Gur et al., 2000, Raz et al., 2004, Salat et al., 1999), cortical thickness of the frontal lobe (FL) specifically prefrontal cortex (PFC), and temporal lobe (TL) are reported to be reduced with age.

Fjell et al. (2009) assessed the consistency of age effects on cortical thickness across 6 different samples with a total of 883 participants age range (18-93 years). The results of their study demonstrated consistent age-related effects across the 6

samples in the superior, middle, and inferior frontal gyri, superior and middle temporal gyri, precuneus, inferior and superior parietal cortices, fusiform and lingual gyri, and the temporo-parietal junction. The strongest effects were noticed in the superior frontal gyri, inferior frontal gyri, and superior parts of the temporal lobe.

Salat et al. (2004) obtained cross-sectional data form 106 participants ranging from 20-90 years old and measured cortical thickness over the entire cortex. They found that the GM of older adults was significantly thinner in the prefrontal cortex and visual regions, but selective preservation was found in the parahippocampal and temporal areas. Consistent with Salat et al. (2004), Ziegler et al. (2010) found large regions of cortical thinning in sensory and motor areas, including the precentral gyrus, the pericalcarine region, and the medial aspect of the superior frontal gyrus. They also noted smaller regions of thinning in the lateral PFC, inferior parietal cortex, and transverse temporal gyri.

Notably, Thambisetty et al. (2010) investigated longitudinal changes in cortical thickness over a mean follow-up interval of 8 years in a cohort of 66 older adults (range 60–84 year). Their main finding was that age-related decline in cortical thickness is widespread, but shows an anterior–posterior gradient with frontal and parietal regions exhibiting greater rates of decline than temporal and occipital. Males showed greater rates of decline than females in the middle frontal, inferior parietal, parahippocampal, postcentral, and superior temporal gyri in the left hemisphere, right precuneus and bilaterally in the superior parietal and cingulate regions. A cross sectional investigation of the influence of aging and sex revealed a highly significant effect of global cortical thickness in males but not females, in the left and right hemispheres (Salat et al., 2004). However, this was not supported by Nopoulos et al, (2000) who recruited a similar sample size and employed identical image analysis

software and method which revealed no significant differences between males and females.

Previous studies analyzing cortical thickness of healthy subjects have successfully related localized variations in prefrontal, posterior and temporal cortices thickness to scores of intelligence (Narr et al., 2007), medial temporal cortical thickness to verbal memory and lateral parietal cortical thickness to visuomotor speed/set (Dickerson et al., 2008). Fjell et al. (2006) also found that older subjects with high fluid intelligence scores (i.e. *t* scores were 50.3, SD = 2.8) had thicker cortex in the right hemisphere, mostly in posterior cingulate cortex, compared to old subjects with average scores (i.e. *t* scores were 38.1, SD = 4.9). In contrast, the same study found no thickness differences between high and low performers on tests of executive function. On the other hand, Ziegler et al. (2010) found no correlations between measures of cognitive performance and cortical thickness. Raz and Rodrigue (2006) suggested that there is no clear relationship between cortical thickness/volume with age and behavioral performance.

In this study, we used an automated, advanced surface-based approach (Fischl and Dale, 2000) to derive measures of cortical thickness across the entire cortical mantle. To do this measurement of cortical thickness, FreeSurfer software, freely downloadable from http://surfer.nmr.mgh.harvard.edu/, was used (Center for Biomedical Imaging, Charlestown, MA). This method provides reliable measures of cortical thickness continuously across the whole cortical mantle without manually defining region of interests (ROIs). Although automated methods may have some disadvantages, such as resolution loss in registration of morphologically different brains to a common stereotactic space, and the need for smoothing, it has several advantages over manual methods. It requires minimal intervention by highly trained

personnel and allows processing of many brains in a reasonable time frame. It is also characterized by very high reliability and repeatability of measures.

We hypothesized that the largest age-related effects on cortical thickness would be found within the FL, while decline in cognitive performance tests would be particularly associated with changes in cortical thickness. We tested for regional differences in cortical thickness for all subjects and within each sex. We also tested for association between cortical thickness and brief executive assessment tests.

7.3 METHODS

7.3.1 Data Analysis:

Cortical Thickness Analyses

Cortical reconstruction and volumetric segmentation was performed with processing the T1-weighted MRI data using the FreeSurfer image analysis tools. This tool of methods was initially proposed in the 1990s (Dale et al., 1999; Fischl et al., 1999a) and has undergone several important improvements over the years (Karnath et al., 2001, Dale and Sereno, 1993, Fischl and Dale, 2000, Fischl et al., 2001, Fischl et al., 2004a, Fischl et al., 1999a, Fischl et al., 1999b, Fischl et al., 2004b, Segonne et al., 2004). With these updates, the current method is fully automated. Briefly, this processing includes motion correction, removal of non-brain tissue using a hybrid watershed/surface deformation procedure (Segonne et al., 2004), automated Talairach transformation, segmentation of the subcortical white matter (WM) and deep GM volumetric structures (Fischl et al., 2002, Fischl et al., 2004a) intensity

normalization (Sled et al., 1998), tessellation of the GM/WM boundary, automated topology correction (Fischl et al., 2001, Segonne et al., 2007), and surface deformation following intensity gradients to optimally place the grey/white and grey/cerebrospinal fluid borders at the location where the greatest shift in intensity defines the transition to the other tissue class (Karnath et al., 2001, Dale and Sereno, 1993, Fischl and Dale, 2000).

The thickness estimation procedure is automated, but requires manual checking of the accuracy of the spatial registration and the WM and GM segmentations. The types of errors that most often require user intervention are insufficient removal of nonbrain tissue and inclusion of vessels adjacent to the cortex. In addition, if large field inhomogeneity exists, small parts of WM may mistakenly be misclassified as GM, thus obscuring the GM/WM boundary. These types of errors are limited in spatial extension, typically seen in a minor area of the brain in a few slices, but are however routinely corrected by manual interventions.

We derived thickness measures at each vertex along the reconstructed surface by calculating the shortest distance from the grey/white border to the outer cortical (pial) surface (Fischl and Dale, 2000).

Statistical Analyses of Cortical Thickness Data

The final statistical data from the FreeSurfer were imported into SPSS format where the analyses were conducted in PASW Statistics v18.0. General linear modeling (GLM) analyses were conducted for sex differences. Multiple linear regressions were performed to find the association between age, and cortical thicknesses. Additionally, in order to investigate whether changes in cortical

thickness predict change in cognitive decline, only cortical regions that demonstrated significant correlation with cognitive assessment tests were included in the subsequent analyses. Age was included as a covariate in all analyses, which were carried out in two steps. First, Pearson partial correlations (age controlled) were examined between cortical thickness and cognitive performance scores. Second, forward stepwise linear regression analysis were performed with change in cortical thickness measures as independent variables, (controlling for age), and change in cognitive performance as the dependent variables.

7.4 RESULTS:

7.4.1 Cognitive Assessment Data:

Results presented in detail in Chapter 6.

7.4.2 Global Cortical Thickness Effect of Aging Among all Subjects:

The correlation between cortical thickness and age was investigated for all subjects using multiple linear regression analyses. Figure 7.1 shows the gyral regions of the human brain atlas developed by (Desikan et al., 2006).

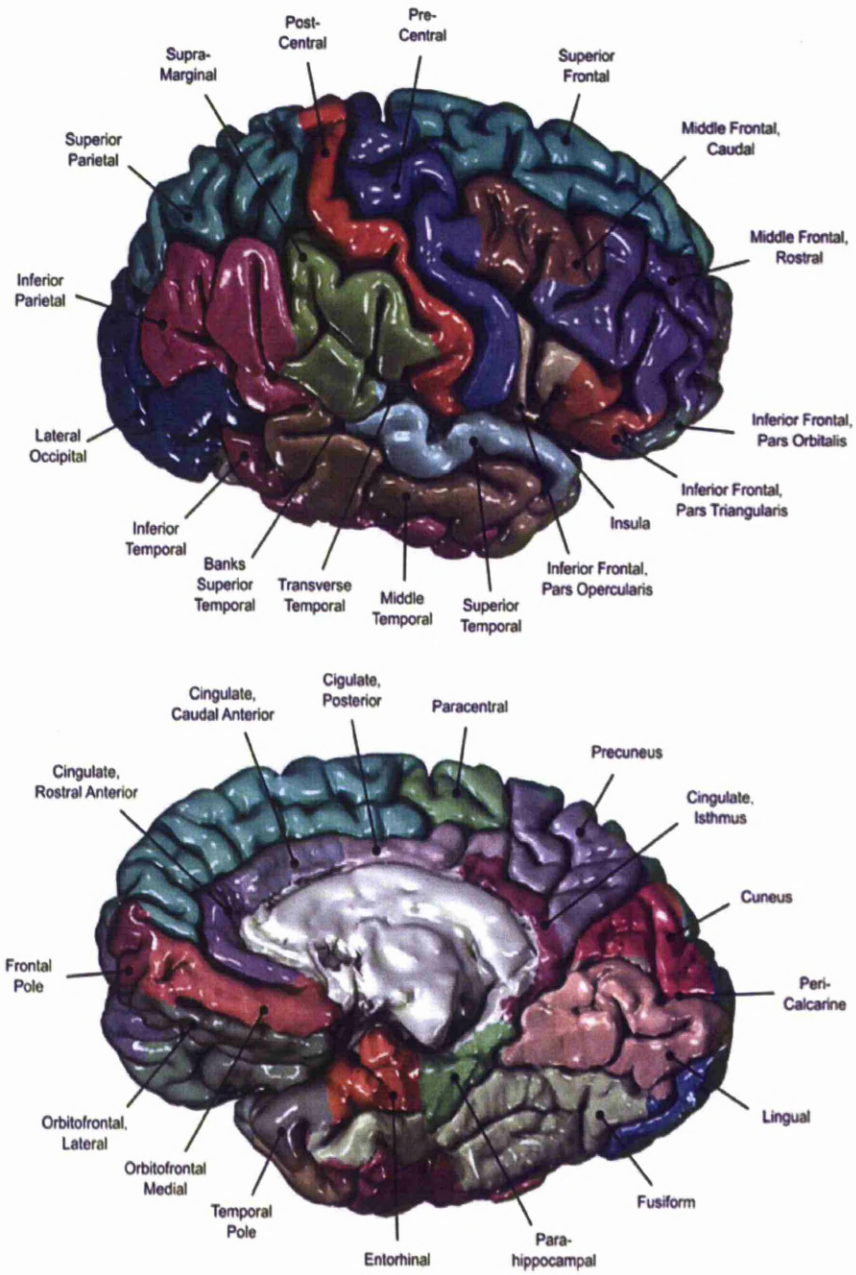

Figure 7.1: Two views showing gyral regions of the human brain. 34 cortical regions were labeled for reference (Desikan et al., 2006).

The results of the multiple regression analysis (using a stepwise method with criteria: probability of F to enter < = 0.05, probability of F to remove > = 0.100 and in which all 68 regions for which cortical thickness had been obtained were entered together with age) are presented in Table 7.1, which summarizes the regression results between cortical thickness and age among all subjects. Left superior frontal (BA 6) was the first predictor for age ($F_{[1,54]}$ =11.05, R^2=0.17, p=0.00), followed by left rostral anterior cingulate (BA 24) ($F_{[2,54]}$ =9.09, R^2=0.26, p=0.02), followed by left supra marginal (BA 40) ($F_{[3,54]}$ =8.30, R^2=0.33, p=0.03), followed by the left pars opercularis (BA 44) ($F_{[4,54]}$ =7.78, R^2=0.38, p=0.04), and finally followed by the right superior temporal (BA 22) ($F_{[5,54]}$ =9.21, R^2=0.42, p=0.02).

Coefficients[a]

Model		Unstandardized Coefficients		Standardized Coefficients		
		B	Std. Error	Beta	t	Sig.
1	(Constant)	174.17	40.00		4.35	.00
	Left Superior Frontal (BA 6)	-47.21	14.20	-.41	-3.32	.00
2	(Constant)	200.35	39.66		5.05	.00
	Left Superior Frontal (BA 6)	-65.92	15.55	-.58	-4.24	.00
	Left Rostral Anterior Cingulate (BA 24)	9.60	3.90	.33	2.46	.02
3	(Constant)	165.36	41.10		4.02	.00
	Left Superior Frontal (BA 6)	-81.91	16.51	-.72	-4.96	.00
	Left Rostral Anterior Cingulate (BA 24)	8.70	3.77	.30	2.31	.02
	Left supra Marginal (BA 40)	31.82	13.92	.31	2.28	.03
4	(Constant)	189.54	41.35		4.58	.00
	Left Superior Frontal (BA 6)	-69.64	16.98	-.61	-4.10	.00
	Left Rostral Anterior Cingulate (BA 24)	5.47	3.95	.19	1.38	.17
	Left supra Marginal (BA 40)	40.34	14.05	.39	2.87	.01
	Left Pars Opercularis (BA 44)	-26.78	12.61	-.28	-2.12	.04
5	(Constant)	210.03	41.38		5.07	.00
	Left Superior Frontal (BA 6)	-51.35	14.76	-.45	-3.48	.00
	Left supra Marginal (BA 40)	48.51	13.41	.47	3.62	.00
	Left Pars Opercularis (BA 44)	-34.37	11.25	-.36	-3.05	.00
	Right Superior Temporal (BA 22)	-20.42	8.64	-.27	-2.36	.02

a. Dependent Variable: age

Table 7.1: Multiple regression analysis coefficients of the brain cortical thickness with age as dependent variable for all subjects. BA= Broadmann's areas.

7.4.3 Global Cortical Thickness Effect of Aging between Sexes:

Sex differences have investigated using repeated measures GLM analyses, with 34 brain regions in 2 hemispheres as within subject variables and age with sex factors as between group factors. There were no significant sex by age interaction ($F_{1,51}$=0.24, p=0.63). However, there were significant differences between sexes in cortical thickness measurements ($F_{1,51}$=4.93, p=0.03). We investigated the

correlation in cortical thickness within each sex for age using multiple linear regression analyses.

Male

Table 7.2 shows the multiple regressions results between cortical thickness and age among the male subjects. Forward stepwise multiple regression analysis first selected left superior frontal (BA 6) ($F_{[1,25]}$ =11.03, R^2=0.31, p=0.00), followed by left inferior parietal (BA 40) ($F_{[2,25]}$ = 9.99, R^2=0.46, p=0.02), finally followed by right isthmus cingulate (BA 26) ($F_{[3,25]}$ = 10.92, R^2=0.59, p=0.01).

Coefficients[a]

Model		Unstandardized Coefficients		Standardized Coefficients		
		B	Std. Error	Beta	t	Sig.
1	(Constant)	282.29	72.74		3.88	.00
	Left Superior Frontal (BA 6)	-86.96	26.18	-.56	-3.32	.00
2	(Constant)	225.70	69.34		3.25	.00
	Left Superior Frontal (BA 6)	-126.04	28.20	-.81	-4.47	.00
	Left Inferior Parietal (BA 40)	67.28	26.48	.46	2.54	.02
3	(Constant)	233.92	64.89		3.60	.00
	Left Superior Frontal (BA 6)	-125.07	26.35	-.81	-4.75	.00
	Left Inferior Parietal (BA 40)	75.48	25.05	.52	3.01	.01
	Right Isthmus Cingulate (BA 26)	-12.47	5.97	-.30	-2.09	.05

a. Dependent Variable: age

Table 7.2: Multiple regression analysis coefficients of the brain cortical thickness with age as dependent variable in males. BA= Broadmann's areas.

Female

Table 7.3 shows the multiple regressions results between cortical thickness and age among the female subjects. Forward stepwise multiple regression analysis first selected Left Pars Opercularis (BA 44) ($F_{[1,28]}$ =15.48, R^2 =0.36, p=0.00), followed by right middle Temporal (BA 21) ($F_{[2,28]}$ = 14.12, R^2 =0.52, p=0.01), followed by right caudal anterior cingulate (BA 24 and 32) ($F_{[3,28]}$ = 12.85, R^2=0.61, p=0.03), followed by left insula (BA 13) ($F_{[4,28]}$ = 13.52, R^2=0.70, p=0.02), finally followed by left superior temporal (BA 22) ($F_{[5,28]}$ = 113.47, R^2=0.74, p=0.04).

Coefficients[a]

Model		Unstandardized Coefficients		Standardized Coefficients		
		B	Std. Error	Beta	t	Sig.
1	(Constant)	199.63	40.20		4.96	.00
	Left Pars Opercularis (BA 44)	-57.53	14.62	-.60	-3.93	.00
2	(Constant)	276.63	44.34		6.24	.00
	Left Pars Opercularis (BA 44)	-56.97	12.94	-.60	-4.40	.00
	Right Middle Temporal (BA 21)	-26.79	9.20	-.40	-2.91	.01
3	(Constant)	260.56	41.53		6.27	.00
	Left Pars Opercularis (BA 44)	-58.90	11.99	-.62	-4.91	.00
	Right Middle Temporal (BA 21)	-33.53	8.98	-.49	-3.73	.00
	Right Caudal Anterior Cingulate (BA 24 & 32)	16.25	6.95	.310	2.34	.03
4	(Constant)	353.60	51.87		6.82	.00
	Left Pars Opercularis (BA 44)	-75.86	12.64	-.80	-6.00	.00
	Right Middle Temporal (BA 21)	-34.30	8.10	-.51	-4.13	.00
	Right Caudal Anterior Cingulate (BA 24 & 32)	22.70	8.10	.43	3.65	.00
	Left Insula (BA 13)	-20.88	8.05	-.36	-2.59	.02
5	(Constant)	352.98	48.23		7.32	.00
	Left Pars Opercularis (BA 44)	-85.74	12.59	-.90	-6.81	.00
	Right Middle Temporal (BA 21)	-38.68	7.80	-.57	-4.96	.00
	Right Caudal Anterior Cingulate (BA 24 & 32)	20.91	6.33	.40	3.30	.00
	Left Insula (BA 13)	-29.49	8.46	-.51	-3.48	.00
	Left Superior Temporal (BA 22)	24.64	11.29	.29	2.18	.04

a. Dependent Variable: age

Table 7.3: Multiple regression analysis coefficients of the brain cortical thickness with age as dependent variable in females. BA= Broadmann's areas.

7.4.4 Cortical Thickness Correlations with Cognitive Performance:

In this analysis, association between cortical thickness and cognitive measures (controlling for age), which showed strong correlations with age among all subjects and in each sex, were investigated using stepwise linear regression analysis.

All Subjects

Digit span forward

The results of the regression analysis are summarized in Table 7.4. Right postcentral (BA 1, 2 and 3) explained significant variance in digit span forward ($F_{[2,54]}$ =2.34, R^2=0.08, p=0.04).

Coefficients[a]

Model		Unstandardized Coefficients		Standardized Coefficients	t	Sig.
		B	Std. Error	Beta		
1	(Constant)	9.40	.89		10.54	.00
	Age	.01	.02	.045	.32	.75
2	(Constant)	4.98	2.24		2.23	.03
	Age	.00	.02	.03	.23	.82
	Right postcentral (BA 1, 2 & 3)	1.99	.93	.28	2.14	.04

a. Dependent Variable: Digit Span Forward

Table 7.4: Multiple regression analysis coefficients of the brain cortical thickness with digit span forward as dependent variable (controlling for age) in all subjects. BA= *Broadmann's areas.*

Digit span backward

The results of the regression analysis are summarized in Table 7.5. Right medial orbitofrontal (BA 10 and 11) explained significant variance in digit span backward ($F_{[2,54]}$ =3.08, R^2 =0.11, p=0.02).

Coefficients[a]

Model		Unstandardized Coefficients		Standardized Coefficients		
		B	Std. Error	Beta	t	Sig.
1	(Constant)	9.11	1.05		8.70	.00
	Age	-.01	.02	-.07	-.52	.60
2	(Constant)	3.47	2.54		1.36	.18
	Age	.00	.02	-.00	-.03	.97
	Right Medial Orbitofrontal (BA 10 & 11)	2.08	.86	.32	2.42	.02

a. Dependent Variable: Digit Span Backward

Table 7.5: Multiple regression analysis coefficients of the brain cortical thickness with digit span backward as dependent variable (controlling for age) in all subjects. BA= *Broadmann's areas.*

Digit symbol

The results of the regression analysis are summarized in Table 7.6. Right rostral middle frontal (BA 10 and 46) explained significant variance in digit symbol ($F_{[2,54]}$ =15.07, R^2 =0.37, p=0.01).

Coefficients[a]

Model	Unstandardized Coefficients		Standardized Coefficients		
	B	Std. Error	Beta	t	Sig.
1 (Constant)	82.36	4.16		19.80	.00
Age	-.43	.09	-.53	-4.57	.00
2 (Constant)	37.57	17.47		2.15	.04
Age	-.35	.09	-.44	-3.80	.00
Right Rostral Middle Frontal (BA10, 46)	16.87	6.41	.30	2.63	.01

a. Dependent Variable: Digit Symbol

Table 7.6: Multiple regression analysis coefficients of the brain cortical thickness with digit symbol as dependent variable (controlling for age) in all subjects. BA= *Broadmann's areas.*

Male

Digit span forward

Table 7.7 shows the multiple regressions results between cortical thickness and digit span forward test (controlling for age) among the male subjects. Forward stepwise multiple regression analysis first selected right pars opercularis (BA 44) ($F_{[2,25]}$ = 5.22, R^2 =0.31, p=0.01), followed by right pars triangularis (BA 45) ($F_{[3,25]}$ = 6.42, R^2 =0.48, p=0.02). No other cortical regions contributed to the digit span forward test.

Coefficients[a]

Model		Unstandardized Coefficients		Standardized Coefficients		
		B	Std. Error	Beta	t	Sig.
1	(Constant)	6.91	1.35		5.13	.00
	Age	.05	.03	.31	1.63	.12
2	(Constant)	24.84	6.83		3.64	.00
	Age	.02	.03	.16	.85	.40
	Right Pars Opercularis (BA 44)	6.26	2.35	.49	2.67	.01
3	(Constant)	8.64	8.89		.97	.34
	Age	.02	.03	.11	.67	.51
	Right Pars Opercularis (BA 44)	7.53	2.17	.59	3.47	.00
	Right Pars Triangularis (BA 45)	7.74	3.07	.40	2.53	.02

a. Dependent Variable: Digit Span Forward

Table 7.7: Multiple regression analysis coefficients of the brain cortical thickness with digit span forward as dependent variable (controlling for age) in males. BA= *Broadmann's areas.*

Digit span backward

Table 6.8 shows the multiple regressions results between cortical thickness and digit span backward test (controlling for age) among the male subjects. Forward stepwise multiple regression analysis first selected right pars opercularis (BA 44) ($F_{[2,25]}$ = 5.50, R^2=0.32, p=0.00), followed by right pars triangularis (BA 45) ($F_{[3,25]}$ = 5.81, R^2=0.44, p=0.04). No other cortical regions contributed to the digit span forward test.

Coefficients[a]

Model		Unstandardized Coefficients		Standardized Coefficients		
		B	Std. Error	Beta	t	Sig.
1	(Constant)	5.73	1.50		3.83	.00
	Age	.06	.03	.32	1.64	.11
2	(Constant)	26.14	7.54		3.47	.00
	Age	.03	.03	.16	.85	.40
	Right Pars Opercularis (BA 44)	7.13	2.60	.50	2.75	.01
3	(Constant)	12.38	9.45		1.31	.20
	Age	.02	.03	.09	.51	.61
	Right Pars Opercularis (BA 44)	9.23	2.60	.65	3.56	.00
	Right Pars Triangularis (BA 45)	7.90	3.65	.37	2.16	.04

a. Dependent Variable: Digit Span Backward

Table 7.8: Multiple regression analysis coefficients of the brain cortical thickness with digit span backward as dependent variable (controlling for age) in males. BA= *Broadmann's areas.*

Digit symbol

There were no significant correlation between cortical thicknesses and digit symbol test in males (controlling for age).

Female

Digit span forward

There were no significant correlation between cortical thicknesses and digit span forward test in females (controlling for age).

Digit span backward

Table 7.9 shows the multiple regressions results between cortical thickness and digit span backward test (controlling for age) among the female subjects. Forward stepwise multiple regression analysis first selected right lateral orbitofrontal (BA 47) ($F_{[2,28]}$ = 6.85, R^2 =0.34, p=0.01), followed by right medial orbitofrontal (BA 11) ($F_{[3,28]}$ = 6.75, R^2 =0.45, p=0.04). No other cortical regions contributed to the digit span backward test.

Coefficients[a]

Model		Unstandardized Coefficients		Standardized Coefficients		
		B	Std. Error	Beta	t	Sig.
1	(Constant)	11.74	1.30		9.01	.00
	Age	-.06	.03	-.39	-2.18	.04
2	(Constant)	-7.23	6.91		-1.05	.30
	Age	-.04	.03	-.26	-1.55	.13
	Right Lateral Orbitofrontal (BA 47)	6.54	2.45	.46	2.78	.01
3	(Constant)	-11.46	6.76		-1.69	.10
	Age	-.02	.03	-.15	-.89	.38
	Right Lateral Orbitofrontal (BA 47)	6.22	2.20	.44	2.82	.01
	Right Medial Orbitofrontal (BA 11)	1.75	.81	.34	2.15	.04

a. Dependent Variable: Digit Span Backward

Table 7.9: Multiple regression analysis coefficients of the brain cortical thickness with digit span backward as dependent variable (controlling for age) in females. BA= *Broadmann's areas.*

Digit symbol

Table 7.10 shows the multiple regressions results between cortical thickness and digit symbol test (controlling for age) among the female subjects. Left caudal anterior cingulate (BA 24 and 32) explained significant variance in digit symbol ($F_{[2,28]}$ =14.86, R^2=0.53, p=0.02). No other cortical regions contributed to the digit symbol test.

Coefficients[a]

Model		Unstandardized Coefficients		Standardized Coefficients		
		B	Std. Error	Beta	t	Sig.
1	(Constant)	90.31	5.41		16.70	.00
	Age	-.52	.12	.64	-4.37	.00
2	(Constant)	77.58	6.97		11.13	.00
	Age	-.54	.11	-.66	-4.94	.00
	Left Caudal Anterior Cingulate (BA 24 & 32)	5.30	2.05	.35	2.58	.02

a. Dependent Variable: Digit Symbol

Table 7.10: Multiple regression analysis coefficients of the brain cortical thickness with digit symbol as dependent variable (controlling for age) in females. BA= *Broadmann's areas.*

7.5 DISCUSSION AND CONCLUSION

This study explored age-related changes in cortical thickness in a representative healthy population (age ranged 18-71 years). The objectives of this study were to evaluate the effect of global cortical thickness and age among all subjects and in each sex, as well as to evaluate the relationships between cortical thickness and performance on cognitive tests.

Effects of age on cortical thickness in each sex:

Among all subjects, linear regression analysis between cortical thickness and age showed a significant thinning in the left superior frontal gyrus (BA 6), left pars opercularis (BA 44), and right superior temporal gyrus (BA 22). However, we found cortical thickness measures increased with age in the left supra marginal gyrus (BA 40).

In males, regression analysis between cortical thickness and age showed a significant thinning in the left superior frontal gyrus (BA 6) and right isthmus cingulate (BA 26). However, we found cortical thickness measures increased with age in the left inferior parietal cortex (BA 40).

In females, cortical thickness decreased most significantly with age in the left pars opercularis (BA 44) (β=-0.85, p=0.00), right middle temporal gyrus (BA 21), left insular cortex (BA 13), and left superior temporal gyrus (BA 22). However, cortical thickness measures increased with age in the right caudal anterior cingulate (BA 24 and 32).

These results of age-related changes in cortical thickness are similar to some earlier reports (see Table 7.11). Certain results, including prominent thinning of the

frontal cortex specifically prefrontal and some parts of the temporal cortex, met with previous findings from volumetric neuroimaging studies (Cowell et al., 2007, Cowell et al., 1994, Gur et al., 2000, Raz et al., 1997, Raz et al., 2004, Salat et al., 1999). We also observed increases in cortical thickness with age in the left supra marginal gyrus (BA 40), left inferior parietal gyrus (BA40) and right caudal anterior cingulate (BA 24 and 32) regions. Other studies have observed similar increases in cortical thickness with age in different regions (Salat et al., 2009, Thambisetty et al., 2010). Although interestingly, we have not directly addressed the likely mechanisms underlying this observation. One plausible explanation suggested by Thambisetty et al. (2010) is that decreases in grey-white contrast during aging might result in apparent increases in cortical thickness estimates. It has also been observed that in some brain regions, statistical effects of changes in grey–white contrast during aging may be stronger than those attributable to cortical thinning (Salat et al., 2009).

Lobe	Region of Thinned Cortex	Study by
Frontal	Superior frontal gyrus (present study)	(Fjell et al., 2009, Ziegler et al., 2010)
	Middle frontal gyrus (present study)	(Fjell et al., 2009)
	Inferior frontal gyrus (present study)	(Fjell et al., 2009, Salat et al., 2004)
	Inferior lateral prefrontal cortex	(Salat et al., 2004)
	Precentral gyrus	(Salat et al., 2004, Ziegler et al., 2010)
	Medial orbitofrontal gyrus	(Salat et al., 2004)
Temporal	Superior temporal gyrus (present study)	(Fjell et al., 2009)
	Middle temporal gyrus (present study)	(Fjell et al., 2009)
	Temporo parietal junction	(Fjell et al., 2009)
	Transverse temporal gyrus	(Ziegler et al., 2010)
	Banks of the superior temporal sulcus	(Salat et al., 2004, Ziegler et al., 2010)
	Fusiform gyrus	(Fjell et al., 2009)
	Parahippocampal guys	(Fjell et al., 2009)
Occipital	Lingual gyrus	(Fjell et al., 2009)
	Cuneus	(Fjell et al., 2009, Salat et al., 2004,
	Calcarine sulcus	(Ziegler et al., 2010)
	Precuneus	(Fjell et al., 2009)
	Pericalcarine cortex	(Fjell et al., 2009, Ziegler et al., 2010)
Parietal	Inferior parietal cortices (present study)	(Fjell et al., 2009, Ziegler et al., 2010)
	Superior parietal cortices	(Fjell et al., 2009)
	Postcentral gyrus	(Salat et al., 2004)
Cingulate	Cingulate (present study)	(Salat et al., 2004, Ziegler et al., 2010)

Tale 7.11: Results of previous cortical studies, shown regions of thinning cortex with age.

Correlation of Cortical Thickness with Cognitive Performance:

In this study the hypothesis was tested that age-related declines in cognitive functioning are associated with changes of the cortical thickness. It was expected that reductions in cortical thickness would be related to a decline in performance on cognitive tests. We investigated the relation between cortical thickness, digit span forward, digit span backward and digit symbol tests which were significantly correlated with age in each sex (West, 1996).

Among all subjects, cortical thickness of regions of the right postcentral (BA 1, 2 and 3) was significantly positively associated with digit span forward. With digit span backward, cortical thickness of the right medial orbitofrontal (BA10 and 11) was significantly positively associated. With digit symbol, there was significant positive association in the right rostral middle frontal (BA 10 and 46).

In males, cortical thickness of regions of the right pars triangularis (BA 45) and right pars opercularis (BA 44) were significantly positively associated with digit span forward and digit span backward. There were no associations between cortical thickness and digit symbol performance in males.

In females, cortical thickness of regions of the right lateral orbitofrontal (BA 47) and right medial orbitofrontal (BA 11) were significantly positively associated with digit span backward (see Table 7.8). With digit symbol, cortical thickness of the left caudal anterior cingulate (BA 24 and 32) was significantly positively associated (see Table 7.9). There were no associations between cortical thickness and digit span forward performance in females.

Our results showed some association between cortical thicknesses of some regions of the frontal, cingulate, parietal and performance on specific cognitive tasks. The most prominent correlations were found in the inferior frontal gyrus, which were especially pronounced in the right hemisphere, including the pars opercularis (BA 44), pars triangularis (BA 45), medial orbitofrontal (BA 10 and 11), as well as parts of the rostral middle frontal (BA 10 and 46). As parts of the frontal and prefrontal cortex, these structures are close to areas involved in working memory and executive and control functions necessary in performance on neuropsychological tests. The right inferior frontal cortex, known to be important for response inhibition (Aron et al., 2004). Evidence from functional and structural neuroimaging studies suggests that the right inferior frontal gyrus is heavily involved in cognitive control processes related to inhibiting or delaying responses (Aron et al., 2007, Aron et al., 2003, Aron et al., 2004). It is also recruited during attentional processing (Hampshire et al., 2010).

The right postcentral (BA 1, 2 and 3) and left caudal anterior cingulate (BA 24 and 32) also correlated significantly with cognitive performance. The postcentral regions were reported to have correlations with visuospatial cognition (Hanggi et al., 2010). The anterior cingulate gyri, and in particular the caudal aspects, are implicated in a range of cognitive conflict processing (Bush et al., 2000, Cabeza and Nyberg, 2000) and have also been shown to be activated in the attention network test (Fan et al., 2003, Fan et al., 2005) as well as in other cognitive control tasks (Wager et al., 2005).

Previous volumetric studies have provided some evidence of associations between neuroanatomical changes with age in specific regions and performance on specific cognitive tasks. For instance, poorer performances on age-sensitive tests of attention and executive functions have been linked to the reduced global cortical volumes and reduced volumes of the prefrontal cortices (Gunning-Dixon and Raz, 2003, Raz et al., 1998, Zimmerman et al., 2006). Some other studies reported an association between regional brain volumes decrement and cognitive functioning, such as hippocampal volume and memory performance (Golomb et al., 1994), between the PFC volume and mental imagery (Raz et al., 1999), between the limbic structures and memory (Raz et al., 1998), and between medial prefrontal and fluid intelligence (Gong et al., 2005). Other studies have not found any evidence for such a relation between brain volume and cognitive performance with age (Raz et al., 1998, Tisserand et al., 2000, Tisserand and Jolles, 2003). In a recent study, older adults with high fluid intelligence scores had large regions of thicker cortex in the right hemisphere, most markedly in posterior cingulate cortex, compared to older adults with average scores (Fjell et al., 2006). In contrast, the same study found nearly no thickness differences between high and low performers on tests of executive function, which also matched the result found by Ziegler et al. (2010). It has been suggested that structural changes in the frontal lobe do not necessarily involve changes in the thickness of cortex (Fjell et al., 2006).

In summary, we have found that cortical structure–function relationships are different for each sex. For example, some areas show positive correlation with digit span forward scores in males, but no correlation in females. Conversely, some areas show positive correlation with digit symbol scores in females, but no correlation in males. The main finding in this study is that age-related reduction in cortical

thickness is widespread, but the frontal regions, in general, exhibiting greater thickness changes than parietal, temporal and occipital. This observation is in agreement with pervious studies that demonstrated similar patterns of widespread age-related reduction in cortical thickness (Fjell et al., 2009, Salat et al., 2004, Ziegler et al., 2010).

7.6 Methodological Considerations

The conclusions from the present study should be drawn with caution, and limitations should be noted: first, the sample size of the study groups here are not large. A larger sample size would have needed to provide adequate statistical power. Second, it is important to consider individual variability due to sex differences and age-extrinsic biomedical factors (i.e. blood pressure, diabetes mellitus, chronic respiratory disease, and hormones) when interpreting age effect on brain structure (for review see (Tisserand and Jolles, 2003)). Third, the signal to noise ratio (SNR) of the images was suboptimal due to MRI scans being acquired with the use of parallel imaging (Madore and Pelc, 2001).

CHAPTER 8: Summary

8.1 Summary

Previous MRI and fMRI studies documented that the brain undergoes several changes with the ageing process. This thesis has focused on the application of calibrated fMRI, VBM-DARTEL and FreeSurfer software in studying neurovascular and morphological alterations with age. This work is seen as a first attempt to show the outcomes and results of structural, functional and cognitive data collected on the same set of subjects. Results derived from the present study identify the correlation between structural, functional and cognitive changes with age.

A general discussion of the results of each study is presented below.

Chapter 5 highlighted the use of hyperoxia-calibrated fMRI during a Stroop task to study age related neurovascular differences in healthy subjects (age between 18-71 years) in brain regions associated with cognition. Globally, the blood-oxygenation-level-dependent (BOLD) response to the Stroop task was found to increase significantly with age, in agreement with previous work (Langenecker et al., 2004, Milham et al., 2002, Zysset et al., 2007). However, there was a reduction in the estimated cerebral metabolic rate of oxygen ($\Delta CMRO_2$) with increasing age, that would be consistent with neurodegeneration (Uylings and de Brabander, 2002). We also observed a reduction in the parameter M with age, which may be a reflection of the direct proportionality with baseline blood volume, which is known to decrease with age (Leenders et al., 1990). Cerebral blood flow response (ΔCBF) did not change with age, suggesting that the increased BOLD response with age is due primarily to a reduction in $CMRO_2$ response with age. Regionally, we found the age-

related BOLD increase to be greatest in the left and right middle frontal gyrus (MFG) (BA6) and in the primary motor cortex (M1) (BA 4), in broad agreement with previous studies (Cabeza et al., 2002, Cabeza et al., 2003, Langenecker et al., 2004, Milham et al., 2002, Nielson et al., 2002, Zysset et al., 2007). However, $\Delta CMRO_2$ is found to decrease in these areas, which supports the findings from the global analysis that the increased BOLD response with increasing age is due to a reduction in $\Delta CMRO_2$. Increased BOLD response in the frontal cortex is interpreted in previous studies as increased neural activity (Langenecker et al., 2004, Zysset et al., 2007); compensatory activity in the older group to aid performance. However, our results suggest that increased BOLD response is a result of reduced neural activation in those regions, which is inconsistent with the previously mentioned studies.

With respect to cognitive performance, we found that the low performers in the older age group showed increased BOLD response and reduced $CMRO_2$ response in LMFG (BA 6) and M1 (BA 4) compared to the young group. This suggests that reduced neural processing in these regions is impacting negatively on performance. Thus, rather than compensatory activity, increased BOLD response in these regions could be interpreted as an indication of neurodegeneration, resulting in lower performance.

To support our findings, we considered the structural data in chapter 6 and 7 looking for age-related grey matter and cortical changes in these area as well as global changes.

In **(chapter 6)** study, we used the new VBM-DARTEL method to investigate the effects of age and sex on the global grey matter density and to study the relation between grey matter density and decline in performance on brief executive

assessment tests. In the VBM method, signal intensity in every voxel of the acquired brain volume is used to measure regional variations in structural properties of the imaged tissue. The index derived from this approach is local tissue "density". Decline in density estimated by this method is assumed to indicate atrophy (Raz and Rodrigue, 2006).

In this study, some regions of the frontal, partial, and temporal lobes showed a decline in density with increasing age, similar to what has been reported by previous volumetric studies (Cowell et al., 1994, Good et al., 2001b, Gur et al., 1999, Murphy et al., 1996, Raz et al., 1997). The total brain volume, grey matter and white matter partitions were larger in males compared with females in accordance with previous studies (Coffey et al., 1998, Good et al., 2001b, Gur et al., 1991, Gur et al., 1999, Murphy et al., 1996, Raz et al., 1997, Smith et al., 2007). For all subjects, there was a significant decline of global grey matter volume with age (Good et al., 2001b, Smith et al., 2007). Significant decline of grey matter volume was found in both sexes. There were no significant correlations between age and white matter density among all subjects or in each sex in accordance with previous findings (Taki et al., 2004). Similar to the previous findings, these results clearly indicate that the main factor contributing to brain atrophy with ageing is the volume reduction of the grey matter.

The regional changes of grey matter density with aging in our study were most prominent in the frontal cortices. Among all subjects, the strongest correlation with age was seen in the paracentral gyrus (BA 4 and 6), supplementary motor area (SMA) (B6), superior frontal gyrus (BA 6), and inferior frontal gyrus (BA 44 and 45). Similar regions were found in both sexes. These findings are in agreement with previous standard VBM studies (Good et al., 2001b, Taki et al., 2004). This study also showed a consistent GM density difference in the older groups of subjects. We

identified regions of increased GM density in groups less than 50 years old in comparison to above 50 years old in each sex.

In this study the correlation between cognitive performance and changes in grey matter density was also investigated. It was expected that reductions in grey matter brain density would be related to a decline in performance on brief cognitive tests. Indeed we found a significant positive correlation could be established between grey matter density and the digit symbol test performance among all subjects in the left superior frontal gyrus (BA 6), left paracentral lobule (BA 4a and 6), left SMA (BA 6), bilateral superior medial frontal gyrus (BA 6), bilateral inferior frontal gyrus (BA 45), bilateral middle cingulate cortex (BA 6), right middle orbital gyrus (BA 11) and right middle frontal gyrus (BA 6). VBM result form this study also shows a similar positive correlation between grey matter density in some of these regions and digit symbol test in both sexes. These regions could be highly associated with improved performance on the specific cognitive test. Better performance had been observed to be associated with larger frontal cortices on some executive tasks (Driscoll et al., 2003, Gunning-Dixon and Raz, 2003, Head et al., 2008, Raz et al., 1999, Raz et al., 1998, Raz et al., 2008, Raz and Rodrigue, 2006). Prefrontal cortex volumes has been found to be associated with performance on executive tasks such as Wisconsin Card Sorting Test (Gunning-Dixon and Raz, 2003, Raz et al., 1998) as well as with performance in visuospatial skills (Raz et al., 1999), episodic memory performance (Head et al., 2008) and fluid intelligence (Raz et al., 2008). The association between performance on cognitive tests and changes in regional GM volumes remains inconclusive (Raz and Rodrigue, 2006). Van Petten et al. (2004) gave an overview of many studies of healthy participants and concluded that it has been difficult to determine strong associations between

neuropsychological functioning and brain morphometry. When structure cognition relations are found, they are not easily replicated and appear sensitive to the choice of cognitive tests (Raz and Rodrigue, 2006).

A further investigation of the relationship between whole brain $\Delta CMRO_2$ and changes in GM density for all subjects tested using a voxel-based multiple regression analysis tool SPM8. There were no GM regions that were significantly correlated (either positively or negatively) with $\Delta CMRO_2$.This suggests that the reduction in $CMRO_2$ response is not related to a reduction in grey matter density. However, it could still relate in general to neurodegeneration as opposed to neural loss. Age-related shrinkage of cortical grey matter may indeed reflect reduction in the size or the density of neurons that make up these cortical regions (Raz and Rodrigue, 2006). The reduction in grey matter volume could include: loss of neuronal bodies (Pakkenberg and Gundersen, 1997), shrinkage and dysmorphology of neurons (Haug, 1985), reduction in synaptic density (Morrison and Hof, 1997), and loss of dendrites (Jacobs et al., 1997).

In the last study of this thesis **(chapter 7),** additional investigation of the structural data was carried out using an automated, advanced surface-based approach (FreeSurfer software) to measure cortical thickness of the frontal lobe as well as the entire cortical mantle. This chapter illustrated the significant and strong correlation observed between cortical thickness and age. Cortical thickness in certain regions was shown to decrease with advancing age. Consistent with many volumetric studies, marked thinning was noted in the frontal cortex. Among all subjects, significant thinning found in the left superior frontal gyrus (BA 6), left pars opercularis (BA 44), and right superior temporal gyrus (BA 22). These results of age-related changes in cortical thickness are similar to results reported earlier (Fjell

et al., 2009, Salat et al., 2004, Sowell et al., 2007) and met with previous findings from volumetric neuroimaging studies (Cowell et al., 1994, Gur et al., 2000, Raz et al., 1997, Raz et al., 2004, Salat et al., 1999).

In this study, further stepwise linear regression test between cognitive performance and changes in cortical thickness (controlling for age) was done using SPSS. It was expected that reductions in cortical thickness would be related to a decline in performance on cognitive tests. Indeed, the results showed strong positive association between cortical thicknesses of some regions of the cingulate and frontal cortex and cognitive performance.

The most prominent correlations were found in the frontal lobe, specifically, in the pars opercularis (BA 44), pars triangularis (BA 45), lateral orbitofrontal (BA 47), medial orbitofrontal (BA 11), rostral middle frontal gyrus (BA 10, 46), and caudal anterior cingulate (BA 24 and 32). As parts of the frontal and prefrontal cortex, these structures are close to areas involved in working memory and executive and control functions necessary in performance on neuropsychological tests. The frontal lobe, specifically the inferior frontal gyrus, is heavily involved in cognitive control processes related to inhibiting or delaying responses (Aron et al., 2007, Aron et al., 2003, Aron et al., 2004). The inferior frontal gyrus is also recruited when relevant cues are detected, regardless of whether that detection is followed by an inhibition of a motor response, the generation of a motor response, or no external process at all (Hampshire et al., 2010), which demonstrates the relevance to attentional processing. The caudal anterior cingulate (BA 24 and 32) are implicated in a range of cognitive conflict processing (Bush et al., 2000, Cabeza and Nyberg, 2000) and have also been shown to be activated in the attention network test (Fan et al., 2003, Fan et al., 2005) as well as in other cognitive control tasks (Wager et al., 2005). Previous studies

analyzing cortical thickness of healthy subjects have successfully related localized variations in prefrontal, posterior and temporal cortices thickness to scores of intelligence (Narr et al., 2007), medial temporal cortical thickness to verbal memory and lateral parietal cortical thickness to visuomotor speed/set (Dickerson et al., 2008). Fjell et al. (2006) also found that older subjects with high fluid intelligence scores (i.e. *t* scores were 50.3, SD = 2.8) had thicker cortex in the right hemisphere, mostly in posterior cingulate cortex, compared to old subjects with average scores (i.e. *t* scores were 38.1, SD = 4.9). In contrast, the same study found no thickness differences between high and low performers on tests of executive function.

Further in this study, we have found that cortical structure–function relationships are different for each sex. For example, some areas show correlation with cognitive scores in males, but no correlation in females. Conversely, some areas show correlation with cognitive scores in females, but no correlation in males.

The main finding in chapter 7 could be summarized as that age-related decline in cortical thickness is widespread, but the frontal regions, in general, exhibit greater thickness changes than parietal, temporal and occipital. This observation is in agreement with one previous study that demonstrated similar patterns of widespread age-related declines in cortical thickness (Fjell et al., 2009).

Results from this chapter were investigated with the results from the previous chapter. Table 8.1 and figure 8.1 illustrate regions of the brain that were found to have significant decline in both grey matter density and cortical thickness. With age, the frontal lobe regions experienced more grey matter density reduction as well as cortical thinning in comparison to the other brain lobes. Few regions such as the

precentral gyrus, Heschl's gyrus and the insula lobe revealed significant grey mater density reduction with age but no significant changes in cortical thickness. Whereas, the cingulate gyrus, precuneus and the middle temporal gyrus region showed significant cortical thinning with no significant change in grey matter density.

Lobe	Name of the Region	Effect of age
Frontal	Precentral gyrus (BA 4 & 6)	GM reduction
	Inferior frontal gyrus (BA 44 & 45)	GM reduction and Cortical thinning
	Superior frontal gyrus (BA 6)	GM reduction and Cortical thinning
	Middle frontal gyrus (BA 10 & 46)	GM reduction and Cortical thinning
Temporal	Heschl's gyrus (BA 41 & 42)	GM reduction
	Middle temporal gyrus (BA 21)	Cortical thinning
	Superior temporal gyrus (BA 22)	GM reduction and Cortical thinning
Parietal	Inferior parietal gyrus (BA 40)	GM reduction and Cortical thinning
	Postcentral gyrus (BA 1, 2 & 3)	GM reduction and Cortical thinning
	Precuneus (BA 7)	Cortical thinning
	Cingulate gyrus (BA 24)	Cortical thinning
Insular	Insula lobe	GM reduction

Table 8.1: Regions of the brain that have declined in cortical thickness and grey matter density.

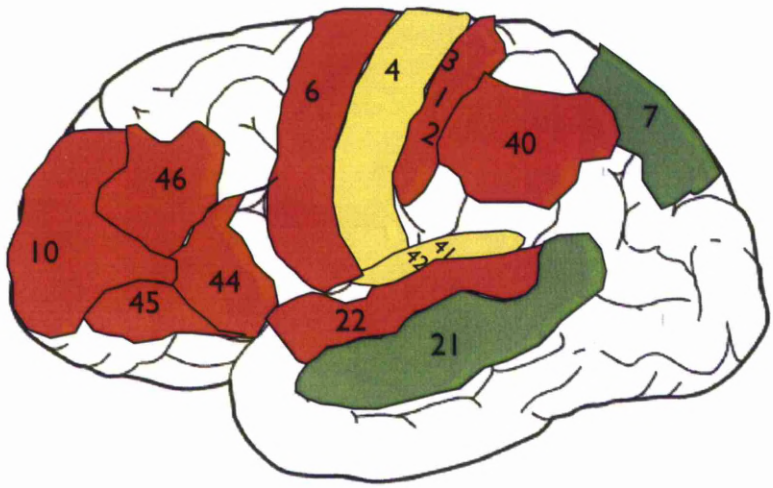

Figure 8.1: Red: regions of both (cortical thinning and grey matter density reduction). Yellow: regions of grey matter density reduction. Green: regions of cortical thinning.

In summary, cognitive and brain functional and structural effects of aging may be interpreted within the framework of the hemispheric asymmetry reduction in older adults (HARLOD) (Cabeza, 2002). This model proposes that task-related changes in functional activity in aging may reflect different mechanisms, including functional compensation and dedifferentiation. While the compensation view proposes that age-related asymmetry reductions counteract age-related cognitive decline, the differentiation perspective suggests that increased functional symmetry may be interpreted as difficulties in recruiting specialized neuronal circuits (Cabeza, 2002). Two contrasting views (the psychogenic view and neurogenic view) were suggested by Cabeza (2002) on the origin of changes in functional asymmetry. The psychogenic view argues that changes in cortical activation result from older

individuals engaging different cognitive strategies from their young counterparts, while the neurogenic view argues that the changes are a result of alterations in actual neural mechanisms (Cabeza, 2002). In the present study, we found relations between brain activation, regional cortical thickness, grey matter density and cognition in aging. The whole body of results derived from this thesis evidences that the strong correlations between age and (BOLD activations, grey matter density, cortical thickness) were found mainly in the frontal cortices. Our results suggest that the increased BOLD response with age is due primarily to a reduction in $CMRO_2$ response with age, which would be consistent with neurodegeneration. Regions with increased BOLD response and decreased $\Delta CMRO_2$ (BA 4 and BA 6) were also the same regions that experienced the most significant decrease in grey matter density and cortical thickness (BA 6). A positive trend towards significance was found between $\Delta CMRO_2$ and cortical thickness in the left medial frontal gyrus (BA 6) ($r = 0.28$, $p = 0.07$). However, thinning of the cortex was also found in regions that did not show significant decrease in grey matter density (i.e. middle temporal gyrus and cingulate gyrus) suggesting that brain shrinkage is not simply related to the cortical thinning. This agrees with what has been suggested previously that structural changes in the frontal lobe do not necessarily involve changes in the thickness of cortex (Fjell et al., 2006). While both cortical thickness and surface area influence volume measurements of cortical grey matter, volume is more closely related to surface area than cortical thickness (Winkler et al., 2010). Previous findings suggest that cortical surface area and cortical thickness are independent, both globally and regionally, and that grey matter volume is a function of these two indicators (Panizzon et al., 2009, Winkler et al., 2010). Better performance had been observed

to be associated with larger frontal grey matter density and thicker cortex on some executive tasks.

The education level is an important influence on neuropsychological test performance. Although all subjects had been recruited as a random sample of the adult population in Liverpool, most of them had an association with the University of Liverpool (as academic staff, postgraduates, technician and mature undergraduate) or as a member of a research volunteer database. Our findings only relate to this recruited group, as they are not representative of the entire population and cannot draw inferences to the general population. It is possible that a less-well educated group would have produced different results. Possibly larger effects of ageing in a group drawn from the general population would have been seen. Several studies have demonstrated a strong association between educational level and performance on various neuropsychological measures (Ardila et al., 2000, Rosselli and Ardila, 2003). With regard to the question of whether age or education level is the most significant determinant of cognitive change, Leibovici et al. (1996) suggested that education may have a more important impact on changes in secondary memory and language functioning, but that elsewhere age is the more important factor. Elderly persons with a high level of education appear to show greatest resistance to age-related change but only on tests with a high learned component that is, tests of language and secondary memory (Leibovici et al., 1996). They also suggested that on cognitive functions such as attention, implicit memory and visuospatial analysis level of education seems to make relatively little difference to the rate of change over time.

Finally, caution should be taken when automatic methods of image analysis are used. For example, although much of the processing and analysis is automated in SPM and FreeSurfer, many methodological decisions remain such as the templates to use for normalization, the level and type of correction to use and threshold for statistical map display, as well as the choice of appropriate smoothing kernel size (Henley et al., 2010, Ridgway et al., 2008). As in current study, adoption of additional techniques such as DARTEL for registration and FreeSurfer for surface deformation could be time consuming and skill demanding. However, automated methods also have several advantages over manual methods. They require minimal intervention by highly trained personnel, allow processing of many brains in a reasonable time frame and are characterized by high reliability and repeatability of measures (Fischl et al., 2002).

The focus of research in the normal aging human brain is indeed gradually moving from an interest in the whole brain to specific regions of interest in relation to aging and age-related diseases (i.e. Alzheimer). Importantly, no single functional neuroimaging method can fully address developmental questions centred on the issue of functional and structural interactions across areas. Therefore, converging method approaches are crucial in studying effects of healthy ageing. Furthermore, functional imaging studies alone cannot establish that a brain area is necessary for a particular cognitive process (Fellows and Farah, 2005) and converging evidence from structural and functional imaging studies are therefore highly valuable.

Application of the calibrated BOLD technique in normal populations allow further exploration of the effects of aging and also allow determination of baseline values that could serve as a biomarker for individuals at subsequent risk for disease. Complementing this technique with analysis of high quality structural 3D MRI data

provides unique insight into within subjects inter-relationship between the brain's metabolic and cortical activity together with structural integrity and their relationship with cognitive performance. Future research will build on this work by investigating structural and functional connectivity across the adult life span. Results from these future studies may raise the possibility of earlier diagnosis and precise or personalised treatment and management for neurological diseases, and may help physicians and scientists to develop new diagnostic tools to explore the brain differences. Understanding the development of normal brain, from cradle to grave, and differences between the sexes is important for the interpretation of clinical imaging studies.

References

AGUIRRE, G. K., DETRE, J. A., ZARAHN, E. & ALSOP, D. C. 2002. Experimental design and the relative sensitivity of BOLD and perfusion fMRI. *Neuroimage,* 15, 488-500.

ALLEN, J. S., BRUSS, J., BROWN, C. K. & DAMASIO, H. 2005. Methods for studying the aging brain: Volumetric analyses versus VBM. *Neurobiology of Aging,* 26, 1275-1278.

ALLMAN, J. M., HAKEEM, A., ERWIN, J. M., NIMCHINSKY, E. & HOF, P. 2001. The anterior cingulate cortex. The evolution of an interface between emotion and cognition. *Ann N Y Acad Sci,* 935, 107-17.

AMUNTS, K., WEISS, P. H., MOHLBERG, H., PIEPERHOFF, P., EICKHOFF, S., GURD, J. M., MARSHALL, J. C., SHAH, N. J., FINK, G. R. & ZILLES, K. 2004. Analysis of neural mechanisms underlying verbal fluency in cytoarchitectonically defined stereotaxic space-The roles of Brodmann areas 44 and 45. *Neuroimage,* 22, 42-56.

ANCES, B. M., LIANG, C. L., LEONTIEV, O., PERTHEN, J. E., FLEISHER, A. S., LANSING, A. E. & BUXTON, R. B. 2009. Effects of aging on cerebral blood flow, oxygen metabolism, and blood oxygenation level dependent responses to visual stimulation. *Hum Brain Mapp,* 30, 1120-32.

ANKNEY, C. D. 1992. Differences in brain size. *Nature,* 358, 532.

ARBEEV, K. G., UKRAINTSEVA, S. V., AKUSHEVICH, I., KULMINSKI, A. M., ARBEEVA, L. S., AKUSHEVICH, L., CULMINSKAYA, I. V. & YASHIN, A. I. 2011. Age trajectories of physiological indices in relation to healthy life course. *Mech Ageing Dev,* 132, 93-102.

ARDILA, A., OSTROSKY-SOLIS, F., ROSSELLI, M. & GOMEZ, C. 2000. Age-related cognitive decline during normal aging: the complex effect of education. *Arch Clin Neuropsychol,* 15, 495-513.

ARON, A. R., BEHRENS, T. E., SMITH, S., FRANK, M. J. & POLDRACK, R. A. 2007. Triangulating a cognitive control network using diffusion-weighted magnetic resonance imaging (MRI) and functional MRI. *J Neurosci,* 27, 3743-52.

ARON, A. R., FLETCHER, P. C., BULLMORE, E. T., SAHAKIAN, B. J. & ROBBINS, T. W. 2003. Stop-signal inhibition disrupted by damage to right inferior frontal gyrus in humans. *Nat Neurosci,* 6, 115-6.

ARON, A. R., ROBBINS, T. W. & POLDRACK, R. A. 2004. Inhibition and the right inferior frontal cortex. *Trends Cogn Sci,* 8, 170-7.

ASHBURNER, J. 2007. A fast diffeomorphic image registration algorithm. *Neuroimage,* 38, 95-113.

ASHBURNER, J. & FRISTON, K. J. 2000. Voxel-based morphometry--the methods. *Neuroimage,* 11, 805-21.

ASHBURNER, J. & FRISTON, K. J. 2001. Why voxel-based morphometry should be used. *Neuroimage,* 14, 1238-43.

ATTWELL, D. & IADECOLA, C. 2002. The neural basis of functional brain imaging signals. *Trends Neurosci,* 25, 621-5.

AUGUSTINE, J. R. 1996. Circuitry and functional aspects of the insular lobe in primates including humans. *Brain Res Brain Res Rev,* 22, 229-44.

BANICH, M. T., MILHAM, M. P., ATCHLEY, R., COHEN, N. J., WEBB, A., WSZALEK, T., KRAMER, A. F., LIANG, Z. P., WRIGHT, A., SHENKER, J. & MAGIN, R. 2000. fMri studies of Stroop tasks reveal unique roles of anterior and posterior brain systems in attentional selection. *J Cogn Neurosci,* 12, 988-1000.

BARBAS, H. 1995. Anatomic basis of cognitive-emotional interactions in the primate prefrontal cortex. *Neurosci Biobehav Rev,* 19, 499-510.

BARBAS, H. 2000. Complementary roles of prefrontal cortical regions in cognition, memory, and emotion in primates. *Adv Neurol,* 84, 87-110.

BARBAS, H., GHASHGHAEI, H., DOMBROWSKI, S. M. & REMPEL-CLOWER, N. L. 1999. Medial prefrontal cortices are unified by common connections with superior temporal cortices and distinguished by input from memory-related areas in the rhesus monkey. *J Comp Neurol,* 410, 343-67.

BARBAS, H. & ZIKOPOULOS, B. 2007. The prefrontal cortex and flexible behavior. *Neuroscientist,* 13, 532-45.

BECHARA, A. & VAN DER LINDEN, M. 2005. Decision-making and impulse control after frontal lobe injuries. *Curr Opin Neurol,* 18, 734-9.

BENCH, C. J., FRITH, C. D., GRASBY, P. M., FRISTON, K. J., PAULESU, E., FRACKOWIAK, R. S. & DOLAN, R. J. 1993. Investigations of the functional anatomy of attention using the Stroop test. *Neuropsychologia,* 31, 907-22.

BENGTSSON, J., BAKE, B., JOHANSSON, A. & BENGTSON, J. P. 2001. End-tidal to arterial oxygen tension difference as an oxygenation index. *Acta Anaesthesiol Scand,* 45, 357-63.

BERTONI-FREDDARI, C., FATTORETTI, P., DELFINO, A., SOLAZZI, M., GIORGETTI, B., ULRICH, J. & MEIER-RUGE, W. 2002. Deafferentative synaptopathology in physiological aging and Alzheimer's disease. *Ann N Y Acad Sci,* 977, 322-6.

BINDER, J. R., FROST, J. A., HAMMEKE, T. A., BELLGOWAN, P. S., SPRINGER, J. A., KAUFMAN, J. N. & POSSING, E. T. 2000. Human temporal lobe activation by speech and nonspeech sounds. *Cereb Cortex,* 10, 512-28.

BLAKEMORE, S. J. & DECETY, J. 2001. From the perception of action to the understanding of intention. *Nat Rev Neurosci,* 2, 561-7.

BLOCH, F. 1946. Nuclear induction. *Phys. Rev.,* 70.

BLUMBERG, J. & KREIMAN, G. 2010. How cortical neurons help us see: visual recognition in the human brain. *J Clin Invest,* 120, 3054-63.

BONAZ, B. 2003. Visceral sensitivity perturbation integration in the brain-gut axis in functional digestive disorders. *J Physiol Pharmacol,* 54 Suppl 4, 27-42.

BOOKSTEIN, F. L. 2001. "Voxel-based morphometry" should not be used with imperfectly registered images. *Neuroimage,* 14, 1454-62.

BOXERMAN, J. L., BANDETTINI, P. A., KWONG, K. K., BAKER, J. R., DAVIS, T. L., ROSEN, B. R. & WEISSKOFF, R. M. 1995. The intravascular contribution to fMRI signal change: Monte Carlo modeling and diffusion-weighted studies in vivo. *Magn Reson Med,* 34, 4-10.

BROWN, G. G., CLARK, C. & LIU, T. T. 2007a. Measurement of cerebral perfusion with arterial spin labeling: Part 2. Applications. *J Int Neuropsychol Soc,* 13, 526-38.

BROWN, G. G., PERTHEN, J. E., LIU, T. T. & BUXTON, R. B. 2007b. A primer on functional magnetic resonance imaging. *Neuropsychol Rev,* 17, 107-25.

BRUN, C. C., LEPORE, N., LUDERS, E., CHOU, Y. Y., MADSEN, S. K., TOGA, A. W. & THOMPSON, P. M. 2009. Sex differences in brain structure in auditory and cingulate regions. *Neuroreport,* 20, 930-5.

BUCHEL, C., PRICE, C. & FRISTON, K. 1998. A multimodal language region in the ventral visual pathway. *Nature,* 394, 274-7.

BUSH, G., LUU, P. & POSNER, M. I. 2000. Cognitive and emotional influences in anterior cingulate cortex. *Trends Cogn Sci,* 4, 215-222.

BUXTON, R. B. 2002. *Introduction to Functional Magnetic Resonance Imaging: Priniples and Techniques*, Cambridge: Cambridge University

BUXTON, R. B. 2010. Interpreting oxygenation-based neuroimaging signals: the importance and the challenge of understanding brain oxygen metabolism. *Front Neuroenergetics,* 2, 8.

BUXTON, R. B., FRANK, L. R., WONG, E. C., SIEWERT, B., WARACH, S. & EDELMAN, R. R. 1998. A general kinetic model for quantitative perfusion imaging with arterial spin labeling. *Magn Reson Med,* 40, 383-96.

BUXTON, R. B., ULUDAG, K., DUBOWITZ, D. J. & LIU, T. T. 2004. Modeling the hemodynamic response to brain activation. *Neuroimage,* 23 Suppl 1, S220-33.

CABEZA, R. 2001. Cognitive neuroscience of aging: contributions of functional neuroimaging. *Scand J Psychol,* 42, 277-86.

CABEZA, R. 2002. Hemispheric asymmetry reduction in older adults: the HAROLD model. *Psychol Aging,* 17, 85-100.

CABEZA, R., ANDERSON, N. D., HOULE, S., MANGELS, J. A. & NYBERG, L. 2000. Age-related differences in neural activity during item and temporal-order memory retrieval: a positron emission tomography study. *J Cogn Neurosci,* 12, 197-206.

CABEZA, R., ANDERSON, N. D., LOCANTORE, J. K. & MCINTOSH, A. R. 2002. Aging gracefully: compensatory brain activity in high-performing older adults. *Neuroimage,* 17, 1394-402.

CABEZA, R., DASELAAR, S. M., DOLCOS, F., PRINCE, S. E., BUDDE, M. & NYBERG, L. 2004. Task-independent and task-specific age effects on brain activity during working memory, visual attention and episodic retrieval. *Cereb Cortex,* 14, 364-75.

CABEZA, R., LOCANTORE, J. K. & ANDERSON, N. D. 2003. Lateralization of prefrontal activity during episodic memory retrieval: evidence for the production-monitoring hypothesis. *J Cogn Neurosci,* 15, 249-59.

CABEZA, R., MCINTOSH, A. R., TULVING, E., NYBERG, L. & GRADY, C. L. 1997. Age-related differences in effective neural connectivity during encoding and recall. *Neuroreport,* 8, 3479-83.

CABEZA, R. & NYBERG, L. 2000. Imaging cognition II: An empirical review of 275 PET and fMRI studies. *J Cogn Neurosci,* 12, 1-47.

CAPLAN, D., ALPERT, N., WATERS, G. & OLIVIERI, A. 2000. Activation of Broca's area by syntactic processing under conditions of concurrent articulation. *Hum Brain Mapp,* 9, 65-71.

CHAVHAN, G. 2007. *MRI Made Easy*, Anshan Ltd.

CHEE, M. W., CHEN, K. H., ZHENG, H., CHAN, K. P., ISAAC, V., SIM, S. K., CHUAH, L. Y., SCHUCHINSKY, M., FISCHL, B. & NG, T. P. 2009. Cognitive function and brain structure correlations in healthy elderly East Asians. *Neuroimage,* 46, 257-69.

CHEN, X., SACHDEV, P. S., WEN, W. & ANSTEY, K. J. 2007. Sex differences in regional gray matter in healthy individuals aged 44-48 years: a voxel-based morphometric study. *Neuroimage,* 36, 691-9.

CHIARELLI, P. A., BULTE, D. P., GALLICHAN, D., PIECHNIK, S. K., WISE, R. & JEZZARD, P. 2007a. Flow-metabolism coupling in human visual, motor, and supplementary motor areas assessed by magnetic resonance imaging. *Magn Reson Med,* 57, 538-47.

CHIARELLI, P. A., BULTE, D. P., PIECHNIK, S. & JEZZARD, P. 2007b. Sources of systematic bias in hypercapnia-calibrated functional MRI estimation of oxygen metabolism. *Neuroimage,* 34, 35-43.

CHIARELLI, P. A., BULTE, D. P., WISE, R., GALLICHAN, D. & JEZZARD, P. 2007c. A calibration method for quantitative BOLD fMRI based on hyperoxia. *Neuroimage,* 37, 808-20.

CIARAMELLI, E., GRADY, C., LEVINE, B., WEEN, J. & MOSCOVITCH, M. 2010. Top-down and bottom-up attention to memory are dissociated in posterior parietal cortex: neuroimagingand and neuropsychological evidence. *J Neurosci,* 30, 4943-56.

CLARE, S. 1997. *Functional MRI : Methods and Applications.* Doctor of Philosophy, University of Nottingham.

CLARK, D., BOUTROS, N. & MENDEZ, M. 2005. *The Brain and Behavior: An Introduction to Behavioral Neuroanatomy,* New York, Cambridge University Press.

CLARK, D., BOUTROS, N. & MENDEZ, M. 2010. *The Brain and Behavior: An Introduction to Behavioral Neuroanatomy*, Cambridge University Press.

COFFEY, C. E., LUCKE, J. F., SAXTON, J. A., RATCLIFF, G., UNITAS, L. J., BILLIG, B. & BRYAN, R. N. 1998. Sex differences in brain aging: a quantitative magnetic resonance imaging study. *Arch Neurol,* 55, 169-79.

COFFEY, C. E., WILKINSON, W. E., PARASHOS, I. A., SOADY, S. A., SULLIVAN, R. J., PATTERSON, L. J., FIGIEL, G. S., WEBB, M. C., SPRITZER, C. E. & DJANG, W. T. 1992. Quantitative cerebral anatomy of the aging human brain: a cross-sectional study using magnetic resonance imaging. *Neurology,* 42, 527-36.

COLBY, C. L. & GOLDBERG, M. E. 1999. Space and attention in parietal cortex. *Annu Rev Neurosci,* 22, 319-49.

COURCHESNE, E., CHISUM, H. J., TOWNSEND, J., COWLES, A., COVINGTON, J., EGAAS, B., HARWOOD, M., HINDS, S. & PRESS, G.

A. 2000. Normal brain development and aging: quantitative analysis at in vivo MR imaging in healthy volunteers. *Radiology,* 216, 672-82.

COWELL, P. E., ALLEN, L. S., ZALATIMO, N. S. & DENENBERG, V. H. 1992. A developmental study of sex and age interactions in the human corpus callosum. *Brain Res Dev Brain Res,* 66, 187-92.

COWELL, P. E., SLUMING, V. A., WILKINSON, I. D., CEZAYIRLI, E., ROMANOWSKI, C. A., WEBB, J. A., KELLER, S. S., MAYES, A. & ROBERTS, N. 2007. Effects of sex and age on regional prefrontal brain volume in two human cohorts. *Eur J Neurosci,* 25, 307-18.

COWELL, P. E., TURETSKY, B. I., GUR, R. C., GROSSMAN, R. I., SHTASEL, D. L. & GUR, R. E. 1994. Sex differences in aging of the human frontal and temporal lobes. *J Neurosci,* 14, 4748-55.

CROSSMAN, A. R. & NEARY, D. 1998. *Neuroanatomy - an illustrated colour text.*

D'ESPOSITO, M., DEOUELL, L. Y. & GAZZALEY, A. 2003. Alterations in the BOLD fMRI signal with ageing and disease: a challenge for neuroimaging. *Nat Rev Neurosci,* 4, 863-72.

DALE, A. M. & SERENO, M. I. 1993. Improved Localizadon of Cortical Activity by Combining EEG and MEG with MRI Cortical Surface Reconstruction: A Linear Approach. *Journal of Cognitive Neuroscience,* 5, 162-176.

DAVIS, T. L., KWONG, K. K., WEISSKOFF, R. M. & ROSEN, B. R. 1998. Calibrated functional MRI: mapping the dynamics of oxidative metabolism. *Proc Natl Acad Sci U S A,* 95, 1834-9.

DE GUIBERT, C., MAUMET, C., JANNIN, P., FERRE, J. C., TREGUIER, C., BARILLOT, C., LE RUMEUR, E., ALLAIRE, C. & BIRABEN, A. 2011. Abnormal functional lateralization and activity of language brain areas in typical specific language impairment (developmental dysphasia). *Brain,* 134, 3044-58.

DEIBLER, A. R., POLLOCK, J. M., KRAFT, R. A., TAN, H., BURDETTE, J. H. & MALDJIAN, J. A. 2008. Arterial spin-labeling in routine clinical practice, part 1: technique and artifacts. *AJNR Am J Neuroradiol,* 29, 1228-34.

DENNIS, N. A. & CABEZA, R. 2008. *Neuroimaging of healthy cognitive aging,* New York, Psychology Press.

DENNIS, N. A., DASELAAR, S. & CABEZA, R. 2007. Effects of aging on transient and sustained successful memory encoding activity. *Neurobiol Aging,* 28, 1749-58.

DERRFUSS, J., BRASS, M. & VON CRAMON, D. Y. 2004. Cognitive control in the posterior frontolateral cortex: evidence from common activations in task coordination, interference control, and working memory. *Neuroimage,* 23, 604-12.

DESIKAN, R. S., SEGONNE, F., FISCHL, B., QUINN, B. T., DICKERSON, B. C., BLACKER, D., BUCKNER, R. L., DALE, A. M., MAGUIRE, R. P., HYMAN, B. T., ALBERT, M. S. & KILLIANY, R. J. 2006. An automated labeling system for subdividing the human cerebral cortex on MRI scans into gyral based regions of interest. *Neuroimage,* 31, 968-80.

DETRE, J. A., LEIGH, J. S., WILLIAMS, D. S. & KORETSKY, A. P. 1992. Perfusion imaging. *Magn Reson Med,* 23, 37-45.

DETRE, J. A. & WANG, J. 2002. Technical aspects and utility of fMRI using BOLD and ASL. *Clin Neurophysiol,* 113, 621-34.

DEVINSKY, O., MORRELL, M. J. & VOGT, B. A. 1995. Contributions of anterior cingulate cortex to behaviour. *Brain,* 118 (Pt 1), 279-306.

DICKERSON, B. C., FENSTERMACHER, E., SALAT, D. H., WOLK, D. A., MAGUIRE, R. P., DESIKAN, R., PACHECO, J., QUINN, B. T., VAN DER KOUWE, A., GREVE, D. N., BLACKER, D., ALBERT, M. S., KILLIANY, R. J. & FISCHL, B. 2008. Detection of cortical thickness correlates of

cognitive performance: Reliability across MRI scan sessions, scanners, and field strengths. *Neuroimage,* 39, 10-8.

DRISCOLL, I., HAMILTON, D. A., PETROPOULOS, H., YEO, R. A., BROOKS, W. M., BAUMGARTNER, R. N. & SUTHERLAND, R. J. 2003. The aging hippocampus: cognitive, biochemical and structural findings. *Cereb Cortex,* 13, 1344-51.

DUONG, T. Q., KIM, D. S., UGURBIL, K. & KIM, S. G. 2001. Localized cerebral blood flow response at submillimeter columnar resolution. *Proc Natl Acad Sci U S A,* 98, 10904-9.

EICKHOFF, S. B., STEPHAN, K. E., MOHLBERG, H., GREFKES, C., FINK, G. R., AMUNTS, K. & ZILLES, K. 2005. A new SPM toolbox for combining probabilistic cytoarchitectonic maps and functional imaging data. *Neuroimage,* 25, 1325-35.

ENCYCLOPAEDIA BRITANNICA, I. 2008. *Britannica Guide to the Brain,* Chicago, IL, USA, Encyclopaedia Britannica, Inc. and Constable & Robinson.

FAN, J., FOSSELLA, J., SOMMER, T., WU, Y. & POSNER, M. I. 2003. Mapping the genetic variation of executive attention onto brain activity. *Proc Natl Acad Sci U S A,* 100, 7406-11.

FAN, J., MCCANDLISS, B. D., FOSSELLA, J., FLOMBAUM, J. I. & POSNER, M. I. 2005. The activation of attentional networks. *Neuroimage,* 26, 471-9.

FARACI, F. M. & HEISTAD, D. D. 1998. Regulation of the cerebral circulation: role of endothelium and potassium channels. *Physiol Rev,* 78, 53-97.

FELLOWS, L. K. & FARAH, M. J. 2005. Is anterior cingulate cortex necessary for cognitive control? *Brain,* 128, 788-96.

FILIPEK, P. A., RICHELME, C., KENNEDY, D. N. & CAVINESS, V. S., JR. 1994. The young adult human brain: an MRI-based morphometric analysis. *Cereb Cortex,* 4, 344-60.

FISCHL, B. & DALE, A. M. 2000. Measuring the thickness of the human cerebral cortex from magnetic resonance images. *Proc Natl Acad Sci U S A,* 97, 11050-5.

FISCHL, B., LIU, A. & DALE, A. M. 2001. Automated manifold surgery: constructing geometrically accurate and topologically correct models of the human cerebral cortex. *IEEE Trans Med Imaging,* 20, 70-80.

FISCHL, B., SALAT, D. H., BUSA, E., ALBERT, M., DIETERICH, M., HASELGROVE, C., VAN DER KOUWE, A., KILLIANY, R., KENNEDY, D., KLAVENESS, S., MONTILLO, A., MAKRIS, N., ROSEN, B. & DALE, A. M. 2002. Whole brain segmentation: automated labeling of neuroanatomical structures in the human brain. *Neuron,* 33, 341-55.

FISCHL, B., SALAT, D. H., VAN DER KOUWE, A. J., MAKRIS, N., SEGONNE, F., QUINN, B. T. & DALE, A. M. 2004a. Sequence-independent segmentation of magnetic resonance images. *Neuroimage,* 23 Suppl 1, S69-84.

FISCHL, B., SERENO, M. I. & DALE, A. M. 1999a. Cortical surface-based analysis. II: Inflation, flattening, and a surface-based coordinate system. *Neuroimage,* 9, 195-207.

FISCHL, B., SERENO, M. I., TOOTELL, R. B. & DALE, A. M. 1999b. High-resolution intersubject averaging and a coordinate system for the cortical surface. *Hum Brain Mapp,* 8, 272-84.

FISCHL, B., VAN DER KOUWE, A., DESTRIEUX, C., HALGREN, E., SEGONNE, F., SALAT, D. H., BUSA, E., SEIDMAN, L. J., GOLDSTEIN, J., KENNEDY, D., CAVINESS, V., MAKRIS, N., ROSEN, B. & DALE, A.

M. 2004b. Automatically parcellating the human cerebral cortex. *Cereb Cortex,* 14, 11-22.

FJELL, A. M., WALHOVD, K. B., REINVANG, I., LUNDERVOLD, A., SALAT, D., QUINN, B. T., FISCHL, B. & DALE, A. M. 2006. Selective increase of cortical thickness in high-performing elderly--structural indices of optimal cognitive aging. *Neuroimage,* 29, 984-94.

FJELL, A. M., WESTLYE, L. T., AMLIEN, I., ESPESETH, T., REINVANG, I., RAZ, N., AGARTZ, I., SALAT, D. H., GREVE, D. N., FISCHL, B., DALE, A. M. & WALHOVD, K. B. 2009. High consistency of regional cortical thinning in aging across multiple samples. *Cereb Cortex,* 19, 2001-12.

FLYNN, F. G. 1999. Anatomy of the insula functional and clinical correlates. *Aphasiology,* 13, 55-78.

FOX, P. T., RAICHLE, M. E., MINTUN, M. A. & DENCE, C. 1988. Nonoxidative glucose consumption during focal physiologic neural activity. *Science,* 241, 462-4.

FUSTER, J. M. 1995. Memory and planning. Two temporal perspectives of frontal lobe function. *Adv Neurol,* 66, 9-19; discussion 19-20.

FUSTER, J. M. 2002. Frontal lobe and cognitive development. *J Neurocytol,* 31, 373-85.

GE, Y., GROSSMAN, R. I., BABB, J. S., RABIN, M. L., MANNON, L. J. & KOLSON, D. L. 2002. Age-related total gray matter and white matter changes in normal adult brain. Part I: volumetric MR imaging analysis. *AJNR Am J Neuroradiol,* 23, 1327-33.

GEYER, S., LEDBERG, A., SCHLEICHER, A., KINOMURA, S., SCHORMANN, T., BURGEL, U., KLINGBERG, T., LARSSON, J., ZILLES, K. & ROLAND, P. E. 1996. Two different areas within the primary motor cortex of man. *Nature,* 382, 805-807.

GJEDDE, A., MARRETT, S. & VAFAEE, M. 2002. Oxidative and nonoxidative metabolism of excited neurons and astrocytes. *J Cereb Blood Flow Metab,* 22, 1-14.

GOLDBERG, G. 1985. Supplementary motor area structure and function: Review and hypotheses. *Behavioral and Brain Sciences,* 8, 567-588.

GOLDMAN-RAKIC, P. S. 1996. Regional and cellular fractionation of working memory. *Proc Natl Acad Sci U S A,* 93, 13473-80.

GOLDSTEIN, J. M., SEIDMAN, L. J., HORTON, N. J., MAKRIS, N., KENNEDY, D. N., CAVINESS, V. S., JR., FARAONE, S. V. & TSUANG, M. T. 2001. Normal sexual dimorphism of the adult human brain assessed by in vivo magnetic resonance imaging. *Cereb Cortex,* 11, 490-7.

GOLDSTEIN, S. & REIVICH, M. 1991. Cerebral blood flow and metabolism in aging and dementia. *Clin Neuropharmacol,* 14 Suppl 1, S34-44.

GOLOMB, J., KLUGER, A., DE LEON, M. J., FERRIS, S. H., CONVIT, A., MITTELMAN, M. S., COHEN, J., RUSINEK, H., DE SANTI, S. & GEORGE, A. E. 1994. Hippocampal formation size in normal human aging: a correlate of delayed secondary memory performance. *Learn Mem,* 1, 45-54.

GONG, Q. Y., SLUMING, V., MAYES, A., KELLER, S., BARRICK, T., CEZAYIRLI, E. & ROBERTS, N. 2005. Voxel-based morphometry and stereology provide convergent evidence of the importance of medial prefrontal cortex for fluid intelligence in healthy adults. *Neuroimage,* 25, 1175-86.

GOOD, C. D., JOHNSRUDE, I. S., ASHBURNER, J., HENSON, R. N., FRISTON, K. J. & FRACKOWIAK, R. S. 2001a. Cerebral Asymmetry and the Effects of Sex and Handedness on Brain Structure: A Voxel-Based Morphometric Analysis of 465 Normal Adult Human Brains. *Neuroimage,* 14, 685-700.

GOOD, C. D., JOHNSRUDE, I. S., ASHBURNER, J., HENSON, R. N., FRISTON, K. J. & FRACKOWIAK, R. S. 2001b. A voxel-based morphometric study of ageing in 465 normal adult human brains. *Neuroimage,* 14, 21-36.

GOODWIN, J. A., VIDYASAGAR, R., BALANOS, G. M., BULTE, D. & PARKES, L. M. 2009. Quantitative fMRI using hyperoxia calibration: reproducibility during a cognitive Stroop task. *Neuroimage,* 47, 573-80.

GRACHEV, I. D., SWARNKAR, A., SZEVERENYI, N. M., RAMACHANDRAN, T. S. & APKARIAN, A. V. 2001. Aging alters the multichemical networking profile of the human brain: an in vivo (1)H-MRS study of young versus middle-aged subjects. *J Neurochem,* 77, 292-303.

GRADY, C. L. 2000. Functional brain imaging and age-related changes in cognition. *Biol Psychol,* 54, 259-81.

GRADY, C. L., MAISOG, J. M., HORWITZ, B., UNGERLEIDER, L. G., MENTIS, M. J., SALERNO, J. A., PIETRINI, P., WAGNER, E. & HAXBY, J. V. 1994. Age-related changes in cortical blood flow activation during visual processing of faces and location. *J Neurosci,* 14, 1450-62.

GRADY, C. L., MCINTOSH, A. R., HORWITZ, B., MAISOG, J. M., UNGERLEIDER, L. G., MENTIS, M. J., PIETRINI, P., SCHAPIRO, M. B. & HAXBY, J. V. 1995. Age-related reductions in human recognition memory due to impaired encoding. *Science,* 269, 218-21.

GRILL-SPECTOR, K., KUSHNIR, T., HENDLER, T., EDELMAN, S., ITZCHAK, Y. & MALACH, R. 1998. A sequence of object-processing stages revealed by fMRI in the human occipital lobe. *Hum Brain Mapp,* 6, 316-28.

GROSSMAN, M., COOKE, A., DEVITA, C., ALSOP, D., DETRE, J., CHEN, W. & GEE, J. 2002. Age-related changes in working memory during sentence comprehension: an fMRI study. *Neuroimage,* 15, 302-17.

GRUBB, R. L., JR., RAICHLE, M. E., EICHLING, J. O. & TER-POGOSSIAN, M. M. 1974. The effects of changes in PaCO2 on cerebral blood volume, blood flow, and vascular mean transit time. *Stroke,* 5, 630-9.

GUNNING-DIXON, F. M. & RAZ, N. 2003. Neuroanatomical correlates of selected executive functions in middle-aged and older adults: a prospective MRI study. *Neuropsychologia,* 41, 1929-41.

GUR, R. C., MOZLEY, P. D., RESNICK, S. M., GOTTLIEB, G. L., KOHN, M., ZIMMERMAN, R., HERMAN, G., ATLAS, S., GROSSMAN, R., BERRETTA, D. & ET AL. 1991. Gender differences in age effect on brain atrophy measured by magnetic resonance imaging. *Proc Natl Acad Sci U S A,* 88, 2845-9.

GUR, R. C., TURETSKY, B. I., MATSUI, M., YAN, M., BILKER, W., HUGHETT, P. & GUR, R. E. 1999. Sex differences in brain gray and white matter in healthy young adults: correlations with cognitive performance. *J Neurosci,* 19, 4065-72.

GUR, R. E., COWELL, P. E., LATSHAW, A., TURETSKY, B. I., GROSSMAN, R. I., ARNOLD, S. E., BILKER, W. B. & GUR, R. C. 2000. Reduced dorsal and orbital prefrontal gray matter volumes in schizophrenia. *Arch Gen Psychiatry,* 57, 761-8.

HAACKE, E. M., BROWN, R. W., THOMPSON, M. R. & VENKATESAN, R. 1999. *Magnetic Resonance Imaging - physical principples and sequnce design.* .

HALSBAND, U., ITO, N., TANJI, J. & FREUND, H. J. 1993. The role of premotor cortex and the supplementary motor area in the temporal control of movement in man. *Brain,* 116 (Pt 1), 243-66.

HAMPSHIRE, A., CHAMBERLAIN, S. R., MONTI, M. M., DUNCAN, J. & OWEN, A. M. 2010. The role of the right inferior frontal gyrus: inhibition and attentional control. *Neuroimage,* 50, 1313-9.

HANGGI, J., BUCHMANN, A., MONDADORI, C. R., HENKE, K., JANCKE, L. & HOCK, C. 2010. Sexual dimorphism in the parietal substrate associated with visuospatial cognition independent of general intelligence. *J Cogn Neurosci,* 22, 139-55.

HARDER, D. R., ALKAYED, N. J., LANGE, A. R., GEBREMEDHIN, D. & ROMAN, R. J. 1998. Functional hyperemia in the brain: hypothesis for astrocyte-derived vasodilator metabolites. *Stroke,* 29, 229-34.

HARDING, A. J., HALLIDAY, G. M. & KRIL, J. J. 1998. Variation in hippocampal neuron number with age and brain volume. *Cereb Cortex,* 8, 710-8.

HASSON, U., NIR, Y., LEVY, I., FUHRMANN, G. & MALACH, R. 2004. Intersubject synchronization of cortical activity during natural vision. *Science,* 303, 1634-40.

HAUG, H. 1985. Are neurons of the human cerebral cortex really lost during aging? A morphometric examination. *In:* TARBER, J. & GISPEN, W. H. (eds.) *Senile Dementia of Alzheimer Type.* Springer, Berlin.

HAXBY, J. V., GOBBINI, M. I., FUREY, M. L., ISHAI, A., SCHOUTEN, J. L. & PIETRINI, P. 2001. Distributed and overlapping representations of faces and objects in ventral temporal cortex. *Science,* 293, 2425-30.

HEAD, D., RODRIGUE, K. M., KENNEDY, K. M. & RAZ, N. 2008. Neuroanatomical and cognitive mediators of age-related differences in episodic memory. *Neuropsychology,* 22, 491-507.

HENLEY, S. M., RIDGWAY, G. R., SCAHILL, R. I., KLOPPEL, S., TABRIZI, S. J., FOX, N. C. & KASSUBEK, J. 2010. Pitfalls in the use of voxel-based morphometry as a biomarker: examples from huntington disease. *AJNR Am J Neuroradiol,* 31, 711-9.

HOGE, R. D., ATKINSON, J., GILL, B., CRELIER, G. R., MARRETT, S. & PIKE, G. B. 1999a. Investigation of BOLD signal dependence on cerebral blood

flow and oxygen consumption: the deoxyhemoglobin dilution model. *Magn Reson Med,* 42, 849-63.

HOGE, R. D., ATKINSON, J., GILL, B., CRELIER, G. R., MARRETT, S. & PIKE, G. B. 1999b. Linear coupling between cerebral blood flow and oxygen consumption in activated human cortex. *Proc Natl Acad Sci U S A,* 96, 9403-8.

HUBBARD, B. M. & ANDERSON, J. M. 1983. Sex differences in age-related brain atrophy. *Lancet,* 1, 1447-8.

HUETTEL, S. A., SINGERMAN, J. D. & MCCARTHY, G. 2001. The effects of aging upon the hemodynamic response measured by functional MRI. *Neuroimage,* 13, 161-75.

HULVERSHORN, J., BLOY, L., GUALTIERI, E. E., LEIGH, J. S. & ELLIOTT, M. A. 2005a. Spatial sensitivity and temporal response of spin echo and gradient echo bold contrast at 3 T using peak hemodynamic activation time. *Neuroimage,* 24, 216-23.

HULVERSHORN, J., BLOY, L., GUALTIERI, E. E., REDMANN, C. P., LEIGH, J. S. & ELLIOTT, M. A. 2005b. Temporal resolving power of spin echo and gradient echo fMRI at 3T with apparent diffusion coefficient compartmentalization. *Hum Brain Mapp,* 25, 247-58.

HYDER, F. 2004. Neuroimaging with calibrated FMRI. *Stroke,* 35, 2635-41.

HYDER, F., KIDA, I., BEHAR, K. L., KENNAN, R. P., MACIEJEWSKI, P. K. & ROTHMAN, D. L. 2001. Quantitative functional imaging of the brain: towards mapping neuronal activity by BOLD fMRI. *NMR Biomed,* 14, 413-31.

IADECOLA, C. 2004. Neurovascular regulation in the normal brain and in Alzheimer's disease. *Nat Rev Neurosci,* 5, 347-60.

IADECOLA, C. & NEDERGAARD, M. 2007. Glial regulation of the cerebral microvasculature. *Nat Neurosci,* 10, 1369-76.

JACOBS, B., DRISCOLL, L. & SCHALL, M. 1997. Life-span dendritic and spine changes in areas 10 and 18 of human cortex: a quantitative Golgi study. *J Comp Neurol,* 386, 661-80.

JEFFREY D, S. 2004. On the role of frontal eye field in guiding attention and saccades. *Vision Research,* 44, 1453-1467.

JEZZARD, P., HEINEMAN, F., TAYLOR, J., DESPRES, D., WEN, H., BALABAN, R. S. & TURNER, R. 1994. Comparison of EPI gradient-echo contrast changes in cat brain caused by respiratory challenges with direct simultaneous evaluation of cerebral oxygenation via a cranial window. *NMR Biomed,* 7, 35-44.

JEZZARD, P., MATTHEWS, P. M. & SMITH, G. E. 2001. *Functional MRI: An Introduction to Methods*, 1.

KARNATH, H. O., FERBER, S. & HIMMELBACH, M. 2001. Spatial awareness is a function of the temporal not the posterior parietal lobe. *Nature,* 411, 950-3.

KASTRUP, A., KRUGER, G., GLOVER, G. H. & MOSELEY, M. E. 1999a. Assessment of cerebral oxidative metabolism with breath holding and fMRI. *Magn Reson Med,* 42, 608-11.

KASTRUP, A., KRUGER, G., NEUMANN-HAEFELIN, T., GLOVER, G. H. & MOSELEY, M. E. 2002. Changes of cerebral blood flow, oxygenation, and oxidative metabolism during graded motor activation. *Neuroimage,* 15, 74-82.

KASTRUP, A., LI, T. Q., GLOVER, G. H. & MOSELEY, M. E. 1999b. Cerebral blood flow-related signal changes during breath-holding. *AJNR Am J Neuroradiol,* 20, 1233-8.

KELLEY, L. L. & PETERSEN, C. M. 1997. *Sectional Anatomy for Imaging Professionals.*

KEMPER, T. L. 1994. *Neuroanatomical and neuropathological changes during aging and in dementia. In: Clinical neurology of aging,* New York, Oxford University Press.

KIRCHER, T. T., BRAMMER, M. J., LEVELT, W., BARTELS, M. & MCGUIRE, P. K. 2004. Pausing for thought: engagement of left temporal cortex during pauses in speech. *Neuroimage,* 21, 84-90.

KOEHLER, R. C., ROMAN, R. J. & HARDER, D. R. 2009. Astrocytes and the regulation of cerebral blood flow. *Trends Neurosci,* 32, 160-9.

KOLB, B. & WHISHAW, I. 2003. *Fundamentals of human neuropsychology,* New York, NY, Worth Publishers.

KWONG, K. K., BELLIVEAU, J. W., CHESLER, D. A., GOLDBERG, I. E., WEISSKOFF, R. M., PONCELET, B. P., KENNEDY, D. N., HOPPEL, B. E., COHEN, M. S., TURNER, R. & ET AL. 1992. Dynamic magnetic resonance imaging of human brain activity during primary sensory stimulation. *Proc Natl Acad Sci U S A,* 89, 5675-9.

LANGENECKER, S. A., NIELSON, K. A. & RAO, S. M. 2004. fMRI of healthy older adults during Stroop interference. *Neuroimage,* 21, 192-200.

LAU, H. C., ROGERS, R. D., HAGGARD, P. & PASSINGHAM, R. E. 2004. Attention to intention. *Science,* 303, 1208-10.

LAUTERBUR, P. C. 1973. Image formation by induced local interactions. Examples employing nuclear magnetic resonance. 1973. *Clin Orthop Relat Res*, 3-6.

LEENDERS, K. L., PERANI, D., LAMMERTSMA, A. A., HEATHER, J. D., BUCKINGHAM, P., HEALY, M. J., GIBBS, J. M., WISE, R. J., HATAZAWA, J., HEROLD, S. & ET AL. 1990. Cerebral blood flow, blood

volume and oxygen utilization. Normal values and effect of age. *Brain,* 113 (Pt 1), 27-47.

LEIBOVICI, D., RITCHIE, K., LEDESERT, B. & TOUCHON, J. 1996. Does education level determine the course of cognitive decline? *Age Ageing,* 25, 392-7.

LEMAITRE, H., CRIVELLO, F., GRASSIOT, B., ALPEROVITCH, A., TZOURIO, C. & MAZOYER, B. 2005. Age- and sex-related effects on the neuroanatomy of healthy elderly. *Neuroimage,* 26, 900-11.

LEONARD, C. M., TOWLER, S., WELCOME, S., HALDERMAN, L. K., OTTO, R., ECKERT, M. A. & CHIARELLO, C. 2008. Size matters: cerebral volume influences sex differences in neuroanatomy. *Cereb Cortex,* 18, 2920-31.

LEONTIEV, O. & BUXTON, R. B. 2007. Reproducibility of BOLD, perfusion, and CMRO2 measurements with calibrated-BOLD fMRI. *Neuroimage,* 35, 175-84.

LEONTIEV, O., DUBOWITZ, D. J. & BUXTON, R. B. 2007. CBF/CMRO2 coupling measured with calibrated BOLD fMRI: sources of bias. *Neuroimage,* 36, 1110-22.

LEZAK, M. D. 1995. *Neuropsychological Assessment,* New York, Oxford University Press.

LIU, T. T. & BROWN, G. G. 2007. Measurement of cerebral perfusion with arterial spin labeling: Part 1. Methods. *J Int Neuropsychol Soc,* 13, 517-25.

LOGAN, J. M., SANDERS, A. L., SNYDER, A. Z., MORRIS, J. C. & BUCKNER, R. L. 2002. Under-recruitment and nonselective recruitment: dissociable neural mechanisms associated with aging. *Neuron,* 33, 827-40.

LOGOTHETIS, N. K., PAULS, J., AUGATH, M., TRINATH, T. & OELTERMANN, A. 2001. Neurophysiological investigation of the basis of the fMRI signal. *Nature,* 412, 150-7.

LOGOTHETIS, N. K. & WANDELL, B. A. 2004. Interpreting the BOLD signal. *Annu Rev Physiol,* 66, 735-69.

LU, H., XU, F., RODRIGUE, K. M., KENNEDY, K. M., CHENG, Y., FLICKER, B., HEBRANK, A. C., UH, J. & PARK, D. C. 2010. Alterations in Cerebral Metabolic Rate and Blood Supply across the Adult Lifespan. *Cereb Cortex.*

LUDERS, E., NARR, K. L., THOMPSON, P. M., WOODS, R. P., REX, D. E., JANCKE, L., STEINMETZ, H. & TOGA, A. W. 2005. Mapping cortical gray matter in the young adult brain: effects of gender. *Neuroimage,* 26, 493-501.

LUFT, A. R., SKALEJ, M., SCHULZ, J. R. B., WELTE, D., KOLB, R., B√°RK, K., KLOCKGETHER, T. & VOIGT, K. 1999. Patterns of Age-related Shrinkage in Cerebellum and Brainstem Observed In Vivo Using Three-dimensional MRI Volumetry. *Cerebral Cortex,* 9, 712-721.

LUH, W. M., WONG, E. C., BANDETTINI, P. A. & HYDE, J. S. 1999. QUIPSS II with thin-slice TI1 periodic saturation: a method for improving accuracy of quantitative perfusion imaging using pulsed arterial spin labeling. *Magn Reson Med,* 41, 1246-54.

LUH, W. M., WONG, E. C., BANDETTINI, P. A., WARD, B. D. & HYDE, J. S. 2000. Comparison of simultaneously measured perfusion and BOLD signal increases during brain activation with T(1)-based tissue identification. *Magn Reson Med,* 44, 137-43.

MACLEOD, C. M. 1991. Half a century of research on the Stroop effect: an integrative review. *Psychol Bull,* 109, 163-203.

MADDEN, D. J., TURKINGTON, T. G., COLEMAN, R. E., PROVENZALE, J. M., DEGRADO, T. R. & HOFFMAN, J. M. 1996. Adult age differences in regional cerebral blood flow during visual world identification: evidence from H215O PET. *Neuroimage,* 3, 127-42.

MADDEN, D. J., TURKINGTON, T. G., PROVENZALE, J. M., DENNY, L. L., HAWK, T. C., GOTTLOB, L. R. & COLEMAN, R. E. 1999. Adult age differences in the functional neuroanatomy of verbal recognition memory. *Hum Brain Mapp,* 7, 115-35.

MADDEN, D. J., TURKINGTON, T. G., PROVENZALE, J. M., DENNY, L. L., LANGLEY, L. K., HAWK, T. C. & COLEMAN, R. E. 2002. Aging and attentional guidance during visual search: functional neuroanatomy by positron emission tomography. *Psychol Aging,* 17, 24-43.

MADDEN, D. J., TURKINGTON, T. G., PROVENZALE, J. M., HAWK, T. C., HOFFMAN, J. M. & COLEMAN, R. E. 1997. Selective and divided visual attention: age-related changes in regional cerebral blood flow measured by H2(15)O PET. *Hum Brain Mapp,* 5, 389-409.

MADORE, B. & PELC, N. J. 2001. SMASH and SENSE: experimental and numerical comparisons. *Magn Reson Med,* 45, 1103-11.

MANSFIELD, P. & GRANNELL, P. K. 1973. NMR 'diffraction' in solids? *J. Phys. C:Solid State Phys.,* 6.

MARCHAL, G., RIOUX, P., PETIT-TABOUE, M. C., SETTE, G., TRAVERE, J. M., LE POEC, C., COURTHEOUX, P., DERLON, J. M. & BARON, J. C. 1992. Regional cerebral oxygen consumption, blood flow, and blood volume in healthy human aging. *Arch Neurol,* 49, 1013-20.

MARTIN, J. H. 2003. *Neuroanatomy - text and atlas*, McGrawHill.

MARTINI, F. H. 1998. *Fundamentals of Anatomy and Physiology.*

MCROBBIE, D., MOORE, E., GRAVES, M. & PRINCE, M. 2007. *MRI from Picture to Proton*, Cambridge University Press.

MEGA, M. S., CUMMINGS, J. L., SALLOWAY, S. & MALLOY, P. 1997. The limbic system: an anatomic, phylogenetic, and clinical perspective. *J Neuropsychiatry Clin Neurosci,* 9, 315-30.

MILHAM, M. P., ERICKSON, K. I., BANICH, M. T., KRAMER, A. F., WEBB, A., WSZALEK, T. & COHEN, N. J. 2002. Attentional control in the aging brain: insights from an fMRI study of the stroop task. *Brain Cogn,* 49, 277-96.

MILLER, A. K., ALSTON, R. L. & CORSELLIS, J. A. 1980. Variation with age in the volumes of grey and white matter in the cerebral hemispheres of man: measurements with an image analyser. *Neuropathol Appl Neurobiol,* 6, 119-32.

MILLER, K. L., LUH, W. M., LIU, T. T., MARTINEZ, A., OBATA, T., WONG, E. C., FRANK, L. R. & BUXTON, R. B. 2001. Nonlinear temporal dynamics of the cerebral blood flow response. *Hum Brain Mapp,* 13, 1-12.

MORRISON, J. H. & HOF, P. R. 1997. Life and death of neurons in the aging brain. *Science,* 278, 412-9.

MOSCOVITCH, M. & WINOCUR, G. 1995. Frontal lobes, memory, and aging. *Ann N Y Acad Sci,* 769, 119-50.

MUGLER, J. P., 3RD & BROOKEMAN, J. R. 1990. Three-dimensional magnetization-prepared rapid gradient-echo imaging (3D MP RAGE). *Magn Reson Med,* 15, 152-7.

MURPHY, D. G., DECARLI, C., MCINTOSH, A. R., DALY, E., MENTIS, M. J., PIETRINI, P., SZCZEPANIK, J., SCHAPIRO, M. B., GRADY, C. L., HORWITZ, B. & RAPOPORT, S. I. 1996. Sex differences in human brain morphometry and metabolism: an in vivo quantitative magnetic resonance imaging and positron emission tomography study on the effect of aging. *Arch Gen Psychiatry,* 53, 585-94.

NAIRN, J. G., BEDI, K. S., MAYHEW, T. M. & CAMPBELL, L. F. 1989. On the number of Purkinje cells in the human cerebellum: unbiased estimates obtained by using the "fractionator". *J Comp Neurol,* 290, 527-32.

NARR, K. L., WOODS, R. P., THOMPSON, P. M., SZESZKO, P., ROBINSON, D., DIMTCHEVA, T., GURBANI, M., TOGA, A. W. & BILDER, R. M. 2007. Relationships between IQ and regional cortical gray matter thickness in healthy adults. *Cereb Cortex,* 17, 2163-71.

NARUMOTO, J., OKADA, T., SADATO, N., FUKUI, K. & YONEKURA, Y. 2001. Attention to emotion modulates fMRI activity in human right superior temporal sulcus. *Brain Res Cogn Brain Res,* 12, 225-31.

NIELSON, K. A., LANGENECKER, S. A. & GARAVAN, H. 2002. Differences in the functional neuroanatomy of inhibitory control across the adult life span. *Psychol Aging,* 17, 56-71.

NOPOULOS, P., FLAUM, M., O'LEARY, D. & ANDREASEN, N. C. 2000. Sexual dimorphism in the human brain: evaluation of tissue volume, tissue composition and surface anatomy using magnetic resonance imaging. *Psychiatry Res,* 98, 1-13.

NYBERG, L., SANDBLOM, J., JONES, S., NEELY, A. S., PETERSSON, K. M., INGVAR, M. & BACKMAN, L. 2003. Neural correlates of training-related memory improvement in adulthood and aging. *Proc Natl Acad Sci U S A,* 100, 13728-33.

O'SULLIVAN, M., MORRIS, R. G. & MARKUS, H. S. 2005. Brief cognitive assessment for patients with cerebral small vessel disease. *J Neurol Neurosurg Psychiatry,* 76, 1140-5.

OBATA, T., LIU, T. T., MILLER, K. L., LUH, W. M., WONG, E. C., FRANK, L. R. & BUXTON, R. B. 2004. Discrepancies between BOLD and flow dynamics in primary and supplementary motor areas: application of the

balloon model to the interpretation of BOLD transients. *Neuroimage,* 21, 144-53.

OGAWA, S. & LEE, T. M. 1990. Magnetic resonance imaging of blood vessels at high fields: in vivo and in vitro measurements and image simulation. *Magn Reson Med,* 16, 9-18.

OGAWA, S., LEE, T. M., KAY, A. R. & TANK, D. W. 1990a. Brain magnetic resonance imaging with contrast dependent on blood oxygenation. *Proc Natl Acad Sci U S A,* 87, 9868-72.

OGAWA, S., LEE, T. M., NAYAK, A. S. & GLYNN, P. 1990b. Oxygenation-sensitive contrast in magnetic resonance image of rodent brain at high magnetic fields. *Magn Reson Med,* 14, 68-78.

OGAWA, S., MENON, R. S., TANK, D. W., KIM, S. G., MERKLE, H., ELLERMANN, J. M. & UGURBIL, K. 1993. Functional brain mapping by blood oxygenation level-dependent contrast magnetic resonance imaging. A comparison of signal characteristics with a biophysical model. *Biophys J,* 64, 803-12.

OGAWA, S., TANK, D. W., MENON, R., ELLERMANN, J. M., KIM, S. G., MERKLE, H. & UGURBIL, K. 1992. Intrinsic signal changes accompanying sensory stimulation: functional brain mapping with magnetic resonance imaging. *Proc Natl Acad Sci U S A,* 89, 5951-5.

OPPENHEIMER, S. 1993. The anatomy and physiology of cortical mechanisms of cardiac control. *Stroke,* 24, I3-5.

OWEN, A. M. 2000. The role of the lateral frontal cortex in mnemonic processing: the contribution of functional neuroimaging. *Exp Brain Res,* 133, 33-43.

PAKKENBERG, B. & GUNDERSEN, H. J. 1997. Neocortical neuron number in humans: effect of sex and age. *J Comp Neurol,* 384, 312-20.

PANIZZON, M. S., FENNEMA-NOTESTINE, C., EYLER, L. T., JERNIGAN, T. L., PROM-WORMLEY, E., NEALE, M., JACOBSON, K., LYONS, M. J., GRANT, M. D., FRANZ, C. E., XIAN, H., TSUANG, M., FISCHL, B., SEIDMAN, L., DALE, A. & KREMEN, W. S. 2009. Distinct genetic influences on cortical surface area and cortical thickness. *Cereb Cortex,* 19, 2728-35.

PANTANO, P., BARON, J. C., LEBRUN-GRANDIE, P., DUQUESNOY, N., BOUSSER, M. G. & COMAR, D. 1984. Regional cerebral blood flow and oxygen consumption in human aging. *Stroke,* 15, 635-41.

PARDO, J. V., PARDO, P. J., JANER, K. W. & RAICHLE, M. E. 1990. The anterior cingulate cortex mediates processing selection in the Stroop attentional conflict paradigm. *Proc Natl Acad Sci U S A,* 87, 256-9.

PARKES, L. M., RASHID, W., CHARD, D. T. & TOFTS, P. S. 2004. Normal cerebral perfusion measurements using arterial spin labeling: reproducibility, stability, and age and gender effects. *Magn Reson Med,* 51, 736-43.

PARKES, L. M. & TOFTS, P. S. 2002. Improved accuracy of human cerebral blood perfusion measurements using arterial spin labeling: accounting for capillary water permeability. *Magn Reson Med,* 48, 27-41.

PAULESU, E., FRITH, C. D. & FRACKOWIAK, R. S. 1993. The neural correlates of the verbal component of working memory. *Nature,* 362, 342-5.

PETERSEN, E. T., ZIMINE, I., HO, Y. C. & GOLAY, X. 2006. Non-invasive measurement of perfusion: a critical review of arterial spin labelling techniques. *Br J Radiol,* 79, 688-701.

PETRIDES, M. 2000. The role of the mid-dorsolateral prefrontal cortex in working memory. *Exp Brain Res,* 133, 44-54.

PFEFFERBAUM, A., MATHALON, D. H., SULLIVAN, E. V., RAWLES, J. M., ZIPURSKY, R. B. & LIM, K. O. 1994. A quantitative magnetic resonance

imaging study of changes in brain morphology from infancy to late adulthood. *Arch Neurol,* 51, 874-87.

PFEFFERBAUM, A., SULLIVAN, E. V., SWAN, G. E. & CARMELLI, D. 2000. Brain structure in men remains highly heritable in the seventh and eighth decades of life. *Neurobiol Aging,* 21, 63-74.

PURCELL, E. M., TORREY, H. C. & POUND, R. V. 1946. Resonance Absorption by Nuclear Magnetic Moments in a Solid. *Physical Review,* 69, 37-38.

RABBITT, P. 2005. *Methodology of Frontal and Executive Function*, Psychology press Ltd.

RAICHLE, M. E., MACLEOD, A. M., SNYDER, A. Z., POWERS, W. J., GUSNARD, D. A. & SHULMAN, G. L. 2001. A default mode of brain function. *Proc Natl Acad Sci U S A,* 98, 676-82.

RAICHLE, M. E. & MINTUN, M. A. 2006. Brain work and brain imaging. *Annu Rev Neurosci,* 29, 449-76.

RAZ, N. 2000. *Aging of the brain and its impact on cognitive performance: integration of structural and functional findings. In: The handbook of aging and cognition*, Psychology Press, USA

RAZ, N., BRIGGS, S. D., MARKS, W. & ACKER, J. D. 1999. Age-related deficits in generation and manipulation of mental images: II. The role of dorsolateral prefrontal cortex. *Psychol Aging,* 14, 436-44.

RAZ, N., GUNNING, F. M., HEAD, D., DUPUIS, J. H., MCQUAIN, J., BRIGGS, S. D., LOKEN, W. J., THORNTON, A. E. & ACKER, J. D. 1997. Selective aging of the human cerebral cortex observed in vivo: differential vulnerability of the prefrontal gray matter. *Cereb Cortex,* 7, 268-82.

RAZ, N., GUNNING-DIXON, F., HEAD, D., RODRIGUE, K. M., WILLIAMSON, A. & ACKER, J. D. 2004. Aging, sexual dimorphism, and hemispheric

asymmetry of the cerebral cortex: replicability of regional differences in volume. *Neurobiol Aging,* 25, 377-96.

RAZ, N., GUNNING-DIXON, F., HEAD, D., WILLIAMSON, A. & ACKER, J. D. 2001. Age and sex differences in the cerebellum and the ventral pons: a prospective MR study of healthy adults. *AJNR Am J Neuroradiol,* 22, 1161-7.

RAZ, N., GUNNING-DIXON, F. M., HEAD, D., DUPUIS, J. H. & ACKER, J. D. 1998. Neuroanatomical correlates of cognitive aging: evidence from structural magnetic resonance imaging. *Neuropsychology,* 12, 95-114.

RAZ, N., LINDENBERGER, U., GHISLETTA, P., RODRIGUE, K. M., KENNEDY, K. M. & ACKER, J. D. 2008. Neuroanatomical correlates of fluid intelligence in healthy adults and persons with vascular risk factors. *Cereb Cortex,* 18, 718-26.

RAZ, N., LINDENBERGER, U., RODRIGUE, K. M., KENNEDY, K. M., HEAD, D., WILLIAMSON, A., DAHLE, C., GERSTORF, D. & ACKER, J. D. 2005. Regional brain changes in aging healthy adults: general trends, individual differences and modifiers. *Cereb Cortex,* 15, 1676-89.

RAZ, N. & RODRIGUE, K. M. 2006. Differential aging of the brain: patterns, cognitive correlates and modifiers. *Neurosci Biobehav Rev,* 30, 730-48.

RESNICK, S. M., GOLDSZAL, A. F., DAVATZIKOS, C., GOLSKI, S., KRAUT, M. A., METTER, E. J., BRYAN, R. N. & ZONDERMAN, A. B. 2000. One-year age changes in MRI brain volumes in older adults. *Cereb Cortex,* 10, 464-72.

RESNICK, S. M., PHAM, D. L., KRAUT, M. A., ZONDERMAN, A. B. & DAVATZIKOS, C. 2003. Longitudinal magnetic resonance imaging studies of older adults: a shrinking brain. *J Neurosci,* 23, 3295-301.

RESTOM, K., BANGEN, K. J., BONDI, M. W., PERTHEN, J. E. & LIU, T. T. 2007. Cerebral blood flow and BOLD responses to a memory encoding task:

a comparison between healthy young and elderly adults. *Neuroimage,* 37, 430-9.

RESTOM, K., PERTHEN, J. E. & LIU, T. T. 2008. Calibrated fMRI in the medial temporal lobe during a memory-encoding task. *Neuroimage,* 40, 1495-502.

REUTER-LORENZ, P. A., JONIDES, J., SMITH, E. E., HARTLEY, A., MILLER, A., MARSHUETZ, C. & KOEPPE, R. A. 2000. Age differences in the frontal lateralization of verbal and spatial working memory revealed by PET. *J Cogn Neurosci,* 12, 174-87.

RIDGWAY, G. R., HENLEY, S. M., ROHRER, J. D., SCAHILL, R. I., WARREN, J. D. & FOX, N. C. 2008. Ten simple rules for reporting voxel-based morphometry studies. *Neuroimage,* 40, 1429-35.

RIZZOLATTI, G., LUPPINO, G. & MATELLI, M. 1996. The classic supplementary motor area is formed by two independent areas. *Adv Neurol,* 70, 45-56.

ROSSELLI, M. & ARDILA, A. 2003. The impact of culture and education on non-verbal neuropsychological measurements: a critical review. *Brain Cogn,* 52, 326-33.

ROSTRUP, E., LAW, I., BLINKENBERG, M., LARSSON, H. B., BORN, A. P., HOLM, S. & PAULSON, O. B. 2000. Regional differences in the CBF and BOLD responses to hypercapnia: a combined PET and fMRI study. *Neuroimage,* 11, 87-97.

ROTHI, L. J., HEILMAN, K. M. & WATSON, R. T. 1985. Pantomime comprehension and ideomotor apraxia. *J Neurol Neurosurg Psychiatry,* 48, 207-10.

ROY, C. S. & SHERRINGTON, C. S. 1890. On the Regulation of the Blood-supply of the Brain. *J Physiol,* 11, 85-158 17.

RUBY, P., SIRIGU, A. & DECETY, J. 2002. Distinct areas in parietal cortex involved in long-term and short-term action planning: a PET investigation. *Cortex,* 38, 321-39.

RUSHWORTH, M. F., KRAMS, M. & PASSINGHAM, R. E. 2001. The attentional role of the left parietal cortex: the distinct lateralization and localization of motor attention in the human brain. *J Cogn Neurosci,* 13, 698-710.

SAKATA, H., TAIRA, M., KUSUNOKI, M., MURATA, A. & TANAKA, Y. 1997. The TINS Lecture The parietal association cortex in depth perception and visual control of hand action. *Trends in Neurosciences,* 20, 350-357.

SALAT, D. H., BUCKNER, R. L., SNYDER, A. Z., GREVE, D. N., DESIKAN, R. S., BUSA, E., MORRIS, J. C., DALE, A. M. & FISCHL, B. 2004. Thinning of the cerebral cortex in aging. *Cereb Cortex,* 14, 721-30.

SALAT, D. H., KAYE, J. A. & JANOWSKY, J. S. 1999. Prefrontal gray and white matter volumes in healthy aging and Alzheimer disease. *Arch Neurol,* 56, 338-44.

SALAT, D. H., LEE, S. Y., VAN DER KOUWE, A. J., GREVE, D. N., FISCHL, B. & ROSAS, H. D. 2009. Age-associated alterations in cortical gray and white matter signal intensity and gray to white matter contrast. *Neuroimage,* 48, 21-8.

SALTHOUSE, T. A., ATKINSON, T. M. & BERISH, D. E. 2003. Executive functioning as a potential mediator of age-related cognitive decline in normal adults. *J Exp Psychol Gen,* 132, 566-94.

SANDS, M. J. & LEVITIN, A. 2004. Basics of magnetic resonance imaging. *Semin Vasc Surg,* 17, 66-82.

SAXE, R. & KANWISHER, N. 2003. People thinking about thinking people. The role of the temporo-parietal junction in "theory of mind". *Neuroimage,* 19, 1835-42.

SCHLAEPFER, T. E., HARRIS, G. J., TIEN, A. Y., PENG, L., LEE, S. & PEARLSON, G. D. 1995. Structural differences in the cerebral cortex of healthy female and male subjects: a magnetic resonance imaging study. *Psychiatry Res,* 61, 129-35.

SEGONNE, F., DALE, A. M., BUSA, E., GLESSNER, M., SALAT, D., HAHN, H. K. & FISCHL, B. 2004. A hybrid approach to the skull stripping problem in MRI. *Neuroimage,* 22, 1060-75.

SEGONNE, F., PACHECO, J. & FISCHL, B. 2007. Geometrically accurate topology-correction of cortical surfaces using nonseparating loops. *IEEE Trans Med Imaging,* 26, 518-29.

SERENO, M. I., DALE, A. M., REPPAS, J. B., KWONG, K. K., BELLIVEAU, J. W., BRADY, T. J., ROSEN, B. R. & TOOTELL, R. B. 1995. Borders of multiple visual areas in humans revealed by functional magnetic resonance imaging. *Science,* 268, 889-93.

SHERGILL, S. S., BULLMORE, E., SIMMONS, A., MURRAY, R. & MCGUIRE, P. 2000. Functional anatomy of auditory verbal imagery in schizophrenic patients with auditory hallucinations. *Am J Psychiatry,* 157, 1691-3.

SHIMA, K. & TANJI, J. 1998. Both supplementary and presupplementary motor areas are crucial for the temporal organization of multiple movements. *J Neurophysiol,* 80, 3247-60.

SHULMAN, G. L., POPE, D. L., ASTAFIEV, S. V., MCAVOY, M. P., SNYDER, A. Z. & CORBETTA, M. 2010. Right hemisphere dominance during spatial selective attention and target detection occurs outside the dorsal frontoparietal network. *J Neurosci,* 30, 3640-51.

SIMIC, G., KOSTOVIC, I., WINBLAD, B. & BOGDANOVIC, N. 1997. Volume and number of neurons of the human hippocampal formation in normal aging and Alzheimer's disease. *J Comp Neurol,* 379, 482-94.

SLED, J. G., ZIJDENBOS, A. P. & EVANS, A. C. 1998. A nonparametric method for automatic correction of intensity nonuniformity in MRI data. *IEEE Trans Med Imaging,* 17, 87-97.

SMITH, C. D., CHEBROLU, H., WEKSTEIN, D. R., SCHMITT, F. A. & MARKESBERY, W. R. 2007. Age and gender effects on human brain anatomy: a voxel-based morphometric study in healthy elderly. *Neurobiol Aging,* 28, 1075-87.

SOWELL, E. R., PETERSON, B. S., KAN, E., WOODS, R. P., YOSHII, J., BANSAL, R., XU, D., ZHU, H., THOMPSON, P. M. & TOGA, A. W. 2007. Sex differences in cortical thickness mapped in 176 healthy individuals between 7 and 87 years of age. *Cereb Cortex,* 17, 1550-60.

SOWELL, E. R., PETERSON, B. S., THOMPSON, P. M., WELCOME, S. E., HENKENIUS, A. L. & TOGA, A. W. 2003. Mapping cortical change across the human life span. *Nat Neurosci,* 6, 309-15.

SOWELL, E. R., THOMPSON, P. M., HOLMES, C. J., BATTH, R., JERNIGAN, T. L. & TOGA, A. W. 1999. Localizing age-related changes in brain structure between childhood and adolescence using statistical parametric mapping. *Neuroimage,* 9, 587-97.

STIPPICH, C., HEILAND, S., TRONNIER, V., MOHR, A. & SARTOR, K. 2002. [Functional magnetic resonance imaging: Physiological background, technical aspects and prerequisites for clinical use]. *Rofo,* 174, 43-9.

STOLERU, S., GREGOIRE, M. C., GERARD, D., DECETY, J., LAFARGE, E., CINOTTI, L., LAVENNE, F., LE BARS, D., VERNET-MAURY, E., RADA, H., COLLET, C., MAZOYER, B., FOREST, M. G., MAGNIN, F., SPIRA, A. & COMAR, D. 1999. Neuroanatomical correlates of visually evoked sexual arousal in human males. *Arch Sex Behav,* 28, 1-21.

STUART, B. 1993. Functional Neuroanatomy. *The Royal College of Psychiatrists.*

SULLIVAN, E. V., ROSENBLOOM, M., SERVENTI, K. L. & PFEFFERBAUM, A. 2004. Effects of age and sex on volumes of the thalamus, pons, and cortex. *Neurobiol Aging,* 25, 185-92.

TAKI, Y., GOTO, R., EVANS, A., ZIJDENBOS, A., NEELIN, P., LERCH, J., SATO, K., ONO, S., KINOMURA, S., NAKAGAWA, M., SUGIURA, M., WATANABE, J., KAWASHIMA, R. & FUKUDA, H. 2004. Voxel-based morphometry of human brain with age and cerebrovascular risk factors. *Neurobiol Aging,* 25, 455-63.

TAMRAZ, J. C. & COMAIR, Y. G. 2006. *Atlas of regional anatomy of the brain using MRI : with functional correlations,* New York, Springer.

TERRY, R. D., DETERESA, R. & HANSEN, L. A. 1987. Neocortical cell counts in normal human adult aging. *Ann Neurol,* 21, 530-9.

THAMBISETTY, M., WAN, J., CARASS, A., AN, Y., PRINCE, J. L. & RESNICK, S. M. 2010. Longitudinal changes in cortical thickness associated with normal aging. *Neuroimage,* 52, 1215-1223.

THESEN, S., HEID, O., MUELLER, E. & SCHAD, L. R. 2000. Prospective acquisition correction for head motion with image-based tracking for real-time fMRI. *Magn Reson Med,* 44, 457-65.

THOMASON, M. E., FOLAND, L. C. & GLOVER, G. H. 2007. Calibration of BOLD fMRI using breath holding reduces group variance during a cognitive task. *Hum Brain Mapp,* 28, 59-68.

THULBORN, K. R., WATERTON, J. C., MATTHEWS, P. M. & RADDA, G. K. 1982. Oxygenation dependence of the transverse relaxation time of water protons in whole blood at high field. *Biochim Biophys Acta,* 714, 265-70.

TISSERAND, D. J. & JOLLES, J. 2003. On the involvement of prefrontal networks in cognitive ageing. *Cortex,* 39, 1107-28.

TISSERAND, D. J., PRUESSNER, J. C., SANZ ARIGITA, E. J., VAN BOXTEL, M. P., EVANS, A. C., JOLLES, J. & UYLINGS, H. B. 2002. Regional frontal cortical volumes decrease differentially in aging: an MRI study to compare volumetric approaches and voxel-based morphometry. *Neuroimage,* 17, 657-69.

TISSERAND, D. J., VAN BOXTEL, M. P., PRUESSNER, J. C., HOFMAN, P., EVANS, A. C. & JOLLES, J. 2004. A voxel-based morphometric study to determine individual differences in gray matter density associated with age and cognitive change over time. *Cereb Cortex,* 14, 966-73.

TISSERAND, D. J., VISSER, P. J., VAN BOXTEL, M. P. & JOLLES, J. 2000. The relation between global and limbic brain volumes on MRI and cognitive performance in healthy individuals across the age range. *Neurobiol Aging,* 21, 569-76.

TJANDRA, T., BROOKS, J. C., FIGUEIREDO, P., WISE, R., MATTHEWS, P. M. & TRACEY, I. 2005. Quantitative assessment of the reproducibility of functional activation measured with BOLD and MR perfusion imaging: implications for clinical trial design. *Neuroimage,* 27, 393-401.

TOFTS, P. 2003. ed. Quantitative MRI of the brain: measuring changes caused by disease. *Chichester: Wiley.*

TURNER, R., LE BIHAN, D., MOONEN, C. T., DESPRES, D. & FRANK, J. 1991. Echo-planar time course MRI of cat brain oxygenation changes. *Magn Reson Med,* 22, 159-66.

UNCAPHER, M. R. & WAGNER, A. D. 2009. Posterior parietal cortex and episodic encoding: insights from fMRI subsequent memory effects and dual-attention theory. *Neurobiol Learn Mem,* 91, 139-54.

UYLINGS, H. B. & DE BRABANDER, J. M. 2002. Neuronal changes in normal human aging and Alzheimer's disease. *Brain Cogn,* 49, 268-76.

VALLAR, G., LOBEL, E., GALATI, G., BERTHOZ, A., PIZZAMIGLIO, L. & LE BIHAN, D. 1999. A fronto-parietal system for computing the egocentric spatial frame of reference in humans. *Exp Brain Res,* 124, 281-6.

VAN LAERE, K. J. & DIERCKX, R. A. 2001. Brain perfusion SPECT: age- and sex-related effects correlated with voxel-based morphometric findings in healthy adults. *Radiology,* 221, 810-7.

VAN PETTEN, C. 2004. Relationship between hippocampal volume and memory ability in healthy individuals across the lifespan: review and meta-analysis. *Neuropsychologia,* 42, 1394-413.

VILLRINGER, A., PLANCK, J., HOCK, C., SCHLEINKOFER, L. & DIRNAGL, U. 1993. Near infrared spectroscopy (NIRS): a new tool to study hemodynamic changes during activation of brain function in human adults. *Neurosci Lett,* 154, 101-4.

WAGER, T. D. & SMITH, E. E. 2003. Neuroimaging studies of working memory: a meta-analysis. *Cogn Affect Behav Neurosci,* 3, 255-74.

WAGER, T. D., SYLVESTER, C. Y., LACEY, S. C., NEE, D. E., FRANKLIN, M. & JONIDES, J. 2005. Common and unique components of response inhibition revealed by fMRI. *Neuroimage,* 27, 323-40.

WANG, J., AGUIRRE, G. K., KIMBERG, D. Y., ROC, A. C., LI, L. & DETRE, J. A. 2003. Arterial spin labeling perfusion fMRI with very low task frequency. *Magn Reson Med,* 49, 796-802.

WARD, N. L. & LAMANNA, J. C. 2004. The neurovascular unit and its growth factors: coordinated response in the vascular and nervous systems. *Neurol Res,* 26, 870-83.

WATSON, N. A., BEARDS, S. C., ALTAF, N., KASSNER, A. & JACKSON, A. 2000. The effect of hyperoxia on cerebral blood flow: a study in healthy

volunteers using magnetic resonance phase-contrast angiography. *Eur J Anaesthesiol,* 17, 152-9.

WECHSLER, D. 1981. *Wechsler adult intelligence scale–revised,* New York, Psychological Corporation.

WEST, M. J. 1993. Regionally specific loss of neurons in the aging human hippocampus. *Neurobiol Aging,* 14, 287-93.

WEST, R. L. 1996. An application of prefrontal cortex function theory to cognitive aging. *Psychol Bull,* 120, 272-92.

WESTBROOK, C., ROTH, C. & TALBOT, J. 2005. *MRI in practice*, Oxford: Blackwell Publishing Ltd.

WICKER, B., KEYSERS, C., PLAILLY, J., ROYET, J. P., GALLESE, V. & RIZZOLATTI, G. 2003. Both of us disgusted in My insula: the common neural basis of seeing and feeling disgust. *Neuron,* 40, 655-64.

WIMBER, M., HEINZE, H. J. & RICHARDSON-KLAVEHN, A. 2010. Distinct frontoparietal networks set the stage for later perceptual identification priming and episodic recognition memory. *J Neurosci,* 30, 13272-80.

WINKLER, A. M., KOCHUNOV, P., BLANGERO, J., ALMASY, L., ZILLES, K., FOX, P. T., DUGGIRALA, R. & GLAHN, D. C. 2010. Cortical thickness or grey matter volume? The importance of selecting the phenotype for imaging genetics studies. *Neuroimage,* 53, 1135-46.

WISE, S. P., FRIED, I., OLIVIER, A., PAUS, T., RIZZOLATTI, G. & ZILLES, K. J. 1996. Workshop on the anatomic definition and boundaries of the supplementary sensorimotor area. *Adv Neurol,* 70, 489-95.

WONG, E., BUXTON, R. & FRANK, L. 1998. Quantitative imaging of perfusion using a single subtraction (QUIPSS and QUIPSS II). *Magn Reson Med,* 39, 702-708.

WONG, E. C., BUXTON, R. B. & FRANK, L. R. 1997. Implementation of quantitative perfusion imaging techniques for functional brain mapping using pulsed arterial spin labeling. *NMR Biomed,* 10, 237-49.

WRIGHT, P., HE, G., SHAPIRA, N. A., GOODMAN, W. K. & LIU, Y. 2004. Disgust and the insula: fMRI responses to pictures of mutilation and contamination. *Neuroreport,* 15, 2347-51.

XU, J., KOBAYASHI, S., YAMAGUCHI, S., IIJIMA, K., OKADA, K. & YAMASHITA, K. 2000. Gender effects on age-related changes in brain structure. *AJNR Am J Neuroradiol,* 21, 112-8.

YAMAGUCHI, T., KANNO, I., UEMURA, K., SHISHIDO, F., INUGAMI, A., OGAWA, T., MURAKAMI, M. & SUZUKI, K. 1986. Reduction in regional cerebral metabolic rate of oxygen during human aging. *Stroke,* 17, 1220-8.

YANTIS, S., SCHWARZBACH, J., SERENCES, J. T., CARLSON, R. L., STEINMETZ, M. A., PEKAR, J. J. & COURTNEY, S. M. 2002. Transient neural activity in human parietal cortex during spatial attention shifts. *Nat Neurosci,* 5, 995-1002.

YASSA, M. A. & STARK, C. E. 2009. A quantitative evaluation of cross-participant registration techniques for MRI studies of the medial temporal lobe. *Neuroimage,* 44, 319-27.

ZEKI, S. & MOUTOUSSIS, K. 1997. Temporal hierarchy of the visual perceptive systems in the Mondrian world. *Proc Biol Sci,* 264, 1415-9.

ZHOU, J., WILSON, D. A., ULATOWSKI, J. A., TRAYSTMAN, R. J. & VAN ZIJL, P. C. 2001. Two-compartment exchange model for perfusion quantification using arterial spin tagging. *J Cereb Blood Flow Metab,* 21, 440-55.

ZIEGLER, D. A., PIGUET, O., SALAT, D. H., PRINCE, K., CONNALLY, E. & CORKIN, S. 2010. Cognition in healthy aging is related to regional white matter integrity, but not cortical thickness. *Neurobiol Aging,* 31, 1912-26.

ZIMMERMAN, M. E., BRICKMAN, A. M., PAUL, R. H., GRIEVE, S. M., TATE, D. F., GUNSTAD, J., COHEN, R. A., ALOIA, M. S., WILLIAMS, L. M., CLARK, C. R., WHITFORD, T. J. & GORDON, E. 2006. The relationship between frontal gray matter volume and cognition varies across the healthy adult lifespan. *Am J Geriatr Psychiatry,* 14, 823-33.

ZYSSET, S., SCHROETER, M. L., NEUMANN, J. & YVES VON CRAMON, D. 2007. Stroop interference, hemodynamic response and aging: An event-related fMRI study. *Neurobiology of Aging,* 28, 937-946.

APPENDICES

PUBLICATION

Mohtasib, R.S., Lumley, G., Goodwin, J.A., Emsley, H.C., Sluming, V. & Parkes, L.M. 2011. Calibrated fMRI during a cognitive Stroop task reveals reduced metabolic response with increasing age. *Neuroimage.*

ARTICLE IN PRESS

YNIMG-08569; No. of pages: 9; 4C:

NeuroImage xxx (2011) xxx–xxx

Contents lists available at ScienceDirect

NeuroImage

journal homepage: www.elsevier.com/locate/ynimg

Calibrated fMRI during a cognitive Stroop task reveals reduced metabolic response with increasing age

Rafat S. Mohtasib [a,c], Guy Lumley [c], Jonathan A. Goodwin [a,e], Hedley C.A. Emsley [b], Vanessa Sluming [a,c], Laura M. Parkes [a,d,*]

[a] Magnetic Resonance and Image Analysis Research Centre (MARIARC), University of Liverpool, UK
[b] Department of Neurology, Royal Preston Hospital, Preston, Lancashire, UK
[c] School of Health Sciences, University of Liverpool, Liverpool, UK
[d] Imaging Sciences Research Group, Biomedical Imaging Institute, University of Manchester, UK
[e] Division of Bioengineering and Bioinformatics, Hokkaido University, Japan

ARTICLE INFO

Article history:
Received 25 March 2011
Revised 16 June 2011
Accepted 30 July 2011
Available online xxxx

Keywords:
Calibrated BOLD
Arterial spin labeling
Oxygen metabolism
Aging
fMRI
Stroop

ABSTRACT

fMRI studies of aging have revealed increased blood oxygenation level dependent (BOLD) response to tasks of executive function with advancing age, which is generally interpreted as increased neural activity. However, changes in the cerebrovascular system with age can alter the BOLD signal, complicating this interpretation. Arterial spin labeling (ASL) allows simultaneous acquisition of BOLD and cerebral blood flow (CBF) information and can be used to quantify the component parts of the BOLD signal. We used this calibrated BOLD approach in 58 healthy participants over an age range of 18–71 years to determine the relative vascular and neuronal contributions to the age-related BOLD changes in response to a Stroop task. The percentage BOLD response increased significantly with increasing age but the percentage CBF response did not alter, such that the BOLD increase is attributed to a significant reduction in the oxygen metabolism response with increasing age. Hence, in this study, the BOLD increase with age should be interpreted as a reduction in neural activity. The greatest percentage BOLD increases with age were found in the left and right medial frontal gyri and the primary motor cortex and were again linked to a reduction in oxygen metabolism. On separating the participants into three groups (young, old high performers and old low performers), age-related differences in percentage BOLD response and oxygen metabolism response could be attributed to the low performing old group. This study demonstrates the need to take into account alterations in vascular–metabolic coupling and resting blood volume when interpreting changes in the BOLD response with aging.

Introduction

Neuroimaging has helped to advance our understanding of the aging process, in particular the relationship between cognitive decline and physiological changes. As a person ages, notable changes occur in cellular metabolism (Simic et al., 1997), cortical density (Good et al., 2001; Sowell et al., 2003; Tisserand et al., 2004; Van Laere and Dierckx, 2001) and cerebrovascular function (Leenders et al., 1990; Parkes et al., 2004). Structural studies of the aging brain indicate that the frontal lobe cortices experience a high degree of age-related atrophy (Coffey et al., 1992; Cowell et al., 1994; Good et al., 2001). However, even with the susceptibility of the frontal cortex to aging, greater frontal cortex blood-oxygenation-level-dependent (BOLD) activation with increasing age, suggesting *increased* neural activity, has been revealed in many fMRI studies of aging (Cabeza et al., 2002; Langenecker et al., 2004; Milham et al., 2002; Zysset et al., 2007).

fMRI relies on the detection of hemodynamic changes that accompany neural activity. As such, the BOLD signal is an indirect measure of neural activity and may also reflect changes in the cerebrovascular system due to age (D'Esposito et al., 2003; Lu et al., 2011; Restom et al., 2007). Therefore, it is difficult to conclude if age-related differences in the BOLD signal develop from age-related neural plasticity or age-related cerebrovascular changes. We aimed to address this question through the use of calibrated fMRI during a cognitive Stroop task. Ances et al. (2009) used a similar approach to investigate the age-related decline in BOLD response in the visual cortex. Using calibrated fMRI they were able to quantify the component parts of the BOLD response, concluding that the reduced BOLD response in the visual cortex with aging does not reflect lower neural activity, but rather differences in neurovascular properties.

Calibrated fMRI is a non-invasive approach that allows quantification of the component parts of the BOLD signal, namely changes in the cerebral metabolic rate of oxygen ($CMRO_2$) and cerebral blood

* Corresponding author at: Imaging Sciences Research Group, School of Cancer and Enabling Sciences, University of Manchester, Stopford Building, Oxford Rd, Manchester, M13 9PT, UK. Fax: +44 161 2755145.
E-mail address: Laura.Parkes@manchester.ac.uk (L.M. Parkes).

1053-8119/$ – see front matter © 2011 Elsevier Inc. All rights reserved.
doi:10.1016/j.neuroimage.2011.07.092

Please cite this article as: Mohtasib, R.S., et al., Calibrated fMRI during a cognitive Stroop task reveals reduced metabolic response with increasing age, NeuroImage (2011), doi:10.1016/j.neuroimage.2011.07.092

flow (CBF) (Davis et al., 1998; Hoge et al., 1999). A calibration constant, M, reflecting baseline vascular properties is also determined. Estimates of $\Delta CMRO_2$ may be particularly useful as it is reported to have a closer link with changes in neural activity than the BOLD signal (Davis et al., 1998; Hyder, 2004). Calibrated fMRI uses an arterial spin labeled (ASL) pulse sequence which allows simultaneous measurements of the BOLD and CBF response. Addition of either a hypercapnic (Ances et al., 2009; Kastrup et al., 2002; Rostrup et al., 2000; Thomason et al., 2007) or hyperoxic (Chiarelli et al., 2007; Goodwin et al., 2009) gas challenge allows additional quantification of the change in $CMRO_2$. In our study, hyperoxia calibration was chosen over hypercapnia as it is more comfortable and better tolerated, important when studying an older population. In addition, hyperoxia calibration does not rely on noisy ASL-derived CBF measurements which are required for hypercapnic calibration.

We chose to use a form of the Stroop task (Stroop, 1935) as the cognitive challenge, as it has been proven to be a powerful, simple task which can examine age-related changes in the neural substrates of executive function (Banich et al., 2000; Bench et al., 1993; Pardo et al., 1990). Several studies using it have shown an increased BOLD response with increasing age in the frontal cortex (Langenecker et al., 2004; Milham et al., 2002; Zysset et al., 2007). In our study, BOLD activation during an incongruent Stroop task was compared to rest (rather than a congruent task) in order to robustly activate large regions of the brain, allowing individual analysis and regional comparison of the calibrated fMRI measurements. A comparison of incongruent and congruent (or neutral) conditions would have been of additional interest, allowing the isolation of the inhibitory executive function. However, the differences in BOLD signal between these conditions (Zysset et al., 2007) are likely to be too small to provide reliable estimates of the change in oxygen metabolism (Goodwin et al., 2009). In addition, previous work (Zysset et al., 2007) shows an age-related increase in BOLD response to the incongruous condition compared to rest, which is attributed to increased neural processing.

We measured $\Delta BOLD$, ΔCBF, and estimated $\Delta CMRO_2$ and M in regions activated by the Stroop task and considered whether these parameters are affected by age. M can be considered as a 'baseline' parameter that is expected to be independent of cognitive task (Hyder, 2004), reflecting the general physiological state of the brain. We aimed to replicate previous findings of an age-related increased BOLD response in the frontal cortex and determined whether this is due primarily to alterations in the metabolic ($CMRO_2$) or the vascular (CBF) response to neural activity. Finally, we aimed to determine which of the parameters are most related to performance change with increasing age.

Methods

Participants

58 healthy, volunteers (28 male, 30 female, mean age 41 years, SD 16 years, age range 18–71 years) were recruited and scanned in a 3 T MR imaging system. This study was approved by the University of Liverpool research ethics committee, and written informed consent was obtained from all subjects. All subjects had normal vision (no color-blindness), were right handed and had English as a first language. Years of education were recorded. Subjects were excluded if they were taking any psychoactive or vasoactive medication, or if they had any history of significant neurological, psychiatric or cardiovascular disease, including migraine, stroke, hypertension, and diabetes. A brief cognitive assessment test (O'Sullivan et al., 2005) was administered to further screen out subjects with any cognitive deficits. Tests comprised: digit symbol, verbal fluency, trail-making (B–A) and digit span backwards from which a composite score was calculated. Subjects performing below 0.57 on the composite score (see Table 2 of O'Sullivan et al., 2005) were excluded.

Stroop task

An incongruent color–word Stroop task was used as a functional stimulus, similar to the one used in the studies by Zysset et al. (2007) and Goodwin et al. (2009). Participants had to decide (with a choice of two buttons using the right hand), if the meaning of the bottom word matched the print color of the top word (Fig. 1). Subjects were instructed to respond as quickly and accurately as possible. Fifteen stimuli were presented in each block. Stimuli were self-paced but with a minimum of 2 s between each stimulus, during which a fixation cross was presented. Eight active blocks of approximately 30 s were interspersed with a 30 s fixation cross on a black screen. To become familiar with the task all participants first practiced the task for 4 min outside of the scanner prior to scanning. For each participant we calculated mean response time and accuracy of responses recorded during the scanning session.

Hyperoxia calibration

Hyperoxia was induced by breathing 100% oxygen delivered through an open mask over the mouth and nose at a flow-rate of 15 L/min, following the same procedure as described in Goodwin et al. (2009). The protocol comprised 2 min of air, 3 min of oxygen, 3 min of air and 3 min of oxygen (Fig. 2). Respiratory composition was continuously monitored using an oxygen analyser (Model S-3A) (AEI Technologies, Pittsburgh, PA, USA), which was calibrated prior to each scan against an oxygen depletion monitor (GasMonitor4) situated in the scanner room. Respiratory data logging was performed at intervals of 1 ms using Powerlab software (ADInstruments, Colorado Springs, USA). End-tidal values were extracted from the data using code created in Matlab (The MathWorks Inc., Massachusetts, USA).

Image acquisition

Imaging was carried out on a 3 T whole-body Siemens Trio system (Siemens, Erlangen, Germany). An eight-channel radiofrequency (RF) head coil was used with foam padding to comfortably restrict head motion. For the functional arterial spin labeling (ASL) acquisitions, we recorded control and tagged images using a PICORE tagging scheme with the QUIPSS II modification (Wong et al., 1998) that enables simultaneous collection of BOLD signal and quantitative CBF data (Wong et al., 1998). The sequence parameters were: TR = 2.13 s, TE = 25 ms, tag-saturation time (TI_1) = 0.7 s, tag-saturation end-time (TI_{1stop}) = 1.3 s, time between label and readout (TI_2) = 1.4 s, 10-cm tag width, a 10-mm tag-slice gap and crusher gradients with b = 5 mm s^{-1}. Control and label acquisitions were interleaved, such that the labeling was applied every two TR. We acquired a total of twelve slices of 3.5-mm thickness and 0.35 mm gap that covered the frontal, motor and parietal cortices (Fig. 3). Prospective motion correction (PACE) (Thesen et al., 2000) was included in the pulse sequence. In order to avoid T_1 relaxation effects, we discarded two

Fig. 1. Stimulus paradigm: the incongruent Stroop task. Subjects had to decide if the meaning of the bottom word matched the color of the top word (red in this case). (For interpretation of the references to color in this figure legend, the reader is referred to the web version of this article.)

Please cite this article as: Mohtasib, R.S., et al., Calibrated fMRI during a cognitive Stroop task reveals reduced metabolic response with increasing age. NeuroImage (2011), doi:10.1016/j.neuroimage.2011.07.092

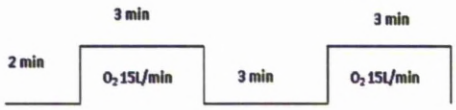

Fig. 2. The hyperoxia paradigm.

'dummy' scans at the start of each functional run. To produce quantitative CBF maps we collected a calibration image at the end of each functional run, using the identical QUIPSS II sequence with labeling switched off and a TR of 10 s. In addition to these scans, a 1 mm isotropic structural 3D MPRAGE image was also collected (Mugler and Brookeman, 1990).

Data analysis

Matlab software (The MathWorks Inc., Massachusetts, USA) was first used to process the ASL data for the Stroop and hyperoxia runs in order to extract BOLD and CBF time-courses. Label and control images were added to produce a time-course of BOLD images; or subtracted to produce a time-course of perfusion-weighted images. Perfusion-weighted images were converted into quantitative CBF maps using a single blood compartment model described by Parkes and Tofts (2002).

BOLD and CBF time-course data were analyzed using BrainVoyager QX software. Pre-processing included spatial (FWHM 6 mm) and temporal (FWHM 10 s) smoothing and linear trend removal. Temporal smoothing was applied to increase the signal to noise ratio in the exported time-courses, to allow more precise estimates of BOLD and CBF change. The BOLD and CBF images were then co-registered to the structural T_1-weighted image and transformed into Talairach space. The regressor for the Stroop task was generated by convolving the timing of the Stroop blocks (using subject-specific onset and offset times for the whole block) with the hemodynamic response function as implemented in BrainVoyager. A group-wise analysis was then performed using both the BOLD and CBF time-courses from all individuals to determine regions where the model accounted for significant variance in the data at a threshold of $p<0.05$ (corrected for false-discovery rate (FDR)), i.e. regions that are responsive to the Stroop task.

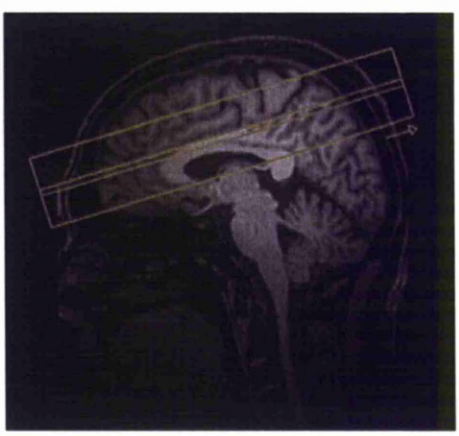

Fig. 3. Slice coverage. Limited coverage of the ASL sequence restricted our acquisition to cover frontal, motor and parietal regions.

The estimation of $\Delta CMRO_2$ requires precise measurements of BOLD and CBF signal change, and so is usually done on a regional rather than a voxel-wise basis (Leontiev et al., 2007) in order to increase the signal to noise ratio. Hence, when considering age-related effects we performed analysis on a regional basis, using signal time-courses from those regions defined as significantly active during the Stroop task in the group analysis (FDR $p<0.05$). These regions are then employed for the analyses of both the Stroop and the hyperoxia runs.

Within each region, a volume of 1 cm^3 was defined, composed of the voxels with the most significant activity (derived from a general linear model using both BOLD and CBF data as described above). BOLD and CBF signal time-courses were recorded for both the Stroop and hyperoxia runs, averaged over all the voxels within each region for each individual. For hyperoxia, the percentage change in the BOLD signal was found in each region by comparing the mean signal over the last minute of each hyperoxia period compared to 1 min prior to each hyperoxia period. For the Stroop activation, the BOLD and CBF time-courses were averaged over the 8 activation blocks and the percentage change in BOLD and CBF between the maximum and minimum response was found.

Quantification of oxygen metabolism change

The analysis procedure to extract the calibration constant M and the change in $CMRO_2$ followed the same approach as in Goodwin et al. (2009), where a more detailed description can be found. In brief, the fractional BOLD signal change ($\Delta BOLD/BOLD_0$) can be modeled as a function of the relative changes in CBF and $CMRO_2$ according to Eq. (1).

$$\frac{\Delta BOLD}{BOLD_0} = M\left(1-\frac{CBF}{CBF_0}^{\alpha-\beta}\frac{CMRO_2}{CMRO_{20}}^{\beta}\right) \quad (1)$$

Where $\Delta BOLD$ refers to the change in BOLD signal during activation and CBF and $CMRO_2$ are the values for these parameters during activation. The subscript 0 denotes the baseline values. In steady-state, the parameter α is the Grubb constant (assumed to be 0.38, accounting for an assumed fixed relationship between changes in cerebral blood volume (CBV) and CBF) (Grubb et al., 1974). β describes the oxygenation and field strength dependence of the BOLD effect and was assumed to be 1.5 (Boxerman et al., 1995; Davis et al., 1998). The parameter M is the calibration constant, which corresponds to the maximum BOLD change for complete removal of deoxyhemoglobin in the voxel. M was estimated using the Chiarelli and Bulte model (Chiarelli et al., 2007), as given in Eq. (2).

$$\frac{\Delta BOLD_{HO}}{BOLD_0} = M\left[1-\left(\frac{CBF_{HO}}{CBF_0}\right)^{\alpha}\left(\frac{[dHb]_{HO}}{[dHb]_0}+\frac{CBF_0}{CBF_{HO}}-1\right)^{\beta}\right] \quad (2)$$

Where $\Delta BOLD_{HO}$ is the change in the BOLD signal during hyperoxia, CBF_{HO} is the CBF during hyperoxia, and $[dHb]_{HO}$ is the concentration of deoxygenated hemoglobin in the venous vasculature during hyperoxia. The subscript 0 refers to these parameters at baseline. Values for $[dHb]_{HO}/[dHb]_0$ were calculated from the end-tidal measurements (averaged over the same time-periods as for the BOLD response) following the procedure described in Chiarelli et al.(2007). We assumed a baseline oxygen extraction fraction of 0.4 based on previous data (Raichle et al., 2001), and a reduction in CBF of 5% during hyperoxia (Chiarelli et al., 2007). Note that an assumed reduction in CBF was used as the ASL signal is too noisy to allow reliable estimates of such a small change in CBF. On a regional basis, values for M, $\Delta BOLD$ and ΔCBF are substituted into Eq. (1) and $\Delta CMRO_2$ is found.

Please cite this article as: Mohtasib, R.S., et al., Calibrated fMRI during a cognitive Stroop task reveals reduced metabolic response with increasing age, NeuroImage (2011), doi:10.1016/j.neuroimage.2011.07.092

Table 1
Age, end-tidal O_2 values and Stroop task performance accuracy for the three groups.

Group	Number	Mean age (years)	Mean end-tidal O_2 (% ± SE)	Mean accuracy (% ± SE)	Mean reaction time (s ± SE)
Young	15	21 (18–29)	60 ± 2.0	98.9 ± 0.2	910 ± 50
Old high performers	15	55 (42–67)	65 ± 2.0	98.9 ± 0.2	1010 ± 40
Old low performers	14	55 (43–71)	63 ± 2.0	95.7 ± 0.7	1220 ± 100

Table 2
Performance on the cognitive assessment tests and relation to age.

Test	Mean	SD	Correlation coefficient	Significance (p-value)
Trail making B–A	20	12	−0.11	0.4
Verbal fluency total	53	14	0.17	0.2
Digit span back	8.5	2.6	−0.23	0.09
Digit symbol	67	11	−0.54	<0.0001

Statistical analysis

We first rejected any regional data where M or $\Delta CMRO_2$ were negative, as this was deemed physiologically implausible (4% of data rejected). We then considered the global response from all of the activated regions. The estimated ΔCBF, $\Delta BOLD$, $\Delta CMRO_2$, and M values were correlated with age using bivariate correlation, with significance accepted at $p<0.05$. The benefit of looking first for a global effect is that the signal to noise of the measurements will be increased such that an age effect is more likely to become apparent. In addition, the numbers of statistical comparisons are kept low.

We then considered regional differences, as it is predicted that any age-related effects will be largest in the frontal cortices. We first determined the magnitude of any BOLD increase with age in each of the identified regions. In regions showing a significant BOLD age-effect we consider age-related changes in ΔCBF, $\Delta CMRO_2$, and M.

The final aim was to establish whether there is a relationship between the physiological parameters and performance change with increasing age. We found the variance in performance levels increased with increasing age, such that we could define two older groups with the same age distribution but relatively 'high' and 'low' performance. Thus we split the participants into 3 groups, young, old high performers and old low performers (Table 1). Performance accuracy was significantly better for the old high performers compared to the old low performers ($p=0.0006$, unpaired two-tailed t-test), with a trend towards lower reaction times ($p=0.07$, unpaired two-tailed t-test). There was no significant difference in age between the old groups and no significant difference in performance accuracy or reaction times between the young and old high performing groups.

Within the regions showing a significant change in BOLD response with increasing age, we compared the measured/estimated parameters between the young and the low performing old group and the young and the high performing old group. This determined which of the parameters are related to the drop in performance with age. A further comparison between the two old groups determined whether the changes could be attributed to a difference in performance per-se.

Results

The data from three subjects were excluded: one subject did not complete the experiment (due to claustrophobia), in another the images were too severely degraded by artifact, and one performed very badly on the Stroop task (accuracy more than 3 standard deviations from the mean) and reported falling asleep during the scan. Thus, 26 male subjects (mean age 40.5 years, SD 15 years) and 29 female subjects (mean age 42 years, SD 17 years) were included in the analyses. The mean years of education was 17 years, SD 3.2 years with no significant effect of age ($r=-0.02$, $p=0.9$, Pearson correlation). No subjects were excluded on the basis of their performance on the out-of-scanner cognitive assessment tests. Mean performance on these tests are given in Table 2, along with age-related regression coefficients.

Behavioral data

All participants performed the Stroop task correctly with mean accuracy of 98% and standard deviation of 2%. Mean response time was 1040 ms with a standard deviation of 278 ms. The behavioral results showed a trend towards lower accuracy ($p=0.07$) (Fig. 4a) and longer response times ($p=0.09$) with increasing age (Fig. 4b). Mean duration of each Stroop block was 30.7 s with a standard deviation of 0.7 s. There was no significant correlation between block duration and age ($p=0.5$).

Gas data

To determine whether there were any age-related differences in the end-tidal O_2 levels, we performed regression analysis of the mean end-tidal values (averaged over both periods of O_2 administration) against age. Fig. 5 shows an unexpected increase in end-tidal O_2 with increasing age ($r=0.37$, $p=0.01$). Theoretically the estimate of the calibration constant M is independent of the level of end-tidal O_2, as the venous hemoglobin deoxygenation is calculated directly from the O_2 measurements (Chiarelli et al., 2007). As such, this age-dependence should not affect our results. This assumes that the arterial tension of oxygen can be inferred directly from the end-tidal O_2 measurements (Chiarelli et al., 2007), which in general appears valid as the measures are very tightly correlated in normoxia (Bengtsson et al., 2001).

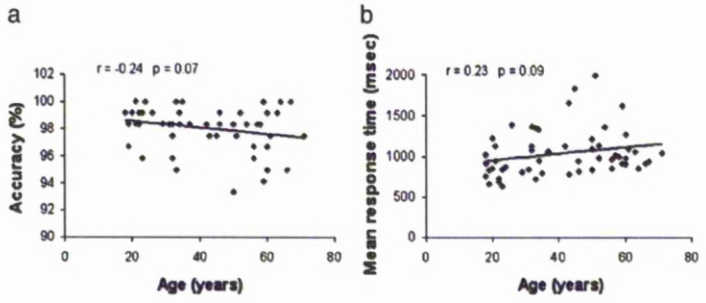

Fig. 4. Stroop task performance with age for a) accuracy and b) response time.

Please cite this article as: Mohtasib, R.S., et al., Calibrated fMRI during a cognitive Stroop task reveals reduced metabolic response with increasing age, NeuroImage (2011), doi:10.1016/j.neuroimage.2011.07.092

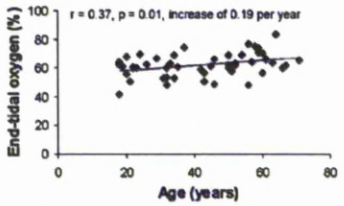

Fig. 5. Effect of age on end-tidal O_2. Mean end-tidal O_2 (averaged over two periods of O_2 administration) measurements for each individual are plotted against age.

One possible contributory reason for the increase in end-tidal O_2 is a reduction in pulmonary function with increasing age. This could increase the dead-space in the lung, resulting in a reduction in oxygen transfer and hence increased end-tidal O_2 (Bengtsson et al., 2001). This would lead to an overestimation of arterial tension of oxygen with increasing age, leading to an underestimation of M with increasing age.

To further assess the effect of the age-dependence of end-tidal O_2, the analysis was repeated using data within a narrower range of end-tidal O_2 values from 47 to 77%, centered on the mean value of 62%. This excluded 3 subjects and removed the age-dependence of end-tidal O_2 values ($r=0.25$, $p=0.1$). Additional analysis was not performed for the group-wise data as there was found to be no significant difference in end-tidal O_2 values between the groups (Table 1).

fMRI data

Mean response over all activated regions

Group analysis over all subjects revealed ten regions to be significantly activated at $p<0.05$ (corrected for False Detection Rate), as shown in Fig. 6 with Talairach coordinates for the 10 regions shown in Table 3. Anatomical locations were determined using the Talairach daemon (www.talairach.org) (Lancaster et al., 2000), choosing the closest gray matter region if the peak activation fell in white matter.

Table 3
Talairach coordinates of the active regions shown in Fig. 5.

Anatomical region	Tal. coordinates
Left pre-central gyrus BA4 primary motor cortex (M1)	−35 −23 54
Medial frontal gyrus BA 6 supplementary motor area (SMA)	−3 −5 53
Left parietal lobe BA7 (LPL)	−24 −61 45
Right parietal lobe BA7 (RPL)	31 −57 45
Left middle frontal gyrus BA6 (LMFG)	−40 1 40
Right middle frontal gyrus BA6 (RMFG)	44 8 38
Left middle frontal gyrus BA9 dorsolateral pre-frontal cortex (LDLPFC)	−40 18 26
Right middle frontal gyrus BA9 dorsolateral pre-frontal cortex (RDLPFC)	36 18 30
Left insular (LI)	−33 14 11
Right insular (RI)	30 16 11

Averaged over all regions the BOLD response increased significantly ($r=0.30$, $p=0.03$) with increasing age (Fig. 7a). There was a significant reduction in the $CMRO_2$ response with increasing age ($r=-0.31$, $p=0.03$) (Fig. 7b), the calibration constant M decreased significantly with increasing age ($r=-0.29$, $p=0.04$) (Fig. 7c) but CBF did not change with age (Fig. 7d). Re-analysis using the data within the restricted end-tidal O_2 range showed similar results for BOLD response ($r=0.35$, $p=0.01$), $CMRO_2$ response ($r=-0.34$, $p=0.02$) and CBF response (no change with age), but the age-dependence of M was no longer present ($r=-0.23$, $p=0.1$). As a further check for the influence of end-tidal O_2 differences, a regression of end-tidal measurements against $CMRO_2$ response was performed (using the full dataset). This showed no significant relationship ($r=-0.14$, $p=0.3$).

Regional differences

Regression results of all four parameters within each of the ten regions are shown in Table 4. We first considered the magnitude of the BOLD increase with age in the ten individual regions. The greatest BOLD increase with age was found in M1, LMFG and RMFG (Table 4)

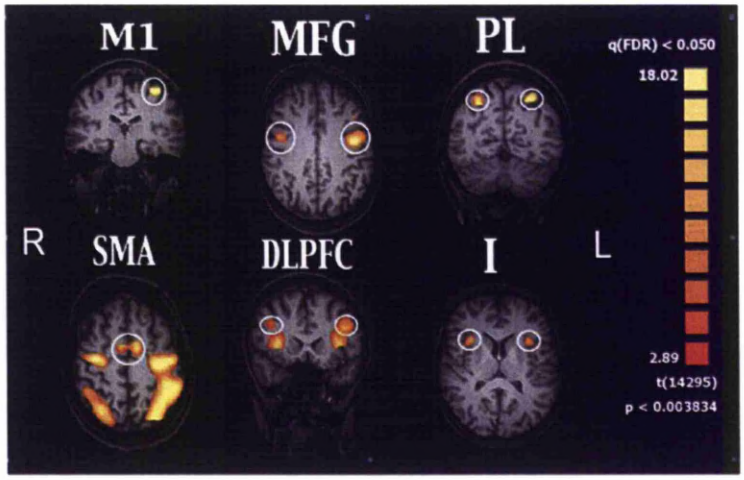

Fig. 6. Regions of activation during the Stroop task. Results from the group analysis at FDR $p<0.05$, using a general linear model incorporating both BOLD and CBF data. Ten regions were identified, as indicated by the white circles. M1 = primary motor cortex, SMA = supplementary motor area, MFG = middle frontal gyrus, DLPFC = dorsolateral pre-frontal cortex,PL = parietal lobe, I = Insular.

Please cite this article as: Mohtasib, R.S., et al., Calibrated fMRI during a cognitive Stroop task reveals reduced metabolic response with increasing age, NeuroImage (2011), doi:10.1016/j.neuroimage.2011.07.092

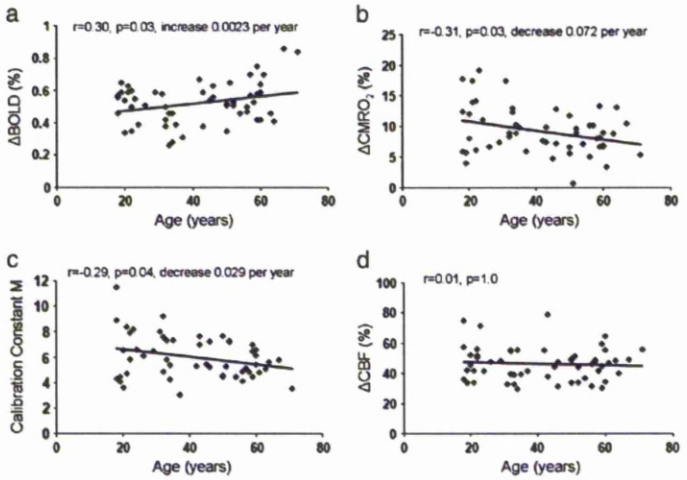

Fig. 7. The age-related change in the measured/estimated parameters ((a) ΔBOLD, (b) $\Delta CMRO_2$, (c) *M* and (d) ΔCBF), averaged over the ten activated regions. Each point shows the average value for an individual over the ten activated regions.

and, indeed, the increase was significant in these regions: M1 ($p = 0.003$), LMFG ($p = 0.02$) and RMFG ($p = 0.02$). Further regression tests on the other 3 parameters within these 3 regions show no significant change for ΔCBF and *M*, but a significant reduction in $\Delta CMRO_2$ within M1 and LMFG (Table 4). Regions showing the largest change in calibration constant *M* were the left insular, left DLPFC and right DLPFC.

Re-analysis using the data within the restricted end-tidal O_2 range showed very similar results to Table 4, identifying the same three regions with the largest, and significant, age-related increase in BOLD response. None of the results in Table 4 changed in terms of their significance (i.e. results remained above or below the $p = 0.05$ threshold), except for *M* within the right DLPFC where p increased from 0.01 to 0.06.

Relationship with performance

We determined the relationship between the measured/estimated parameters and performance accuracy in the 3 regions showing an age-related effect (L and R MFG and M1) in the BOLD response. We split the subjects into 3 groups as described in the Methods (Table 1): young, old high performers and old low performers. Table 5 shows the mean parameter estimates across each of these groups in each of the regions. It can be seen that in LMFG and M1, the BOLD and $\Delta CMRO_2$ responses are significantly different for the low performing old group in comparison to the young group. In LMFG the BOLD response (but not the $\Delta CMRO_2$ response) is significantly different for the low performing old group in comparison to the high performing old group. None of the parameters showed any significant difference between the high performing old group and the young group.

Discussion

Mean response over all activated regions

Initially, the estimated calibration constant *M* was found to decline with increasing age (Fig. 7c), consistent with a previous study considering age-related alterations in the response of the visual cortex (Ances et al., 2009). However, on re-analysis within a narrow range of end-tidal values, this age-dependence is no longer present, suggesting that the age-related differences in end-tidal O_2 were driving the changes seen in *M*. *M* reflects the amount of deoxyhemoglobin present in the baseline state. As such, *M* depends on a number of physiological parameters including baseline CBV, resting oxygen extraction fraction (OEF), the constant β, and the hematocrit,

Table 4
Regression of the measured/estimated parameters with age in the 10 activated regions. Slope represents the change in the measured/estimated value per year. Significant values ($p < 0.05$) are highlighted in bold.

Region	ΔBOLD			M			ΔCBF			$\Delta CMRO_2$		
	Slope × 10^{-3}	r	p	Slope	r	p	Slope	r	p	Slope	r	p
M1	**4.9**	**0.40**	**0.003**	−0.02	−0.26	0.06	−0.03	−0.06	0.7	**−0.13**	**−0.42**	**0.004**
SMA	1.0	0.06	0.7	−0.03	−0.17	0.2	−0.14	−0.20	0.1	**−0.13**	**−0.30**	**0.03**
LPL	1.5	0.10	0.4	−0.03	−0.20	0.2	0.09	0.16	0.2	0.008	0.02	0.9
RPL	1.4	0.09	0.5	−0.02	−0.12	0.4	0.09	0.20	0.1	−0.03	−0.10	0.5
LMFG	**4.8**	**0.31**	**0.02**	−0.02	−0.22	0.1	−0.04	−0.07	0.6	**−0.12**	**−0.34**	**0.03**
RMFG	**5.1**	**0.31**	**0.02**	−0.01	−0.14	0.4	0.09	0.16	0.2	−0.05	−0.15	0.3
LDLPFC	−1.3	−0.10	0.4	**−0.05**	**−0.37**	**0.008**	−0.11	−0.16	0.2	**−0.15**	**−0.38**	**0.01**
RDLPFC	−1.7	−0.19	0.1	**−0.04**	**−0.35**	**0.01**	0.06	0.01	0.9	−0.03	−0.09	0.5
LI	−0.02	0.00	1.0	**−0.05**	**−0.31**	**0.03**	0.05	0.08	0.5	−0.07	−0.19	0.2
RI	0.08	0.01	0.9	0.001	0.01	0.9	0.02	0.04	0.8	−0.07	−0.28	0.06

Please cite this article as: Mohtasib, R.S., et al., Calibrated fMRI during a cognitive Stroop task reveals reduced metabolic response with increasing age, NeuroImage (2011), doi:10.1016/j.neuroimage.2011.07.092

all of which could potentially change with age. There is evidence that CBV declines with age (Leenders et al., 1990), which would predict a reduction in M with age. Hematocrit remains fairly stable up to the age of 65 and then declines (Arbeev et al., 2011), so is unlikely to affect M over the age range we have studied. OEF has been found to remain stable (Leenders et al., 1990; Pantano et al., 1984; Yamaguchi et al., 1986) or increase with age (Lu et al., 2011), predicting an increase in M with age.

The BOLD response to the Stroop task was found to increase with age (Fig. 7a), in agreement with previous work (Langenecker et al., 2004; Milham et al., 2002; Zysset et al., 2007). However, we found a reduction in the estimated $\Delta CMRO_2$ with increasing age (Fig. 7b), that would be consistent with neurodegeneration (Uylings and de Brabander, 2002). ΔCBF did not change with age, suggesting that the increased BOLD response with age is due primarily to a reduction in $CMRO_2$ response with age. Hence caution should be exercised in interpreting the BOLD signal increase with age as increased neural activity. Previous studies using combined ASL and BOLD in aging have focussed on other brain regions. One study (Ances et al., 2009) found reduced BOLD response in the visual cortex with increasing age, but no significant alteration in $\Delta CMRO_2$. Another study (Restom et al., 2007) found increased BOLD and CBF response with increasing age in the medial temporal lobe during memory encoding, consistent with increased $\Delta CMRO_2$ with age. However a calibration scan was not included and so baseline effects could not be accounted for. These two studies consider responses in different brain regions and to different tasks and so would not necessarily be expected to show the same age-related changes as in our present study.

Regional differences

Considering regional changes, we found the age-related BOLD increase to be greatest in the left and right MFG (BA6) and in the primary motor cortex (Table 4), in broad agreement with previous studies (Cabeza et al., 2002, 2003; Langenecker et al., 2004; Milham et al., 2002; Nielson et al., 2002; Zysset et al., 2007) using similar tasks. Langenecker et al. (2004) reported that older adults exhibited greater BOLD response in many frontal areas during a Stroop task, including the left inferior frontal gyrus (IFG). Milham et al. (2002) showed greater BOLD response to a Stroop task for younger subjects compared to elderly subjects across a number of brain regions including frontal and parietal lobes. However, older adults had greater BOLD response compared to young adults in the inferior frontal gyrus (IFG). Finally, in a recent study by Zysset et al. (2007) middle-aged adults showed increased BOLD response to a Stroop task in several task-related regions, mainly in the inferior frontal junction (IFJ) area (bilaterally) and the pre-supplementary motor area. The Talairach coordinates of the IFJ and IFG given in the studies by Langenecker and Zysset are within 1 cm of the regions we identify as L and R MFG (Table 3).

Considering the other parameters (Table 4), only $\Delta CMRO_2$ is found to have an age dependence in LMFG and M1. This supports the findings from the global analysis (Fig. 7), that the increased BOLD response with increasing age is due to a reduction in $\Delta CMRO_2$. Increased BOLD response in the frontal cortex is interpreted in previous studies as increased neural activity (Langenecker et al., 2004; Zysset et al., 2007); compensatory activity in the older group to aid performance. Our results suggest caution in this interpretation, suggesting instead that increased BOLD response is related to a reduction in neural processing in this context.

The regions showing the largest decline in M with age were the left insular and left and right DLPFC. The insular and frontal cortex have also been found to show the largest decline in CBV with age (Leenders et al., 1990), consistent with the view that regional alterations in M are due to CBV changes.

Table 5
Mean (±SE) values for the measured/estimated parameters in the young, old high performers and old low performers in the three regions showing an age-related response.

	M	ΔBOLD (%)	ΔCBF (%)	ΔCMRO2 (%)
LMFG				
Young	5.6 ± 0.7	0.63 ± 0.04*	27.6 ± 3.1	10.4 ± 2.0*
Old high	5.1 ± 0.3	0.65 ± 0.04†	23.4 ± 2.5	7.1 ± 1.0
Old low	4.6 ± 0.4	0.85 ± 0.07*†	24.7 ± 2.3	4.2 ± 1.0*
RMFG				
Young	6.0 ± 0.6	0.55 ± 0.04	24.1 ± 2.2	8.7 ± 1.8
Old high	5.9 ± 0.3	0.54 ± 0.04	24.7 ± 2.5	9.3 ± 0.9
Old low	4.9 ± 0.5	0.67 ± 0.11	27.9 ± 2.6	6.7 ± 1.2
M1				
Young	5.7 ± 0.5	0.49 ± 0.06*	25.2 ± 1.7	11.9 ± 1.3**
Old high	4.9 ± 0.3	0.59 ± 0.06	22.9 ± 1.0	8.2 ± 1.1
Old low	4.9 ± 0.4	0.64 ± 0.03*	21.7 ± 2.0	5.3 ± 1.2**

*and † indicates pairs of values that are significantly different at $p<0.05$.
** indicates pairs of values that are significantly different at $p<0.005$.

Relationship with performance

Despite the very high performance of all participants in this study (Table 1 and Fig. 4), we were able to define two groups of older adults, those with high performance and those with 'low' performance (Table 1). We found that the low performers showed a significant difference in the measured/estimated parameters compared to the young group (Table 5), whereas the older group of high performers had values indistinguishable from the young group (Table 6). The low performers showed increased BOLD response and reduced $CMRO_2$ response in LMFG and M1 compared to the young group. This suggests that reduced neural processing in these regions is impacting negatively on performance. Thus, rather than compensatory activity, increased BOLD response in these regions could be interpreted as an indication of neurodegeneration, resulting in lower performance. The comparison of the two old groups indicated increased BOLD response in LMFG for the low performers, but no difference in $CMRO_2$ response, suggesting it is age-related differences in performance (not performance alone) that is leading to the altered $CMRO_2$ responses between young and old.

Methodological considerations

The end-tidal O_2 values showed an unexpected increase with age which could influence our findings of reduced M and $\Delta CMRO_2$ with increasing age. Re-analysis using data within a restricted range of end-tidal O_2 values did remove the apparent age-dependence of M, but not $\Delta CMRO_2$. We find an increase in % end-tidal O_2 of 0.19 per year. Calculations show that this would lead to a reduction in M of 0.03 per year and a decline in $\Delta CMRO_2$ of 0.03 per year. Hence, this could be responsible for the reduction in M that we see (decline of 0.03 per year averaged over all regions, maximum regional decline of 0.05 per year in left DLPFC). However, the reduction in % $\Delta CMRO_2$ per year is much greater (0.07 per year averaged over all regions, maximum regional decline of 0.15 in left DLPFC), which cannot be entirely accounted for by errors in the arterial tension of oxygen.

The hyperoxia calibration model assumes fixed values for a number of physiological parameters, including Grubb's constant α, the field-dependent parameter β and the baseline oxygen extraction fraction (OEF). It is possible that all 3 of these parameters could change with age, thus affecting our conclusions. To address this problem, we have performed simulations using plausible age-related changes in these parameters. For the simulations we have taken average values of end-tidal O_2 (17% during rest and 62% during hyperoxia), BOLD response (0.52%) and CBF response (24%) from our data, along with values of OEF = 0.4, $\alpha = 0.38$ and $\beta = 1.5$. We calculate values for M and $\Delta CMRO_2$ using Eq. (2) along with the

Please cite this article as: Mohtasib, R.S., et al., Calibrated fMRI during a cognitive Stroop task reveals reduced metabolic response with increasing age, NeuroImage (2011), doi:10.1016/j.neuroimage.2011.07.092

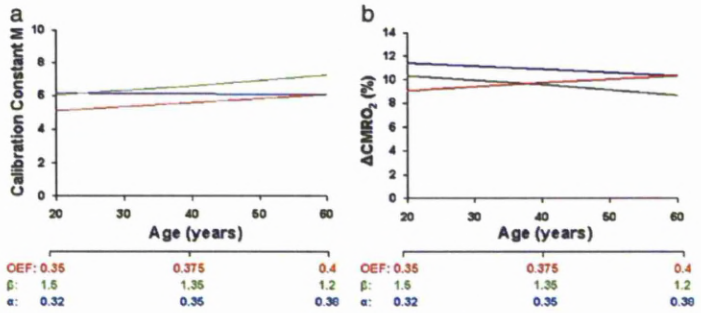

Fig. 8. Sensitivity of the calculated parameters M and $\Delta CMRO_2$ to the assumed values for OEF (red), α (blue) and β (green) as they would be estimated to vary across an age span from 20 to 60 years.

equations in (Chiarelli et al., 2007) for calculating $[dHb]_{HO}/[dHb]_0$, while altering one parameter at a time as described below. Results of the simulations are shown in Fig. 8.

First, considering OEF, a number of previous studies revealed no significant age-related changes in OEF (Leenders et al., 1990; Pantano et al., 1984; Yamaguchi et al., 1986). However, one recent study of a large sample size (232 subjects) revealed an increase in OEF with age (Lu et al., 2011) from 0.35 at 20 years up to approximately 0.40 at 60 years (from Lu et al., 2011). Substituting these values into the model, produces an increase in M of 0.02 per year and an increase in $\Delta CMRO_2$ of 0.03 per year (Fig. 8). Thus, assuming a fixed value of OEF of 0.4 for all ages, as we have done, would tend to overestimate M and $\Delta CMRO_2$ at the younger age, producing an apparent decline in M and $\Delta CMRO_2$.

The relaxation parameter R_2^* depends on the concentration of deoxygenated hemoglobin raised to the power of β (Davis et al., 1998). β is dependent on the composition of vessel sizes and increases as the proportion of smaller vessels increases (Buxton et al., 2004). With increasing age, it might be expected that the relative proportion of smaller vessels reduces, due to sub-clinical vascular disease, leading to a reduction in β. It is difficult to estimate by how much β might decline with age. It is known that gray matter perfusion declines by approximately 0.5% per year (Parkes et al., 2004), hence a similar reduction in β seems reasonable (i.e. from $\beta = 1.5$ at 20 years to $\beta = 1.2$ at 60 years). Substituting these values into the model, produces an increase in *M* of 0.03 per year and a decrease in $\Delta CMRO_2$ of 0.04 per year (Fig. 8). Thus, assuming a fixed value of β of 1.5 for all ages, as we have done, would tend to underestimate *M* and overestimate $\Delta CMRO_2$ at the older age, producing an apparent decline in *M* and an apparent increase in $\Delta CMRO_2$.

The relationship between changes in CBV and CBF (from baseline to a new steady state) is governed by the Grubb constant, α (Grubb et al., 1974), according to $\Delta CBV = \Delta CBF^{\alpha}$. Following an increase in neural activity the venous vessels are thought to expand passively due to increased pressure, producing an increase in CBV. It is difficult to predict how and by how much α might change with increasing age, but it seems likely that α would increase due to loss of elasticity in the vessel walls, i.e. there would be a larger change in CBV for a given change in CBF. Again we assume an increase in α of 0.5% per year (from 0.32 at 20 years to 0.38 at 60 years). Substituting these values into the model, produces a decline in *M* of 0.002 per year (negligible) and a decrease in $\Delta CMRO_2$ of 0.03 per year (Fig. 8). Thus, assuming a fixed value of α of 0.38 for all ages, as we have done, would tend to underestimate *M* and $\Delta CMRO_2$ at the younger age, producing an apparent increase in *M* and $\Delta CMRO_2$.

Our data shows a decline in *M* of 0.03 per year averaged over all regions, with a maximum regional decline of 0.05 per year in the left DLPFC. Given the above simulations, it seems entirely possible that this decline is artifactual and due instead to the incorrect assumption that OEF and β are fixed across the lifespan.

However, our data also shows a much larger decline in $\Delta CMRO_2$ of 0.07 per year averaged over all regions, with a maximum regional decline of 0.15 in the left DLPFC. This decline is two to five-fold larger than what would be expected if the assumption of fixed OEF is incorrect. In fact, the simulations show that the age-related decline in $\Delta CMRO_2$ we find is probably conservative due to our assumptions of fixed α and β.

In our application of the hyperoxia calibration model, a fixed value for CBF reduction in response to hyperoxia is used. However, there is evidence that this CBF reduction may reduce with increasing age (Watson et al., 2000), which would lead to overestimated values for M and $\Delta CMRO_2$ in the older subjects. If true this would suggest the age related decline in M and $\Delta CMRO_2$ that we found, may in fact be conservative.

In conclusion, this study demonstrates the need to take into account alterations in vascular-metabolic coupling and resting blood volume when interpreting changes in the BOLD response with aging. It also highlights the added benefit that calibrated fMRI offers in terms of interpreting the underlying physiological changes that give rise to the measured BOLD response.

Acknowledgments

This work was partly funded by the Medical Research Council. We would also like to thank Val Adams and Bill Bimson for their assistance with scanning.

References

Ances, B.M., Liang, C.L., Leontiev, O., Perthen, J.E., Fleisher, A.S., Lansing, A.E., Buxton, R.B., 2009. Effects of aging on cerebral blood flow, oxygen metabolism, and blood oxygenation level dependent responses to visual stimulation. Hum. Brain Mapp. 30, 1120–1132.

Arbeev, K.G., Ukraintseva, S.V., Akushevich, I., Kulminski, A.M., Arbeeva, L.S., Akushevich, L., Culminskaya, I.V., Yashin, A.I., 2011. Age trajectories of physiological indices in relation to healthy life course. Mechanisms of Ageing and Development 132, 93–102.

Banich, M.T., Milham, M.P., Atchley, R., Cohen, N.J., Webb, A., Wszalek, T., Kramer, A.F., Liang, Z.P., Wright, A., Shenker, J., Magin, R., 2000. fMRI studies of Stroop tasks reveal unique roles of anterior and posterior brain systems in attentional selection. J. Cogn. Neurosci. 12, 988–1000.

Bench, C.J., Frith, C.D., Grasby, P.M., Friston, K.J., Paulesu, E., Frackowiak, R.S., Dolan, R.J., 1993. Investigations of the functional anatomy of attention using the Stroop test. Neuropsychologia 31, 907–922.

Bengtsson, J., Bake, B., Johansson, A., Bengtson, J.P., 2001. End-tidal to arterial oxygen tension difference as an oxygenation index. Acta Anaesthesiol. Scand. 45, 357–363.

Boxerman, J.L., Bandettini, P.A., Kwong, K.K., Baker, J.R., Davis, T.L., Rosen, B.R., Weisskoff, R.M., 1995. The intravascular contribution to fMRI signal change –

Monte-Carlo modeling and diffusion-weighted studies in-vivo. Magn. Reson. Med. 34, 4–10.
Buxton, R.B., Uludag, K., Dubowitz, D.J., Liu, T.T., 2004. Modeling the hemodynamic response to brain activation. NeuroImage 23, S220–S233.
Cabeza, R., Anderson, N.D., Locantore, J.K., McIntosh, A.R., 2002. Aging gracefully: compensatory brain activity in high-performing older adults. NeuroImage 17, 1394–1402.
Cabeza, R., Locantore, J.K., Anderson, N.D., 2003. Lateralization of prefrontal activity during episodic memory retrieval: evidence for the production-monitoring hypothesis. J. Cogn. Neurosci. 15, 249–259.
Chiarelli, P., Bulte, D., Wise, R., Gallichan, D., Jezzard, P., 2007. A calibration method for quantitative BOLD fMRI based on hyperoxia. NeuroImage 37, 808–820.
Coffey, C.E., Wilkinson, W.E., Parashos, I.A., Soady, S.A., Sullivan, R.J., Patterson, L.J., Figiel, G.S., Webb, M.C., Spritzer, C.E., Djang, W.T., 1992. Quantitative cerebral anatomy of the aging human brain: a cross-sectional study using magnetic resonance imaging. Neurology 42, 527–536.
Cowell, P.E., Turetsky, B.I., Gur, R.C., Grossman, R.I., Shtasel, D.L., Gur, R.E., 1994. Sex differences in aging of the human frontal and temporal lobes. J. Neurosci. 14, 4748–4755.
D'Esposito, M., Deouell, L.Y., Gazzaley, A., 2003. Alterations in the bold fMRI signal with ageing and disease: a challenge for neuroimaging. Nat. Rev. Neurosci. 4, 863–872.
Davis, T.L., Kwong, K.K., Weisskoff, R.M., Rosen, B.R., 1998. Calibrated functional MRI: mapping the dynamics of oxidative metabolism. Proc. Natl. Acad. Sci. U. S. A. 95, 1834–1839.
Good, C.D., Johnsrude, I.S., Ashburner, J., Henson, R.N.A., Friston, K.J., Frackowiak, R.S.J., 2001. A voxel-based morphometric study of ageing in 465 normal adult human brains. NeuroImage 14, 21–36.
Goodwin, J.A., Vidyasagar, R., Balanos, G.M., Bulte, D., Parkes, L.M., 2009. Quantitative fMRI using hyperoxia calibration: reproducibility during a cognitive Stroop task. NeuroImage 47, 573–580.
Grubb, R.L., Raichle, M.E., Eichling, J.O., Terpogos, M.M., 1974. Effects of changes in Paco2 on cerebral blood volume, blood flow, and vascular mean transit time. Stroke 5, 630–639.
Hoge, R.D., Atkinson, J., Gill, B., Crelier, G.R., Marrett, S., Pike, G.B., 1999. Linear coupling between cerebral blood flow and oxygen consumption in activated human cortex. Proc. Natl. Acad. Sci. U. S. A. 96, 9403–9408.
Hyder, F., 2004. Neuroimaging with calibrated fMRI. Stroke 35, 2635–2641.
Kastrup, A., Kruger, G., Neumann-Haefelin, T., Glover, G.H., Moseley, M.E., 2002. Changes of cerebral blood flow, oxygenation, and oxidative metabolism during graded motor activation. NeuroImage 15, 74–82.
Lancaster, J.L., Woldorff, M.G., Parsons, L.M., Liotti, M., Freitas, E.S., Rainey, L., Kochunov, P.V., Nickerson, D., Mikiten, S.A., Fox, P.T., 2000. Automated Talairach Atlas labels for functional brain mapping. Hum. Brain Mapp. 10, 120–131.
Langenecker, S.A., Nielson, K.A., Rao, S.M., 2004. fMRI of healthy older adults during Stroop interference. NeuroImage 21, 192–200.
Leenders, K.L., Perani, D., Lammertsma, A.A., Heather, J.D., Buckingham, P., Healy, M.J.R., Gibbs, J.M., Wise, R.J.S., Hatazawa, J., Herold, S., Beaney, R.P., Brooks, D.J., Spinks, T., Rhodes, C., Frackowiak, R.S.J., Jones, T., 1990. Cerebral blood-flow, blood-volume and oxygen utilization — normal values and effect of age. Brain 113, 27–47.
Leontiev, O., Dubowitz, D.J., Buxton, R.B., 2007. CBF/CMRO2 coupling measured with calibrated BOLD fMRI: sources of bias. NeuroImage 36, 1110–1122.
Lu, H., X., F., Rodrigue, K.M., Kennedy, K.M., Cheng, Y., Flicker, B., Hebrank, A.C., Uh, J., Park, D.C., 2011. Alterations in cerebral metabolic rate and blood supply across the adult lifespan. Cereb. Cortex 21, 1426–1434.
Milham, M.P., Erickson, K.I., Banich, M.T., Kramer, A.F., Webb, A., Wszalek, T., Cohen, N.J., 2002. Attentional control in the aging brain: insights from an fMRI study of the Stroop task. Brain Cogn. 49, 277–296.
Mugler III, J.P., Brookeman, J.R., 1990. Three-dimensional magnetization-prepared rapid gradient-echo imaging (3D MP RAGE). Magn. Reson. Med. 15, 152–157.
Nielson, K.A., Langenecker, S.A., Garavan, H., 2002. Differences in the functional neuroanatomy of inhibitory control across the adult life span. Psychol. Aging 17, 56–71.
O'Sullivan, M., Morris, R.G., Markus, H.S., 2005. Brief cognitive assessment for patients with cerebral small vessel disease. J. Neurol. Neurosurg. Psychiatry 76, 1140–1145.
Pantano, P., Baron, J.C., Lebrungrandie, P., Duquesnoy, N., Bousser, M.G., Comar, D., 1984. Regional cerebral blood-flow and oxygen-consumption in human aging. Stroke 15, 635–641.
Pardo, J.V., Pardo, P.J., Janer, K.W., Raichle, M.E., 1990. The anterior cingulate cortex mediates processing selection in the Stroop attentional conflict paradigm. Proc. Natl. Acad. Sci. U. S. A. 87, 256–259.
Parkes, L.M., Rashid, W., Chard, D.T., Tofts, P.S., 2004. Normal cerebral perfusion measurements using arterial spin labeling: reproducibility, stability, and age and gender effects. Magn. Reson. Med. 51, 736–743.
Parkes, L.M., Tofts, P.S., 2002. Improved accuracy of human cerebral blood perfusion measurements using arterial spin labeling: accounting for capillary water permeability. Magn. Reson. Med. 48, 27–41.
Raichle, M.E., MacLeod, A.M., Snyder, A.Z., Powers, W.J., Gusnard, D.A., Shulman, G.L., 2001. A default mode of brain function. Proc. Natl. Acad. Sci. U. S. A. 98, 676–682.
Restom, K., Bangen, K.J., Bondi, M.W., Perthen, J.E., Liu, T.T., 2007. Cerebral blood flow and BOLD responses to a memory encoding task: a comparison between healthy young and elderly adults. NeuroImage 37, 430–439.
Rostrup, E., Law, I., Blinkenberg, M., Larsson, H.B., Born, A.P., Holm, S., Paulson, O.B., 2000. Regional differences in the CBF and BOLD responses to hypercapnia: a combined PET and fMRI study. NeuroImage 11, 87–97.
Simic, G., Kostovic, I., Winblad, B., Bogdanovic, N., 1997. Volume and number of neurons of the human hippocampal formation in normal aging and Alzheimer's disease. J. Comp. Neurol. 379, 482–494.
Sowell, E.R., Peterson, B.S., Thompson, P.M., Welcome, S.E., Henkenius, A.L., Toga, A.W., 2003. Mapping cortical change across the human life span. Nat. Neurosci. 6, 309–315.
Stroop, J.R., 1935. Studies of interference in serial verbal reactions. J. Exp. Psychol. 18, 643–662.
Thesen, S., Heid, O., Mueller, E., Schad, L.R., 2000. Prospective acquisition correction for head motion with image-based tracking for real-time fMRI. Magn. Reson. Med. 44, 457–465.
Thomason, M.E., Foland, L.C., Glover, G.H., 2007. Calibration of BOLD fMRI using breath holding reduces group variance during a cognitive task. Hum. Brain. Mapp. 28, 59–68.
Tisserand, D.J., van Boxtel, M.P.J., Pruessner, J.C., Hofman, P., Evans, A.C., Jolles, J., 2004. A voxel-based morphometric study to determine individual differences in gray matter density associated with age and cognitive change over time. Cereb. Cortex 14, 966–973.
Uylings, H.B., de Brabander, J.M., 2002. Neuronal changes in normal human aging and Alzheimer's disease. Brain Cogn. 49, 268–276.
Van Laere, K.J., Dierckx, R.A., 2001. Brain perfusion SPECT: age-and sex-related effects correlated with voxel-based morphometric findings in healthy adults. Radiology 221, 810–817.
Watson, N.A., Beards, S.C., Altaf, N., Kassner, A., Jackson, A., 2000. The effect of hyperoxia on cerebral blood flow: a study in healthy volunteers using magnetic resonance phase-contrast angiography. Eur. J. Anaesthesiol. 17, 152–159.
Wong, E., Buxton, R., Frank, L., 1998. Quantitative imaging of perfusion using a single subtraction (QUIPSS and QUIPSS II). Magn. Reson. Med. 39, 702–708.
Yamaguchi, T., Kanno, I., Uemura, K., Shishido, F., Inugami, A., Ogawa, T., Murakami, M., Suzuki, K., 1986. Reduction in regional cerebral metabolic-rate of oxygen during human aging. Stroke 17, 1220–1228.
Zysset, S., Schroeter, M.L., Neumann, J., von Cramon, D.Y., 2007. Stroop interference, hemodynamic response and aging: an event-related fMRI study. Neurobiol. Aging 28, 937–946.

Please cite this article as: Mohtasib, R.S., et al., Calibrated fMRI during a cognitive Stroop task reveals reduced metabolic response with increasing age, NeuroImage (2011), doi:10.1016/j.neuroimage.2011.07.092